Auditory decision making in mice:

Behavioural characterisation and neural correlates in auditory cortex

Florian Raphael Steinfeld

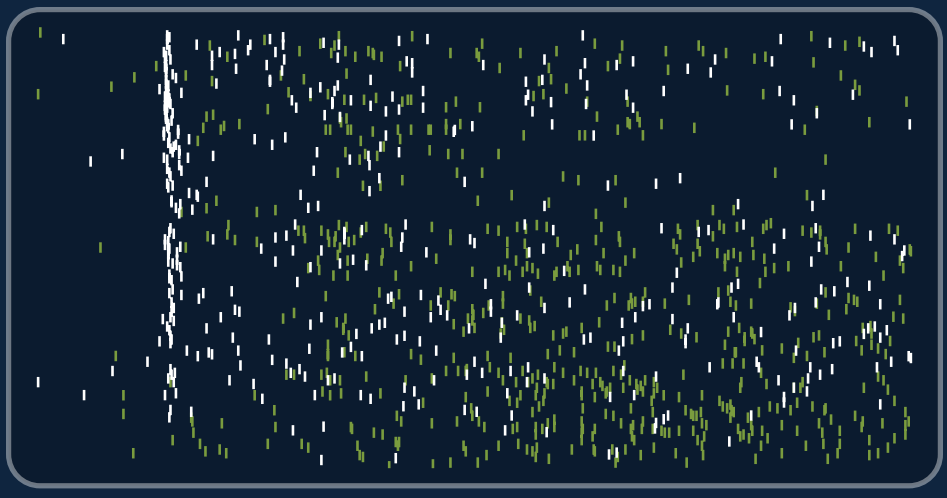

Dissertation presented to obtain the Ph.D degree in Neuroscience

Instituto de Tecnologia Química e Biológica António Xavier | Universidade Nova de Lisboa

Oeiras,
December, 2020

UNIVERSIDADE NOVA DE LISBOA

Auditory decision making in mice: Behavioural characterisation and neural correlates in auditory cortex

Florian Raphael Steinfeld

Dissertation presented to obtain the Ph.D degree in Neuroscience

Instituto de Tecnologia Química e Biológica António Xavier | Universidade Nova de Lisboa

Research work coordinated by:

Champalimaud Foundation

FCT

Fundação para a Ciência e a Tecnologia

MINISTÉRIO DA EDUCAÇÃO E CIÊNCIA

UNIVERSIDADE NOVA DE LISBOA

Oeiras, December, 2020

Acknowledgements:

I want to begin this thesis by thanking my supervisor Alfonso Renart for the opportunity to pursue my PhD in his lab, the open ear for good and the patience with bad ideas as well as for the many hours spent explaining new mathematical concepts to me.
I also want to thank the present and former members of the Renart lab for the supportive atmosphere, the good friendships that I had the privilege of finding there, as well as some memorable karaoke nights. Special thanks here go to José for helping me settling into the lab, Davide for the great spirit and enthusiasm whatever the obstacle, Mafalda for the friendship, the stories and all the Portuguese and most of all to André, whose energy and enthusiasm made all of this possible.

Abstract:

Forming appropriate decisions based on the state of the outside world is an essential skill animals need to survive. While several tasks to study rodent decision making have been proposed, many aspects of perceptual decision making and their neural correlates remain poorly understood. In this thesis we focused on three separate aspects of auditory decision making in mice, each represented by one of the following chapters.
We started by demonstrating the involvement of the auditory cortex in performance of a delayed frequency discrimination task. Moreover, we showed a laminar and temporal separation of sensory and action related signals across the layers of the auditory cortex as mice perform in that task. In the following chapter, we investigated the influence of baseline neural activity on the discrimination accuracy of the following trial. We found that baseline firing rate and cortical synchronisation affected task accuracy only in trials following mistakes. Therefore, our data represents the first demonstration of response-outcome dependent brain state influences on frequency discrimination accuracy in mice.
In the last chapter of the thesis, we deeply characterised the behavioural strategy of animals performing a simple frequency discrimination in a two alternative forced choice paradigm. We revealed the formation of a general, asymmetric response strategy across animals and frequency ranges. Our analysis provides strong evidence that this response strategy developed in response to sensory and control limitations. Taken together, our data highlights the richness of mouse behavioural strategies, even in presumably simple and symmetric task paradigms.

Resumo:

Tomar decisões apropriadas com base no estado do mundo exterior é uma capacidade essencial para a sobrevivência de um animal. Embora várias tarefas para o estudo da tomada de decisão tenham sido propostas , muitas das suas características e paralelos neuronais continuam sem ser compreendidos. Nesta tese, concentrámo-nos em três aspectos individuais da tomada de decisão, por parte de murganhos, com base em evidências auditivas.
Começámos por demonstrar o envolvimento do córtex auditivo na realização de uma tarefa de discriminação retardada de frequência. Além disso, mostrámos uma separação laminar e temporal, ao longo das camadas corticais, por parte dos sinais relacionados com as componentes sensorial e referente à ação.
No capítulo seguinte, investigámos a influência da actividade neuronal basal na precisão do ensaio seguinte. Descobrimos que a qualidade da resposta do animal é influenciada pelo ritmo de actividade basal e pela sincronização do córtex exclusivamente depois de respostas incorretas. Desta forma, os nossos dados demonstram, pela primeira vez, que o ritmo basal e a sincronização do córtex influenciam a performance de murganhos na discriminação de frequência de uma forma que depende do resultado da resposta anterior.
No capítulo final desta tese, caracterizámos de forma aprofundada a estratégia comportamental dos animais ao efectuarem uma discriminação de frequências simples, num paradigma de duas alternativas e escolha forçada. Revelámos a formação de uma estratégia geral, de resposta assimétrica entre animais e grupos de frequências. A nossa análise destes dados providencia fortes evidências de que esta estratégia comportamental foi desenvolvida em resposta a limitações sensoriais e de controlo. No seu todo, os nossos dados realçam a complexidade das estratégias comportamentais dos murganhos, até em tarefas, à primeira vista, simples e simétricas.

Author contributions:

In the following we want to acknowledge our collaborators and clarify their contributions to the respective chapters of this thesis. Moreover we want to take the opportunity to recognise and thank for specific support obtained when establishing the project. All work presented here was performed under the supervision of Dr. Alfonso Renart.

- **Chapter 2:** We thank André Monteiro for help with behavioural training and Julien Fiorilli for his help establishing the the junction-potential based lick port system. Furthermore, we want to thank Dr. José Pardo-Vazquez for his help establishing the recording system and his instructions for performing acute silicone probe recordings. Mostly, we want to thank Dr. Alfonso Renart for the scientific guidance.
- **Chapter 3:** The contents of this chapter represent the collaborative efforts of the author with Dr. Davide Reato. The data analysed was acquired by the author and a collaborative effort for analysis of the effects of brain state on discrimination accuracy was started after the author's initial observations of synchronisation-dependent changes in task accuracy.
- **Chapter 4:** The contents of this chapter represent the collaborative efforts of the author with Dr. Davide Reato and Juan Castiñeiras. The behavioural task was developed by the author and all modifications described in the chapter to establish the behavioural phenotype represent collaborative efforts with Dr. Davide Reato. Theoretical considerations described in this chapter were contributed by Juan Castiñeiras and Dr. Davide Reato and implemented in a signal detection theory framework by the author.

This work was funded by a scholarship from the Fundação para a Ciência e a Tecnologia of the Portuguese Ministry of Education and Science (SFRH/BD/52219/2013), and by the Champalimaud Foundation.

Table of Contents

List of Figures

List of Tables

List of Acronyms

2AFC Two Alternative Forced Choice
A1 Primary Auditory Cortex
AAF Anterior Auditory Field
ACx Auditory Cortex
AUC Area under the ROC Curve
CD Coding Direction
CSD Current Source Density
DA Dorsoanterior Field
DM Dorsomedial Field
DP Dorsoposterior Field
DV Decision Variable
FR Firing Rate
GLM Generalised Linear Model
GLMM Generalised Linear Mixed Model
ITI Intertrial Interval
LFP Local Field Potential
MSE Mean Squared Error
MGN Medial Geniculate Nucleus
MAD Median Absolute Deviation
MI Mutual Information
MUA Multi Unit Activity

OF Optic Flow

PBS Phosphate Buffered Saline

PSTH Peristimulus Time Histogram

ROI Region of Interest

SDT Signal Detection Theory

SEM Standard Error of the Mean

VCx Visual Cortex

Chapter 1

Introduction

HIGHLIGHTS

- In this first chapter, we review literature and theoretical concepts essential for the following chapters of the thesis.
- We begin by reviewing important concepts and methodology of studying rodent perceptual decision making.
- We then introduce key features of the auditory system with a focus on the laminar structure and distinction of cortical areas in the mouse.
- We furthermore review the literature on state modulations observed in the auditory cortex.
- We conclude the chapter by presenting the structure of this thesis and clarifying the motivation behind each scientific question studied.

1.1 Sensory decision making

We are what we are because of the way we perceive the world and how we relate to it, because of what we have learned and how we combine all these factors into our decisions and actions. Studying this process therefore represents a fundamentally important gateway into understanding the human condition.

1.1.1 Psychophysics

A decision is the process that results in a deliberate commitment to a categorical proposition [78]. A common framework to study such processes in neuroscience is sensory-motor decision making, where subjects are required to form decisions about certain features of sensory stimuli. Such features can be the direction of cohesively moving dots [178], the frequency of a sound [115] or the location of its source [197]. These decisions then need to be reported by the execution - or omission - of defined actions. Subjects are therefore tasked to infer the state of the outside world given the information provided by their sensory systems [78, 126, 205, 259, 281]. Because the stimulus is under direct control of the experimenter, the amount of evidence available to perform a decision can be manipulated. Consequently, sensory-motor tasks can be used to quantify sensory perception, by inferring information about the sensory evidence perceived by the subject through the reported decisions [73, 237].
This application of sensory decision making tasks, known as Psychophysics, was first formulated by Gustav Fechner in the late 19th century and has since then been widely used to study the perceptual limitations of sensory discrimination and detection [64, 263, 234, 51, 127, 91, 199, 52]. Typically, in psychophysical studies, subjects are presented with multiple stimuli varying the sensory feature relevant for the required decision. This feature can be intensity in detection tasks [28], cohesion in case of the random dot movement task [178] or interaural level difference for tasks based on rodent sound localisation [197]. The proportion subjects report one of the two categorical decisions is then calculated for each of the presented stimuli. In discrimination tasks, these fractions typically can be well described by a sigmoidal curve, called the psychometric function or curve. 'Easy' stimuli, provide strong sensory evidence so that the decision making process is not sensory

limited. Therefore the decisions reported for easy stimuli of one condition do not vary strongly. These tails of the psychometric curve therefore indicate the lapse rate of decision behaviour [30]. Only as the sensory evidence for the task categories diminishes, the probability of reporting either category changes with the strength of evidence presented. The slope of this sensory-limited part of the psychometric function therefore measures the sensitivity [30].
Through careful task design, different internal and external factors interfering with the sensory decision process can be studied through their effect on the psychometric curve [30]. Moreover, by conditioning the analysis on the stimulus or decision history, the dependency on internal biases or history effects in the decision making process can be quantified through shifts in the position of the psychometric curve, indicating response biases.

1.1.2 Signal detection theory

To quantify the degree to which animals are able to discriminate or detect stimuli, different theoretical frameworks have been applied [55, 138, 82]. Among those, Signal Detection Theory (SDT) has become highly influential. In this framework the decision is formed based on the value of a Decision Variable (DV) in a particular trial. In the context of psychophysics its value corresponds to the degree of perceptual evidence available in a given trial. In a detection task the DV therefore corresponds to the evidence that a stimulus has been presented while in a discrimination task it represents the evidence available to classify an observed stimulus into one of two categories. The value of the DV observed in individual trials is described by two distributions across the trials of the decision categories (Figure 1.1). In a given trial, the decision is formed by testing if the current DV value is bigger, or smaller, than a threshold. Importantly, overlapping distributions result in DV values that can be observed under both distributions, creating trials of perceptual uncertainty, as the observed perceptual evidence is not uniquely associated with one task condition. The degree to which task conditions can be discriminated is quantified by the difference of the distribution means, relative to the combined standard deviations and is referred to as discriminability index or d-prime [258, 250, 74, 14].
The decision threshold used to determine which distribution a given DV

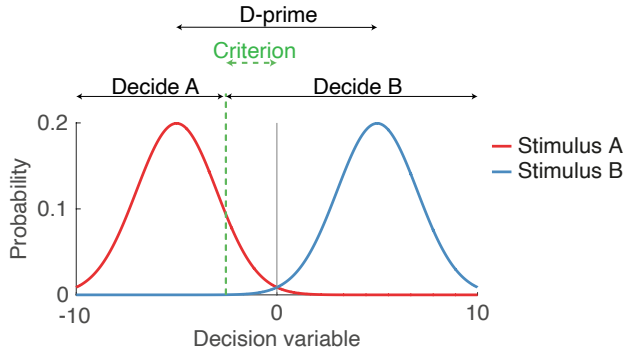

Figure 1.1: ***Distribution of the decision variable across trials of two categories, showing d-prime and the criterion (c).***

value is attributed to is called the criterion (c). The value of the criterion is not necessarily determined exclusively by the DV distributions, but can be subject to internal influences, like motivation, or can be manipulated by the task structure [14, 46]. It can thus reflect the underlying behavioural strategy of the animals independent of the perceptual difficulty. The criterion resulting in the highest decision accuracy is given by the value of the DV that is equally likely observed under both distributions. In this case, all DV values bigger than the criterion are more likely observed under one distribution, and all values smaller are more likely observed under the other. Therefore misclassifications are limited only by the discriminability of the stimulus percepts. However, instead of maximising decision accuracy, the criterion can also minimise the risk of misclassifying trials of one of the two distributions selectively by taking smaller or bigger values [14].

1.1.3 Perceptual decision-making tasks

To generate data suitable to characterise the perceptual decision making process and reveal its neural implementation, appropriate sensory-motor tasks have to be designed that allow for targeted manipulation of the perceptual evidence, while closely monitoring the subjects' behaviour and neural activity [78, 135, 30]. While these tasks have traditionally been developed and applied for studies using primates [198, 78], similar behavioural paradigms have now been established for mice. Given the variety of genetic and optogentic tools available, these tasks facilitate targeted neural manipulations to

probe the resulting behavioural effects [85, 153, 108, 30].
The exact design of the task is an important factor for the training speed and robustness of its findings [283]. Especially in mice, simple Go-NoGo tasks have often been used [6, 245, 101, 2]. In these tasks, one stimulus category (S+) is associated with a response, which has to be omitted in its absence or following presentation of another stimulus (S-). This simple task structure results in relatively short training times [30]. But because the absence of a response action can be triggered by either a dedicated task-decision or correspond to a lack of motivation to engage in the task, the response accuracy is easily confounded. SDT can sometimes disentangle these confounding factors, however especially in the case of stimulus detection tasks, this is not trivial, as an unambiguous separation of the presented stimuli in signal and noise categories is not possible [101]. These shortcomings of Go-NoGo tasks are avoided in symmetric, Two Alternative Forced Choice (2AFC) tasks, in which animals report their decision by executing one of two similar response actions. While changes in the task engagement can still (selectively) alter the fraction of trials in which the animal responded, these motivational effects cannot influence the criterion of the sensory-motor decision process [114, 93].
Apart from different response structures, also distinct classes of behavioural apparatuses for sensory-motor tasks in rodents have been implemented. In freely moving task environments, mice are allowed to explore and walk within the behavioural box voluntarily during the behavioural session. A common apparatus to train freely moving animals consists of a box with three separate nose poke ports. An infrared beam is broken when animals enter these ports, which is considered the voluntary response. Typically, the poke in the centre is used to initiate a trial and thus trigger stimulus presentation, while the two lateral ports are usually sites of the animals' responses and reward delivery [206, 28, 273, 114, 299]. This deliberate trial initiation is a great advantage in task structure as it allows for a self paced progression of trials and limits the trial-by trial fluctuation in motivation of the animals. Contrasting this apparatus for freely moving behaviour, especially behavioural tasks for mice often use behavioural setups that restrict the animals' movements via head-fixation [14, 85, 153, 151]. This restraint of movement greatly facilitates recording of neural data and additionally allows for easy measurements of important behavioural indicators like pupil dilation or movements, which can either be measured by video or by placing the head fixed animal on a

treadmill or tracking ball [153, 225]. In these head fixed preparations, animals can report their decision either by licking at water delivery spouts [85], rotation of a steering wheel [27, 113] or by navigating to a specific location in a virtual environment using a tracking ball [225]. Some head fixed preparations also do allow for voluntary trial initiations by the animal. In instances where mice are fixated while running on a treadmill, specific running speeds have been used for trial initiation [153]. Moreover, a three licking spout paradigm for head fixed mice, analogous to the three nose pokes system, has recently been developed [151].

1.2 Neural coding of sensory information

In all sensory-motor tasks, the brain needs to gather information about the state of the outside world in order to select the appropriate behavioural response. This sensory information is collected by specialised receptor cells outside of the central nervous system. These receptors cells transduce specific features of the present sensory stimuli into neural patterns of activation. This stimulus-evoked neural activity is then propagated into the central nervous system where its processing can lead to a stimulus percept and drive behaviour.
In this study we focus on auditory decision making processes as audition is a salient sensory modality in mice [30]. Moreover, other than somatosensation by whisker movement or olfaction, the detection of sensory stimuli in the auditory domain is not necessarily associated with movement and can therefore be temporally well controlled and easier decoupled from movement influences. In addition, auditory cortical areas are relatively well defined in their location and spatial organisation and can be easily accessed for electrophysiological recordings [271].

1.2.1 The auditory system

The auditory system is specialised to detect and process sound. Sound refers to pressure waves generated by vibrations of air molecules and is the sensory stimulus underlying auditory perception [204]. It is detected by specialised mechano-receptors in the inner ear and its different features correspond to distinct aspects of the resulting auditory percept. Thus, the amplitude of

a sound wave will determine its perceived loudness, while its periodicity is closely related to the perceived pitch [232].
To transform these airborne pressure waves into neural activity patterns, sound waves are gathered by the outer ear and transferred to the cochlear in the inner ear. Pressure waves travelling through the inner ear cause vibrations at the basilar membrane which are transformed into neural activity patterns by hair cells, the sensory receptor cells of the auditory system [204]. Importantly, the basilar membrane systematically changes its flexibility and width, resulting in distinct locations of maximum membrane vibrations for sounds of different frequencies. This structural property of the basilar membrane decomposes sound stimuli into their frequency components and leads to the generation of frequency-specific neural activity patterns by the hair cells [25, 204].
Neurotransmitters released by the hair cells in turn activate neurons of the spiral ganglion, which propagates the resulting activity to the central nervous system [204]. Because these neurons only receive input from one or few hair cells, the frequency decomposition mainly achieved by the physical properties of the basilar membrane is maintained. This frequency-specific organisation in the signal propagation, called tonotopy, represents a hallmark organising principle in the ascending auditory pathway as neighbouring neurons typically have similar characteristic frequencies [25].
In the central nervous system, most sound-triggered neural activity is propagated through multiple relay stations before converging at the inferior colliculus [25]. In mammals, these early processing stages are relatively conserved in their structure and have mostly been implicated in the processing of sound localisation [232, 116, 110, 292, 25]. Activity patterns of the inferior colliculus then are propagated to the the Medial Geniculate Nucleus (MGN) in the thalamus which then gates the activity to the Primary Auditory Cortex (A1) and the striatum [242, 25].

1.2.2 Subdivisions of the mouse auditory cortex

While the anatomical structures that propagate auditory information to the cortex are relatively conserved across mammal species [232], the subdivisions and terminology of different auditory cortical areas greatly vary across species. In general, auditory cortex (ACx) is divided into primary and secondary cortical areas. Primary areas receive direct innervation from the

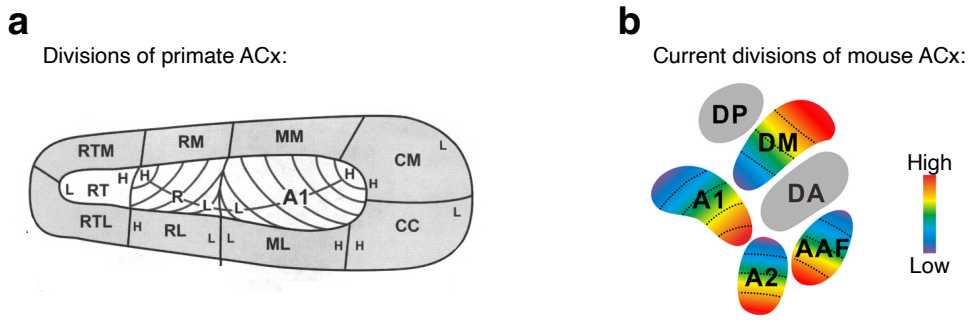

Figure 1.2: ***Subdivisions of the auditory cortex (ACx).*** ***a:*** *Auditory cortical areas in nonhuman primates. Primary areas are primary auditory cortex (A1), rostral area (R) and the rostrotemporal area (RT). Belt areas are referred to by their position as caudolateral (CL), caudomedial (CM), middle lateral (ML), middle medial (MM), rostromedial (RM), anterolateral (AL), rostrotemporal medial and lateral (RTM & RTL). L (Low) and H (High) demarcate the direction of the tonotopic map. Adapted from Kaas & Hackett [119].* ***b:*** *Recent subdivisions of auditory cortical areas of the mouse. Primary areas are primary auditory cortex (A1), dorsomedial (DM) and anterior auditory field (AAF). Secondary areas are secondary auditory cortex (A2), dorsal posterior area (DP) and the dorsal anterior area (DA). Colours indicate the tonotopic map for pure frequency tones. Adapted from Tsukano et al. [268]*

ventral part of the MGN, are tonopopically organised and exhibit certain histological features like dense myelination and elevated expression levels of certain marker proteins [95, 121]. In adjacent primary auditory areas, the direction of the tonotopic map typically inverts [268, 271]. In primates, three primary auditory areas with independent activation by the MGN have been described [164, 109, 168, 207] (Figure 1.2a). These lie in the centre of the ACx and are typically collectively referred to as the core region. The core region is surrounded by secondary auditory fields, called the belt region. These secondary auditory areas are typically innervated by primary cortical areas and show less myelination than core regions [95]. Moreover, some secondary auditory areas are not tonotopically organised, but instead show tuning to higher auditory features [16, 271, 254]. In primates, eight different belt regions are being distinguished according to their histological features.

In the mouse, the differentiation of ACx into smaller areas is not as well

established. Until recently, only two primary areas, the Anterior Auditory Field (AAF) and the A1, with differing response properties, projection targets and thalamic inputs, have been distinguished [254, 144, 84, 112, 171, 246]. However, based on fine scale mapping of tonotopic sound responses and connectivity patterns, recent studies have suggested a division of A1 into Dorsomedial Field (DM) and A1 [268, 269, 271] (Figure 1.2b). Each of these three suggested primary areas receive direct innervation from distinct locations of the MGN and are organised tonotopically. While the Dorsoanterior Field (DA) also receives direct thalamic innervation, it is not considered a primary auditory area because of the absence of tonotopy [102, 104, 270, 268]. A tonotopic map has also been described in the secondary auditory cortex of mice, while neither DA nor Dorsoposterior Field (DP) are activated by pure frequency tones. Instead, responses in these areas are triggered by changes in direction of slow frequency modulated sounds [104, 270, 254].
Importantly, while all primary auditory cortices are arranged along a topnotopic map largely inherited from the cochlea, auditory responses are not limited to pure frequencies. Instead, neurons independently encode multiple sound features, like localisation, frequency and frequency-envelope cues [16, 132] and integrate sound stimuli across different time scales [175, 233]. Moreover, neural responses corresponding to reward expectation and upcoming choices in sensory-motor tasks have been reported [83]. Some studies have reported that neural responses do also vary according to the distance of the cells to the surface, suggesting a depth-dependent segregation of sensory and behavioural information [200, 296].

1.2.3 Laminar organisation of cortex

One hallmark feature of the mammalian neocortex is its stereotypic laminar structure. It is comprised of six main layers, numbered according to their depth. These layers show distinct cell densities and distributions and are connected to each other in a highly stereotypic way, referred to as the canonical cortical microcircuit (Figure 1.3a). The neurons across cortical layers are broadly categorised by the neurotransmitter they release. The principal neurons of cortex, comprising 80% of the neural population, excite their postsynaptic targets by release of glutamate [92]. Because of their morphology, they are commonly referred to as pyramidal cells [92]. While these neurons propagate excitatory inputs locally or across long distances in

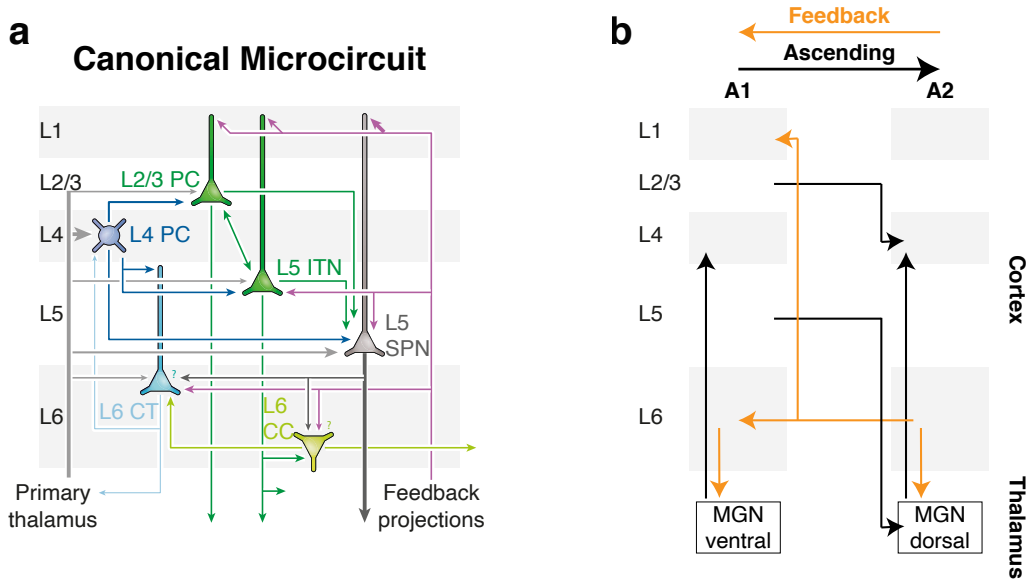

Figure 1.3: ***Connectivity of cortical areas.*** ***a:*** *Canonical cortical microcircuit. Shown are the main excitatory cell types. Line thickness represents the strength of connection. Nomenclature: Corticocortical cells (CC), Corticothalamic cells (CT), Intratelencephalic neurons (ITN), Pyramidal cells (PC), Subcerebral projection neurons (SPN). Adapted from Harris et al. [92].* ***b:*** *Schematic laminar connectivity across the cortical hierarchy.*

the brain, the remaining cortical neurons inhibit firing in their local postsynaptic targets by releasing the neurotransmitter GABA [92].
Both excitatory and inhibitory neurons can be further classified according to their protein expression levels, morphology and typical connectivity. Ascending information from primary thalamus or lower cortical areas primarily excites neurons in cortical layer 4 [243], however in the auditory cortex, strong inputs at the border of cortical layers 5 and 6 have also been observed [222, 92]. Pyramidal cells in layer 4 then strongly innervate neurons in the more superficial layers 2 and 3 [243], but projections to neurons in all layers have also been described [92]. Excitatory neurons in superficial layers 2 and 3 in turn form both local connections to neurons in layer 5 as well as distant projections to higher order cortical areas [243, 92]. Cells in layer 5 fall into two major categories that form connections to either telencephalic or subcerebral areas. Intratelencephalic cells innervate targets like the striatum,

other cortical areas or locally target neurons in layer 2/3 [92]. Subcerebral cells, on the other hand, do not form strong local connections, but project to the ipsilateral striatum as well as secondary thalamic and subcerebral areas [157, 242, 211, 92]. Neurons in the deepest layer of cortex primarily receive descending feedback projections from higher order cortices or thalamus and in turn innervate primary thalamic areas or layer 1 and 6 of lower cortical areas [243, 92]. In primates, local connections of layer 6 neurons preferentially target interneurons in the input layer 4 [242, 260, 92], while a preferential targeting of superficial layer 5 has been observed in rodents [129, 3]. The most superficial layer 1 of cortex is largely free of cell bodies in adult animals and instead a target of projections from higher cortical areas, where they form connections to the ascending dendrites of layer 2/3 and 5 neurons [92] (Figure 1.3a).
This general connectivity of cortical areas forms the basis of the cortical hierarchy (Figure 1.3b). As ascending information primarily excites layer 4 neurons, while descending feedback projections target the extremes of the cortical column, a main directionality or hierarchy in the in the information processing stream can be defined among connected cortical areas [243]. In a given cortical area, the influences of feed forward information in layer 4 and feedback projections to layers 1 and 6 then can be combined in their effects on layer 2/3 and layer 5 neurons. While this characteristic connectivity motif has often been suggested to be associated to a canonical computation of a cortical column, its functional role has not been fully understood. But it is generally believed that the ascending information across the cortical pathway enables the processing of increasingly complex sensory features, while the descending feedback projections play important roles in modulations of cortical processing according to behavioural demands in a particular context [31, 11].

1.3 State dependent activity in ACx

To identify sensory or contextual features relevant for neural activity, feature-dependent activity changes have to be quantified. In a single neuron, the response to a given stimulus is typically described by its average activity at various time points around the stimulus presentation. The hence obtained Peristimulus Time Histogram (PSTH) then gives a description of how the

mean neural activity is affected by the stimulus. In ACx, neurons typically show fast, transient activations at sound onset, but stimulus triggered silencing of neurons and responses to the sound offset have also been described [222, 246, 134].
A different, salient aspect of neural activity in the cortex is its variability [239, 160]. Thus, the firing rates observed during single stimulus presentations or behavioural trials can deviate significantly from another [262, 261]. Sources of such neural variability can be deterministic or random [63]. Deterministic sources of variability in sensory systems can be unintended background stimuli that interfere with the presented stimulus. Alternatively, the observed differences in activity can be rooted in the interconnectivity of the nervous system that allows for complex interactions with contextual information [63, 160, 224, 249]. However, noise can also be truly random and depend on an inherent imperfection in signal detection and/or propagation in the sensory system [63]. To what extent this neural variability is an inherent property of neural systems or explainable by context is still under debate [238, 63, 237].
However, while some of the observed variability might truly be random, behavioural state and context alter cortical activity [224, 249, 160]. Among others, movement, arousal state as well as task engagement and attention have been shown to be important modulators of firing rates in cortex [189, 7, 130, 229, 160]. In the auditory domain, the influence of movement on auditory cortex has been well studied across species [213, 214, 218, 230, 251, 276, 284, 295]. Movement reduces firing rates and frequency responses across all frequencies. This suppression is thought to represent the suppression of expected, self-generated sounds that each movement introduces [216, 24]. In line with this interpretation, the level of suppression observed increases with the familiarity to the environment [231, 229]. In mice, this silencing effect is likely mediated by direct feedback projections from secondary motor cortex (M2), which target both excitatory and inhibitory neurons [176]. Moreover these synapses are strengthened through movement related auditory feedback, and thus may well represent the pathway of suppression of predicted self-generated stimuli [61, 62, 228, 229]. Recently, an additional pathway for motor feedback of upcoming facial movements that selectively activates layer 6 neurons in the ACx has been suggested [42]. Because principal neurons of layer 6 can modulate the cortical response gain through activation of layer 4 interneurons [188], such layer 6 activations represent another possi-

ble pathway of movement-related suppression of activity in ACx. Movement modulations are however not limited to the cortex, but occur on many levels of the auditory pathway [229].
Apart from movement, attention and task engagement also have been demonstrated to control the size of stimulus responses through thalamic gating [288]. More prominently though, they have been reported to alter the width of neural tuning curves [183, 71, 187, 173, 186, 8, 256, 221]. The width of the neural tuning curve describes the range of stimuli that induce firing above the baseline rate. It therefore is an important measure of a neurons' selectivity. When animals are engaged in a task, tuning curves in ACx typically get narrower and baseline firing rates are reduced, resulting in an improved ratio of stimulus representation compared to the noise.
However, these behavioural states do not only affect the firing rate and selectivity of individual neurons alone, but also the degree and level of coordination of neural populations [163, 160] (Figure 1.4). Thus, in the absence

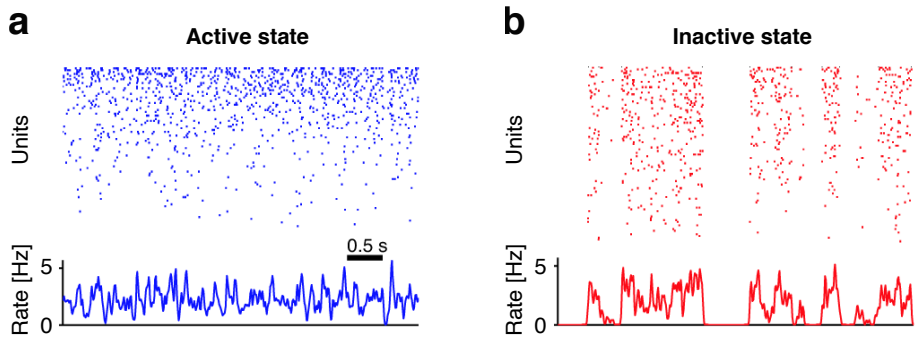

Figure 1.4: ***Examples for active and inactive cortical state in the ACx of anaesthetised rats. a:*** *Raster plot (Top) and PSTH (Bottom) of simultaneously recorded neurons during desynchronised cortical activity.* ***b:*** *Same showing synchronised activity. Adapted from Renart et al. [212]*

of a stimulus, the spontaneous spikes of individual neurons in a population can either occur independent of each other or they can be synchronised, leading to periods of collective firing bursts, called up states, and periods in which spikes are absent in all cells, called down states (Figure 1.4b). The degree of synchrony of spontaneous cortical activity is highly variable across the continuous spectrum between the illustrated extreme states of coordination (Figure 1.4). Moreover the synchrony of cortical activity, also

called brain state, is highly correlated with movement and arousal states, an effect modulated by fluctuations of cholinergic and noradrenegic activity [140, 163, 38, 210]. Thus, both movement and high arousal are associated with desynchronous firing, therefore referred to as active state, while highest degrees of synchronisation are observed across different stages of sleep [253, 159]. However, synchronous firing is not limited to phases of sleep, but can also occur at various degrees during wakefulness [282, 202, 248].
The degree and sign of firing rate correlations can be an important factor for downstream areas, involved in detecting or discriminating stimulus information encoded in that activity [161]. Cortical state of quiescence and mild synchrony can favour the detection of stimuli near detection threshold during down states [161, 160]. However, strong correlations in firing rate likely reduce the specificity of the stimulus signal and discrimination performance [194, 172] (see simplified scheme in Figure 1.5). The active cortical state on the other hand, can facilitate fine-scale discrimination of stimuli, due to the global absence of correlations [212, 160]. In addition, analysis of spontaneous activity in the rat ACx suggests that the active state is maintained through the balanced interaction of two anti-correlated cortical sub-populations [20]. This negative correlation could further increase discriminability for a linear decoder if stimulus tuning across these

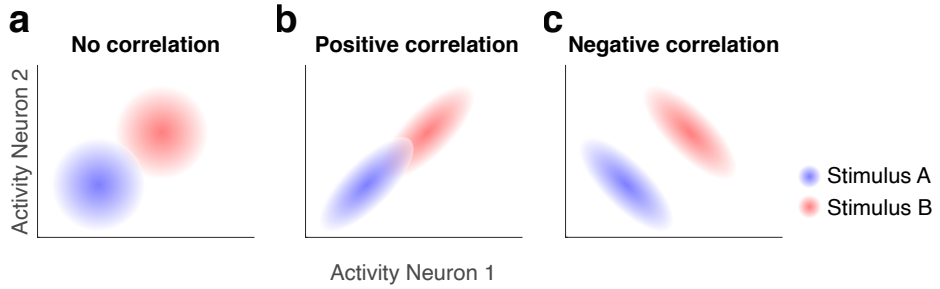

Figure 1.5: ***Effect of correlation in linear coding.*** *Shown are the example histograms of the combined activity of two simulated neurons following the presentation of two stimuli. The colour intensity corresponds to probability of observation.* ***a:*** *No correlation. Firing rates in the two conditions overlap in few instances only.* ***b:*** *Positive correlation. Firing rates overlap strongly, limiting the possibility of correct stimulus discrimination.* ***c:*** *Negative correlation. Noise and stimulus direction in the neural space are orthogonal, strongly increasing the separation of activity.*

sub-populations were positively correlated (Figure 1.5). Indeed, experimental studies have shown that the quality of multi-feature decoding in ACx does depend on the degree of synchrony in cortical spontaneous firing [132]. As recordings in behaving animals have demonstrated a reduction of such correlations with task engagement [57, 163], brain state likely represents an important regulatory mechanism for population function.
Experimentally, many studies have confirmed a correlation of brain state and performance in detection tasks which seems consistent with different levels of task engagement and arousal [44, 161, 224, 249, 160]. However, so far no strong behavioural effect of brain state on stimulus discriminability has been demonstrated in mice [113].

1.4 Structure and aim of this thesis

The aim of this thesis is to study auditory decision making in mice. After this introduction, we investigate the laminar distribution of task correlates in the activity of ACx during frequency discrimination. While previous studies have demonstrated the presence of action related signals in ACx [83, 296], it remains unclear if these signals are predictive of upcoming choices or reflect modulations of ACx by ongoing movements. Moreover, a layer-depended separation of action and stimulus related activity in sensory cortices has been recently suggested [200, 296], but such laminar separations have not yet been observed in mice. We therefore investigate the presence and nature of response signals in the mouse ACx with the aim of dissociating their laminar and temporal profiles during the performance of an auditory decision making task. We demonstrate the necessity of ACx in task performance and a distinct temporal and laminar separation of stimulus and action signals.
In the following chapter, we examine the influence of neural baseline activity prior to stimulus presentation on the task performance. As cortical desynchronisation has been associated with exploratory movements in rodents and visual attention in cats [279, 125], it has been suggested to allow for more accurate representations of sensory stimuli. Consistent with this view, several studies have confirmed a better discriminability of neural stimulus representations during cortical desynchronisation [76, 192, 13, 132]. The behavioural effect of these findings, however is not fully understood yet. In detection

tasks, a clear relationship of neural synchronisation prior to the stimulus presentation and task performance has been established, that mainly reflects changes in the animals' propensity to respond [161, 160]. Moreover, an effect of cortical synchrony on stimulus discrimination accuracy has also been observed in a primate Go-NoGo task [13]. However, when directly comparing the effects of cortical synchronsation on task accuracy and engagement in a 2AFC paradigm, cortical synchrony has been associated with the latter [113]. Here, we revisit the influence of cortical baseline activity on behavioural accuracy during auditory frequency discrimination. We present evidence that neural activity prior to the stimulus presentation selectively correlates with behavioural accuracy in trials following incorrect responses, while no influence of neural activity can be determined in the remaining trials.

In the following chapter we characterise the behavioural strategies of animals during frequency discrimination. A deep understanding of the behavioural strategy is necessary to identify neural implementations of its underlying computations [135]. We present generic task strategies displayed by our animals leading to biased response patterns. While such choice biases have been previously described based on trial history [28, 66, 70, 143] and generic response preferences [77], the underlying limitations causing such biases are not fully understood. We therefore explore asymmetries in sensory processing and limitations in cognitive control as underlying factors. We present evidence for such perceptual asymmetries and further demonstrate that the observed response biases depend on additional control limitations. We then conclude the thesis by recapitulating the major findings presented in each chapter, commenting on their significance and relation to existing work and comment on how remaining questions can be addressed in further studies.

Chapter 2

Laminar distribution of stimulus and choice-related signals in auditory cortex

HIGHLIGHTS

- In this chapter, we introduce a delayed frequency discrimination task for head fixed mice.
- Using pharmacological silencing, we show that the ACx is involved in task execution.
- We demonstrate that single and multi unit activity in the ACx is influenced by both the presented stimulus as well as the upcoming choice of the animal with distinct temporal and laminar profiles.
- We show that coding directions in mid-superficial populations are short-lived and rotating throughout the trial progression, while deep populations display two distinct, stable coding formats during sound presentation and during the delay period.

2.1 Introduction

How the brain transforms sensory information into a behavioural response is a key question in systems neuroscience. The cortex likely plays an important role in this transformation [141, 209], but the underlying processes remain poorly understood. Neocortical areas have a well preserved laminar structure with canonical connectivity patterns [56, 92, 3] and are heavily interconnected, receiving feed forward as well as feedback sources of information [243, 92]. The repetitive laminar structure and connectivity of cortex has been suggested to reflect a common set of computations performed within a cortical column [12, 124]. However, no consensus about the nature of such a cortical computation has been reached. Classical hierarchical models of cortical activity assume that sensory percepts are formed by a series of cortical areas that integrate and filter their inputs along the ascending cortical hierarchy [107, 155, 3]. This model is strongly supported by the encoding of edge orientation in the primary visual cortex [106, 107], but fails to clearly account for the strong presence of feedback signals and context modulation of sensory cortices [65, 136, 229, 50, 32].
Alternatively, a predictive processing framework for cortical function has been suggested [12, 124, 40] where the brain generates predictions about expected sensory input, using an internally generated model. Prediction errors computed with the actual sensory information are then used to update the internal representation of the world. This model is appealing as it provides a simple explanation for feed forward and feedback architecture of cortical areas. Thus, feedback signals to a cortical area can be interpreted as prediction signals that will be locally compared to the sensory information [124, 96]. Observations reporting an activation of sensory cortex by movement in the absence of sensory stimuli [223, 123] and specific responses to the absence of expected stimuli [67] can be well explained under this model. Such mismatch activation signals are more densely found in superficial layers of cortex [223], making these a likely locus of prediction error computation. The internal representation needed to form predictions has been suggested to be maintained in deep layers of cortex as activity there is more sustained [222, 92, 124]. Such representations in the deep layers could then be updated by the strong input received from superficial layers. Moreover deep layers show the necessary connectivity to then broadcast the resulting predictions to lower cortical areas and other modalities [92, 124].

Previous studies reporting a depth-dependent segregation of sensory and behavioural information in cortical layers are consistent with this interpretation [200, 296].
Whatever the appropriate conceptual framework for cortical laminar function is, sensory cortices are not just passively relaying sensory information, but adaptively changing their activity according to contextual demands like movement, reward structure, attention or task engagement [136, 229, 50, 32, 83, 58, 7, 57]. In the ACx, movement has been shown to reduce sound responses through multiple feedback loops [230, 286, 229]. Moreover, ACx has been reported to selectively increase representations of target stimuli in a Go-NoGo task paradigm, indicating a flexible processing of sensory stimuli depending on task demands [10]. In addition to neurons with sensory information, also response-action selective cells have been described previously [83, 296, 272].
Apart from the rich representations of task information and behavioural context, the ACx is not necessarily involved in or required for the execution of auditory guided behaviour. While there are some conflicting reports, lesioning studies have largely shown that the ACx is required for discrimination of complex sounds, like frequency modulated stimuli, but not for frequency discrimination using pure tones [165, 29, 79, 185, 220, 201, 75, 34]. In contrast though, more recent studies, using transient optogenetic or pharmacological silencing methods, have reported strong impairments in frequency discrimination performance during silencing of ACx [257, 190]. This discrepancy between permanent and transient silencing of ACx could be due to stimulus unspecific projections to downstream areas that are acutely required for their function [191]. Alternatively, these differences could indicate a role of ACx in frequency discrimination that can be compensated for in the case of long-term lesions. Indeed, while silencing of ACx during discrimination of easy frequency stimuli significantly reduces task performances [75, 34, 190], only silencing of upstream areas like the thalamus or the superior colliculus can reduce performance to chance level [75, 34]. Therefore, as observed in the lesioning studies, the ACx is not required for frequency discrimination in pure frequency stimuli, but its activity likely contributes to baseline task performance. Because targeted optogenetic manipulation of activity in the ACx has been shown to affect task performance [4, 272] and can directly influence the animal's decision [299], this contribution is more likely due to highly selective output projections instead of an unspecific activation signal

of downstream decision centres. With increasing complexity of the stimulus or the cognitive demands of the task, like memory components or necessary mental transformations, the relevance of this contribution for task performance likely increases [34, 190, 137].
An important feature of a cortical area involved in task execution is its noise correlation structure. As single cell responses to a stimulus are variable [43], the degree of stimulus information available to a downstream decision area depends on the correlations in the sensory responses available as well as the number of neurons in the sensory pool [240]. In uncorrelated sensory populations, noisy stimulus responses can be compensated by integrating across a pool of neurons. However, noise in cortical neurons is typically correlated [43], thus potentially limiting the degree to which their effect on downstream areas can be compensated by integration across the population. Interestingly, noise is typically more strongly correlated in neurons with similar tuning [300, 133]. Moreover, the trial by trial fluctuations in sensory responses have been reported to weakly correlate with the reported decisions [23]. This phenomenon, known as choice probability, has been reported across different cortical areas and behavioural tasks [23, 35, 240, 215, 179, 54, 181, 146, 293, 45]. Its interpretation, however, depends on the source of the underlying noise correlations [47].
In the original feed forward interpretation of choice probability, the correlated noise is reflecting shared and randomly varying sensory input in neurons with similar tuning, causally impacting on the decision. Consistent with this interpretation, choice probability is small in primary sensory areas and increases in the cortical hierarchy as it gets closer to the decision centres [285, 100]. Alternatively, neural populations can be altered by cognitive factors like attention or task engagement [44, 166, 57, 217], thus providing an alternative feedback interpretation of such choice probabilities. This interpretation has been supported by several different observations that are inconsistent with the causal feed forward interpretation. Thus, choice probability forms late during the stimulus presentation while early stimulus presentation is more relevant for the decision process [180]. In addition, negative correlations of stimulus variations and choice as well as orthogonal stimulus and choice representations have been reported [81, 298]. Choice probability therefore might reflect bottom-up as well as top-down signals at different time scales [287].
While choice related activity has been described previously in the rodent

ACx [83, 296], due to the task design applied, these signals were fundamentally confounded by presence of movement, strongly complicating the dissociation of stimulus, decision and action related processes. Moreover, the relationship between sensory tuning and action selectivity has not been directly addressed yet.
We therefore designed a delayed two alternative forced choice task for head fixed mice to study the laminar and temporal distribution of task selective activity in the ACx. We confirmed the involvement of ACx in the default task execution using bilateral pharmacological silencing. Notably, we did not observe a strong reduction in stimulus discriminability, but a significant drop in task engagement, specific to inactivation of ACx. Our analysis confirmed the presence of partially overlapping populations of stimulus as well as action selective neurons. Stimulus selective signals were transient and present across layers, but with a peak in mid-superficial layers. Action selective units, however, were mostly located in the deep output layers of ACx. Importantly, selectivity to the action was not present during sound presentation, but gradually increased throughout the delay period of the task. Therefore, activity in ACx has a distinct temporal and laminar profile that reflects the transformation of sensory information to the behavioural response.

2.2 Methods

2.2.1 Animals

All proceedings were in accordance with standard operating procedures approved by the Champalimaud foundation's animal welfare body under the project #2018/007 'Principles of Sensory- and Memory-guided Auditory Decision Making: Behavior and Neural Basis'. Surgical procedures and training structure were based on protocols established by Guo et al. [85]. All surgeries used standard antiseptic methods. All experiments were performed using male C57BL/6J mice that were housed on a 12h inverted light/dark cycle.

2.2.2 Head bar surgery

During induction of anaesthesia, animals (6-8 weeks of age, 20-22g body weight) were anesthetized with 2-3% (volume in O_2) isoflurane (Vetflurane, Virbac) and subsequently mounted in a stereotactic apparatus (RWD Life Science) on a heating pad (Beurer). Once animals were stably mounted, isoflurane levels were lowered to 1-1.5% and the eyes were covered with ointment (Bepanthen, Bayer Vital). The head was shaved and the scalp cleaned with betadine. A midline incision was performed to expose lambda and bregma, which were subsequently used to align the skull with the horizontal plane of the stereotactic frame by measuring their position with a thin glass capillary (Drummond Scientific). The skull anterior of bregma was exposed by cutting a small area of skin. The exposed area was cleaned with betadine and slightly roughened by scraping it with a surgical blade (Swann-Morton). This procedure improved the attachment of the glue forming the base of the implanted head bar. Subsequently, the skull was dried with sterile cotton swabs and covered with a thin layer of super glue (UHU). To further increase long-term stability, four 0.9mm stainless steel base screws (Antrin Miniature Specialties) were placed in the skull. The exposed skull and base screws were then covered with dental cement (Tap2000, Kerr). A custom designed head bar (22x4x1mm, aluminium, GravoPlot) was lowered into the dental cement while still viscous until the head bar was in contact with the base screws. Subsequently, an extra drop of dental cement was applied to the centre of the head bar in order to fully engulf its medial part. The remaining skin

incision along the midline was then sutured. The animals were injected with buprenorphine (opioid analgesic, 0.05 mg/kg) into the intraperitoneal cavity and allowed to recover for 3-5 days.

2.2.3 Training procedure

After recovery from head bar implantation the animals were water deprived for 12h prior to the first handling session. In handling sessions mice were accustomed to the experimenter and being placed in an aluminium tube to restrain their movement. In the first days of handling, the tube was placed in the animal's home cage. Once the mouse voluntarily entered the tube, it was presented with water delivered manually from a syringe at the end of the tube. This procedure therefore roughly mimicked the water delivery system in the training apparatus. Mice were allowed to drink a max of 1.5ml of water during each handling session (30min). If animals failed to consume sufficient water they were supplemented to a total of 1ml. The aluminium tube remained in the animal's home cage during the entire week of handling to promote adaptation to it. Animals usually learned to enter the tube and drink in their home cage within three sessions. Subsequently, the tube was presented in the experimenter's hand and, once the animal entered the tube, it was lifted out of the home cage before allowing the mouse to drink. Most animals drank at least 1ml in the restraining tube outside of their home cage within two handling sessions. Once mice were accustomed to receiving water in the aluminium tube and being handled by the experimenter, they were placed in the behavioural setup and head fixed with the two water delivery spouts approximately 1cm in front of their mouth. To adapt them to head fixation, free water was delivered upon licking at either of the water delivery spouts. Lick detection was based on junction potential measures between the aluminium restraining tube and the stainless steel lick spout [94]. After triggering and consuming 15 rewards (single reward size: 3μl), training proceeded as summarised in table 2.1.
In the first stage of training, every 3.1s a random high (distribution: 22-40kHz, presented sound randomly selected each trial, category threshold at 14kHz) or low (distribution: 5-8.5kHz) frequency sound was presented to both ears at 60dB for 600ms, indicating at which of the spouts water was available (mapping is counterbalanced within each training cohort). 150ms after sound onset, a green LED flash of 50ms indicated the onset of the

1.5s response period. If the first lick in the response period occurred the correct water spout, a 3μl water reward was delivered. In order to facilitate the animals' engagement, a free water drop was delivered 150ms after sound onset in a random 10% subset of trials. Once mice were readily trying to trigger water rewards by licking at either lick spout after sound presentation (18 in 20 consecutive trials without free water delivery), the sound duration was reduced to 150ms, followed by a 1s response period. The Intertrial Interval (ITI) was drawn from an exponential decay-distribution (mean: 2.5s, truncated at 8s). After mice were engaged in the new timing of the task, free water delivery ceased and incorrect responses were punished by an additional 6s time delay in between sound presentations. As soon as the animals had learned to correctly respond by licking at the appropriate water delivery spout in at least 34 of 40 consecutive trials, the response delay was introduced, by gradually delaying the appearance of the go signal. Impatient licks triggered the abort of the trial and were signalled with white light flashes. The delay period was increased in 10ms increments as long as the animal performed at an accuracy of at least 80% for maximal five increments per session. In the following weeks of training the difficulty of the

Stage	Dur	Stimuli (Low & High)	Priming	Error	Delay
1	600ms	5-8.5kHz & 22-40kHz	10%	none	none
2	150ms	5-8.5kHz & 22-40kHz	10%	none	none
3	150ms	5-8.5kHz & 22-40kHz	none	ITI+6s	none
4	150ms	5-8.5kHz & 22-40kHz	none	ITI+6s	500ms
5	150ms	9.9-13kHz & 15-20kHz	none	ITI+6s	500ms
6	150ms	9.9; 12kHz & 16.3; 20kHz	none	ITI+6s	500ms

Table 2.1: ***Summary of main training stages.*** *Shown are the final parameters at each stage of the training for sound duration, high & low frequencies presented, fraction of primed trials with automatic reward delivery prior to response licks, time punishment after error trials and the duration of the response period.*

presented frequencies was gradually increased by approximating the range of possible low and high frequencies. These increases were performed in 19 increments, depending on a low bias and and high performance (bias $\leq$ 20%; performance $\geq$ 80%, only one change per training session), until a final frequency distribution of low (9.9-13kHz) and high (15-20kHz) frequencies was

reached. Excessive bias or disengagement at any time during the training were corrected by delivering free water at the unpreferred spout right after stimulus presentation until the animal readily responded again. All such intervention trials were excluded from analysis. Session duration depended on the animals' engagement and sessions were terminated after approximately 10 consecutive trial rejections. In case animals failed to drink at least 1ml of water during the behavioural session, animals were supplemented to this amount in their home cages.
After reaching the final frequency distributions, mice were presented with two fixed frequencies per condition (Low: 9.9 and 12kHz; High: 16.3 and 20kHz), with the easy being less likely to be presented (15% of trials). This focus on difficult frequencies enabled us to collect more trials with erroneous outcomes, making it possible to dissociate frequency from response related signals, while the easy frequencies mainly serve to keep the animals' engagement. Psychometric curve fits for behavioural analysis were calculated using the psignifit toolbox [235]. All remaining analysis, if not explicitly stated otherwise, is limited on trials where either a 12 or a 16.3kHz stimulus was presented and the mouse licked at either of the spouts during the response period without any prior lick since sound onset.

2.2.4 Muscimol silencing

The day prior to the first injection, mice were deeply anesthetized with 2-3% (volume in O_2) isoflurane, mounted in a stereotactic apparatus and kept on a thermal blanket. The eyes were covered with ointment. Isoflurane levels were subsequently lowered to 1-1.5%. The animals head was placed in a stereotactic frame using a custom made holder for the head bar. The skin covering the areas above the injection sites and the midline was removed and the exposed skull was cleaned from periostium with a surgical scalpel blade and cleaned with betadine and dried with sterile cotton swabs. Subsequently two craniotomies were performed above the desired needle entry points (2.8mm posterior, 2.2mm medio-lateral to bregma under a 23°medio-lateral angle; drill bit: Meisinger HM1 006). The exposed dura mater and skull were subsequently covered with silicone elastomere (World Precision Instruments) and the animal was injected with buprenorphine (opioid analgesic, 0.05 mg/kg) into the intraperitoneal cavity and allowed to recover over night.

On the days of behavioural manipulation the animals were slightly anaesthetised with 0.5-1.5% isoflurane, placed in the steretactic frame using the implanted head bar and the silicone elastomer was removed. Next, 70nl of either muscimol solution (M1523-5MG Sigma, 1mg/ml in Phosphate Buffered Saline (PBS); 15μl per minute) or just saline were injected (Nanoject2, Drummond scientific) using a thin glass capilary (Drummond scientific, 100µm outer diameter) at the desired depth (ACx: 2.6mm from brain surface VCx: 0.5mm from brain surface under a 23°medio-lateral angle). Subsequently, the craniotomies and skull were covered with silicone elastomere again and the animal was transferred in its home cage to wake up. Behavioural testing started 30min after terminating isuflorane anaesthesia. To allow for an unbiased measurement of trial rejection rates, animals were presented with 350 trials in each behavioural session. Animals that did not receive at least 1ml of water during the behavioural session were later supplemented with free water.
The significance of behavioural alterations due to muscimol injection of each animal was assessed in difficult trials, using a shuffle test procedure. In each of the 50000 shuffle iterations, trials were randomly assigned to either a surrogate auditory silencing or one of two surrogate PBS control sessions while maintaining their original trial numbers. Next, trial rejection rates and the discriminability in valid trials were calculated for each surrogate session. Similarly, trials from the second PBS control session and the visual cortex silencing session were randomly assigned to either group and behavioural measures calculated. The p values were calculated by computing the differences between muscimol injected and PBS groups for trial rejection and discriminability and determining the fraction of surrogates with effect sizes equal or bigger than the observed ones. Finally, to asses the significance of the obtained p values, the significance level α was adjusted for 12 comparisons using Bonferroni correction. To test if the rejection rates during the second ACx silencing are significantly higher than during both visual cortex silencing sessions, the procedure was repeated assigning trials randomly within those three sessions.

2.2.5 Neural recordings

Six to 12 hours prior to the first probe insertion in each hemisphere, mice were deeply anesthetized with 2-3% (volume in O_2) isoflurane, mounted in a

stereotactic apparatus and kept on a thermal blanket. The eyes were covered with ointment. Isoflurane levels were subsequently lowered to 1-1.5%. The animals head was placed in a stereotactic frame using the head bar. The skin covering the areas above the recording sites and the midline was removed and the exposed skull was cleaned from periostium with a surgical scalpel blade and cleaned with betadine and dried with sterile cotton swabs. Subsequently a small craniotomy was performed above the desired recording site (2.8mm posterior, 2.2mm medio-lateral to bregma under a 23°medio-lateral angle). The exposed dura mater was opened using a small needle (BD Microlance^{TM} 0.3 x 13mm) and subsequently the recording silicone probe (BuzA64sp, Neuronexus) was slowly lowered to the desired depth (2.6mm from brain surface, 23°medio-lateral angle). Probes were inserted with the shanks in a medio-lateral orientation, so that the six shanks in the final position approximately span the cortical layers (Figure 2.5a). Neural activity was digitised with an 64 channel headstage (Intan) at 16bit and stored for offline processing using an open ephys acquisition board (open ephys) at a 30kHz sampling rate. Behavioural sessions and storage of recording neural signals were only started 10-20min after probe insertion to allow for tissue relaxation and stabilisation of the recording. Recording sessions were limited to three recordings per hemisphere in each animal due to the tissue damage caused by probe insertion. In the final recording session in each hemisphere the probe was coated with DiI (Vybrant^{TM} DiI, Invitrogen) to confirm correct placement of the recording probe histologically.

2.2.6 Data processing

Because the task engagement in the recording session varied strongly, not all recording files could be used for further analysis. Out of the obtained 36 recording files (three recordings per hemisphere in six animals), only recordings with a minimum of 100 valid trials in total and ten valid trials per combination of stimulus and response were considered for further analysis. Valid trials were defined as above (trials in which the animal responded to either a 12 or 16.3kHz tone in the response period without prior premature licking, no matter if the response was correct or incorrect). Furthermore, the animal's behaviour in valid trials was required to exhibit a minimal d-prime of 0.6 to be included in analysis. The correct placement of all shanks was confirmed analysing the location of the fluorescent traces of the probe's shanks in each

hemisphere and misplaced shanks were excluded for all three recordings in that hemisphere. In the remaining 16 recordings, spike events were detected using Kilosort2 [193] (github.com/MouseLand/Kilosort2) and subsequently manual clustering was performed using phy2 (github.com/cortex-lab/phy). The contamination level of each unit was calculated by dividing the number of spikes in the refractory period by the count expected under a non-stationary Poisson distribution. This was calculated as the average across the corresponding spike-counts during the refractory period in 100 surrogate data sets where each spike time was displaced randomly by a time interval from -20 to 20ms. All multi-units with contamination levels above 0.3 were excluded from further analysis. The remaining units' responsivity to the task was determined by comparing the mean baseline spike counts in the 150ms prior to the sound presentation in each unit with spike counts during sound presentation (0-150ms) and the 150ms prior to the response period for all four combinations of stimulus and action in the task separately. Significance was assessed by randomly assigning trials to baseline or task condition and comparing the distribution of mean firing rate changes across 1000 such assignments with the observed actual firing rate differences. All units that did not exhibit a significant spike count change in either of the tested conditions were excluded from further analysis (175 of 422 units, Figure 2.5b). All further analysis was performed on the activity of the remaining units during valid trials.

2.2.7 Shank alignment across recordings

To allow comparisons across recordings, each shank's position was assigned relative to the shank with maximum frequency information per unit in the early sound response. Mutual information between a unit's activity and the presented frequency was calculated using an iterative process [36]. For this, the empirical joint distribution matrix $\hat{p}(S, R)$ of presented stimuli (S) and spike counts (C) in the first 50ms of sound presentation was formed to calculate mutual information:

$$I\left[\hat{p}(S,C)\right] = \sum_{s,c} \hat{p}(s,c) log\left(\frac{\hat{p}(s,c)}{\hat{p}(s)\hat{p}(c)}\right) \tag{2.1}$$

with the empirical marginal distributions over the stimuli and spike counts $\hat{p}(s) = \sum_c \hat{p}(s,c)$ and $\hat{p}(c) = \sum_s \hat{p}(s,c)$. To reduce the overestimation bias

of mutual information, a correction factor:

$$\frac{\#bins}{2Nlog(2)} \tag{2.2}$$

was subtracted from the empirical estimate, with $\#bins$ being the degrees of freedom of the empirical joint distribution matrix and N the number of trials [36, 174, 264, 195]. In an iterative process, columns of the $\hat{p}(S, R)$ were united, by merging the spike count column with the lowest marginal probability with its neighbour with lower marginal probability [36]. The bias-corrected mutual information was then calculated for the reduced matrix and the steps repeated until the matrix had been reduced to size (2,2). The best information estimate was defined as the maximum information across all reduced matrices. Mutual information was calculated separately in low and high report trials and the average taken as the final information estimate for each unit. Units recorded in shanks medial to the shank with highest mean information per unit were categorised as deep units, remaining units as mid-superficial.

2.2.8 Single cell analysis

To calculate the PSTH of neural activity across time, the activity of each unit was smoothed with a normalised Gaussian kernel with $\sigma = 25$ms (Figure 2.7a & 2.12). When assessing the units' selectivity two smoothing windows were utilised to account for the different time constants of variation during sound presentation and the rest of the trial. Hence, spikes during sound presentation (5-150ms after sound onset) were convolved with a $\sigma = 20$ms gaussian kernel and spikes outside that window with a kernel of $\sigma = 70$ms (see Figure 2.8b for example). Importantly, smoothed neural activity was used for visualisation purposes only, while statistical analysis of observed phenomena was performed using the exact spike counts in specific time windows.

To disentangle stimulus and action related tuning from each other, selectivity of a units activity r between the two presented stimuli s was calculated as the average across the selectivity values conditional on the animals' actions:

$$D'^2_{Stim} = \frac{1}{2}\sum_{act=1}^{2}\left(\frac{(\overline{C1} - \overline{C2})}{\sqrt{0.5(\sigma^2_{C1} + \sigma^2_{C2})}}\right)^2 \tag{2.3}$$

with $C1 := r|s = 1, act$ and $C2 := r|s = 2, act$. Action selectivity was accordingly calculated by taking the average across stimulus-conditional action selectivity values. Signed d prime values were obtained by omitting the squaring step.
To assess if the selectivity to stimulus or action observed in each unit was significantly above chance, stimulus and action selectivity were both calculated during the stimulus presentation (0-150ms) and prior to the response period (450-700ms after sound onset) using the spike counts in these windows (Figure 2.7b right). P values assessing if the obtained average selectivity values were above chance were calculated using a two step shuffling procedure. First, the distribution expected by chance was calculated by creating 1000 surrogate data sets where the trial labels within one condition were randomised for each unit individually. Stimulus and action tuning were then calculated from their respective surrogate data sets for each unit and the average selectivity was calculated for each unit. After determining the chance distribution of selectivity in the population, we tested if the distribution observed in our data had a mean significantly bigger than chance. We therefore calculated the difference of the means of the distributions and tested its significance in a paired shuffle test procedure. We created 10000 surrogate data sets in which chance and observed selectivity were randomly assigned for each unit. Next, the average of the surrogate-observed and surrogate-chance distributions were formed and their difference calculated. Finally p values are given by the fraction of surrogate differences with values more distant or equally distant from zero as the observed value. To assess if the obtained p values were significant, we corrected the significance level α for eight observations (action and stimulus selectivity at two time points in two populations of units) using Bonferroni correction. A separate shuffling procedure was used to determine the number of significantly selective units at each of the two time intervals. In each iteration of this shuffle test, a surrogate data set was created for each unit where the trial identities within one condition were randomised as in the procedure described above. Stimulus and action tuning were then calculated from their respective surrogate data sets. This process was repeated for 1000 shuffle iterations for each measure and then p values were obtained by forming the fraction of surrogate selectivity values with equal or higher selectivity than the observations in the original data set. The significance of the obtained p values was assessed by correcting α for multiple comparisons using Bonferroni correction.

2.2.9 Selectivity in correct and incorrect trials

Given the low number of incorrect trials compared to correct ones, a hierarchical shuffle test procedure was used to allow for their comparison [226]. In each iteration of the bootstrap, ten recordings were drawn randomly (with replacement). In a next step neurons in each of those ten recording were sampled. In each recording the same number of units was drawn with replacement as originally contained in the recording. As a final step, for each of the n obtained units, trials were sub-selected independently. For each of the four combinations of stimulus and action, the number of trials in the real data set were determined and then the smallest of these four observed trial numbers was drawn randomly with replacement from each of the two correct and the two incorrect categories. The D'^2 (spike counts smoothed with a 70ms Gaussian kernel during ITI and delay, with a 20ms kernel during sound presentation) was then calculated for correct and incorrect trials in the surrogate data set and the mean selectivity across the population in correct and incorrect trials was calculated at each time point. This procedure was then repeated for 1000 bootstrap iterations separately for units from mid-superficial and deep units. To assess if the selectivity to correct or incorrect trials observed in each unit was significantly different, this selectivity was calculated in a separate bootstrapping procedure using exact spike counts during the ITI (-500 - 0ms), sound presentation (0-150ms) and prior to the response period (450-700ms after sound onset) in 10000 bootstrap iterations. To determine the p value, the average difference in task discriminability of correct and incorrect trials was determined in each bootstrap iteration. The resulting distribution of these differences was then used to calculate the p value by determining the biggest confidence interval still excluding 0.

2.2.10 Coding directions

The Coding Direction (CD) vectors were calculated for spike counts during sound presentation (0-150ms) and prior to the onset of the response window (450-700ms after sound onset) for correct and incorrect trials separately. The procedure was based on a method introduces by Economo et al. [60]. The CD is the vector specifying the linear combination of neural activity that best distinguishes between high and low frequency trials. Each element

of the vector was calculated by assessing the task selectivity of each unit n:

$$v(n) = \frac{\overline{C_{Low}} - \overline{C_{High}}}{\sqrt{0.5\left(\sigma^2_{Low} + \sigma^2_{High}\right)}} \tag{2.4}$$

with C_{Low} and σ^2_{Low} denoting the mean and variance of activity in low frequency trials. The obtained vector was then normalised with its L2 norm to obtain the unit vector in the CD:

$$CD = \frac{v}{\sqrt{v \cdot v}} \tag{2.5}$$

To address the reliability of this CD measure during the sound presentation and prior to the response period, a hierarchical bootstrapping method similar to the procedure described above was used. In each iteration of the bootstrap, ten recordings were selected with replacement. Subsequently, the neural population of each selected recording was resampled, by drawing (with replacement) as many units as originally contained in that recording. To avoid overlapping data in the the CDs when determining the stability of correct and incorrect coding directions within a session, trials were not resampled. Instead, in each unit the session was randomised and subsequently each of the four possible task categories was split in two parts. CDs were then calculated for the first and second half of the session and their correlation determined by forming their scalar product.
To test if CDs aligned more than expected by chance, random CDs were calculated by assigning the trial types randomly within each selected unit and calculating the resulting CDs. Subsequently, the scalar product of the random directions with the actual cording directions was formed. The full procedure was then repeated for 10000 bootstrap iterations in mid-superficial and deep populations separately. To determine if the observed alignments were bigger than expected by chance, the difference between the two calculated scalar products, one product of two CDs, the other the product of a CD and a random direction, was formed. The resulting distribution of their difference was used to calculate the p value by determining the biggest confidence interval still excluding 0.
When calculating the correlation of CDs in correct trials across time, the data was resampled in a hierarchical shuffle test procedure with additional trial subsampling. Thus, for each selected unit, correct low and high trials

were resampled with replacement to the original number of trials in that category. Spike counts for each selected unit and trial were formed in 100ms bins every 10ms starting 200ms prior to sound presentation until the LED go signal (650ms) resulting in 86 CDs across time in the trial. This procedure was repeated for 1000 iterations of the bootstrap procedure and time points with CDs more aligned than expected by chance were determined as described above. To visualise the the effect size of coding directions with significant correlation compared to expectations by chance, the difference of the mean scalar products of coding directions and the mean scalar products of random directions was formed and analysed at positions were 97.5% of its distribution was bigger than zero.

2.3 Results

2.3.1 Task behaviour

We trained head fixed mice in a delayed response frequency discrimination 2AFC task (Figure 2.1). After a random ITI, mice were presented with either a high or low frequency sound, indicating at which of two water delivery spouts water would be available after a brief delay period. Animals were required to withhold licking during sound presentation and the 500ms delay period until a green LED signalled the onset of the response period. In the response period, licking at the correct spout, indicated by the presented stimulus, triggered a water reward, incorrect responses a time-punishment. Mice learned to correctly time their licks in response to a presented sound

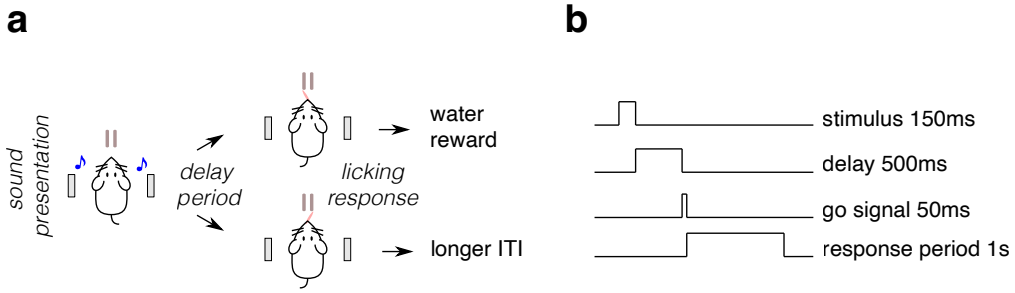

Figure 2.1: ***Task outline.*** ***a:*** *Scheme of delayed response task contingency. Each trial, head fixed mice are presented with high or low frequency sounds from 2 lateral speakers (grey bars). Animals report 'high' or 'low' by licking at one of 2 lateral water delivery spouts (brown lines) during the response period.* ***b:*** *Scheme of timing contingencies in a trial.*

(Figure 2.2a) and showed a good performance in the task. However, animals did not respond during the response period in all trials. We therefore distinguished between completed trials, premature response trials and rejected trials. In completed trials animals responded during the response window at either spout, without any prior licks during either the delay or the sound presentation. These trials were the most common type and can either be correct or incorrect, depending on the stimulus and the location of the response lick. In premature response trials animals did lick prior to the onset of the response period. This premature licking caused the trial to be aborted, signalled by brief light flashes, and the ITI period would start without a prior

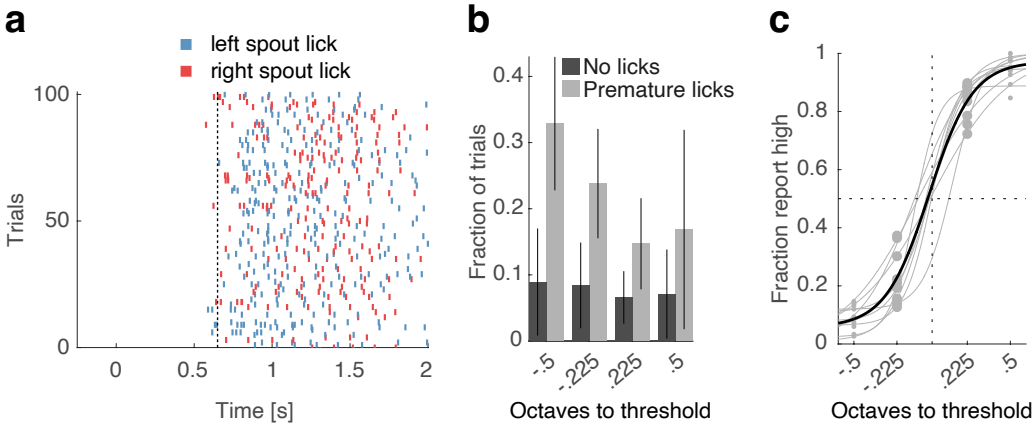

Figure 2.2: ***Task behaviour.*** ***a:*** *Exemplary raster plot of licking behaviour during part of a behavioural session. Dashed line demarcates time of go signal.* ***b:*** *Fraction of invalid (no response or premature response) trials during steady state performance (mean ± SEM, 5 sessions per animal, n=10), sorted by stimulus.* ***c:*** *Psychometric curves of valid trials during steady state. Single animals are shown in grey, black line represents cohort average. Marker size corresponds to the stimulus prevalence.*

response period. To avoid a possibile timing advantage by skipping trials by premature licking, the duration of ITI was increased by the duration of the response period and the fraction of the delay period that the animal had failed to wait. Trials in which animals failed to execute any lick until the end of the response period were termed rejected trials. The probability of trial rejection was not dependent on the presented frequency (Figure 2.2b) and most common towards the end of the end of the behavioural sessions, which was terminated after approximately ten consecutive trial rejections. Premature responses occurred more often in response to low than high frequency sounds (Figure 2.2b). The accuracy of the animals' responses in trials with correctly timed responses was strongly depending on the difficulty, but not the frequency of the presented stimuli. Thus, frequencies half an octave from the category threshold (14kHz) were associated with better performances than frequencies only placed 0.225 octaves from that threshold (Figure 2.2c). Most animals, however, also displayed a slight bias towards low frequency responses, independent of the spout associated with low frequencies. This slight bias however was not reflected on the popula-

tion average. Behavioural sessions typically lasted for approximately 1h, in which animals performed in 200-250 difficult trials.

2.3.2 Involvement of ACx in task execution

To determine the involvement of ACx in this behaviour, we performed bilateral pharmacological silencing experiments and compared the resulting behaviour to injections of saline on the previous and following day. Silencing

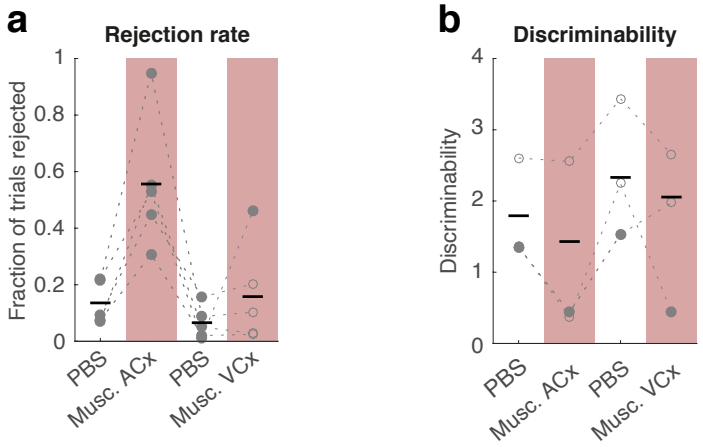

Figure 2.3: ***Silencing of ACx.*** ***a:*** *Trial rejection rate across different manipulations. Pink shades indicate bilateral injection of muscimol in the respective cortical areas, PBS refers to bilateral PBS injections into ACx. Filled dots represent significant muscimol effects compared to PBS injections. Black bars show values obtained in pooled trials per condition.* ***b:*** *Same as a, but showing d-prime in completed trials of each session.*

of ACx strongly altered the behaviour all all five mice. Hence trial rejection rates increased significantly compared to control conditions in all animals (Figure 2.3a; see Table 2.2 for statistical analysis of each animal) to the extent that it was not possible to calculate the d-prime measure for two of the animals (Figure 2.3b). Importantly, animals were presented with the same number of trials across all behavioural manipulations, therefore differences in trial rejection rates are not due to differences in session duration. While animals were rejecting trials much more frequently after silencing ACx, they were still able to detect and consume freely available water drops presented

during the sessions. Therefore, the increased rejection rate was not due to pure motor deficits or a loss of thirst.

Rejection rate (week 1)					
Animal	1	2	3	4	5
PBS_1 & $muscimol_{ACx}$	**<.001**	**<.001**	**<.001**	**<.001**	**<.001**
PBS_2 & $muscimol_{ACx}$	**<.001**	**<.001**	**<.001**	**<.001**	**<.001**
PBS_2 & $muscimol_{VCx}$	.57	.21	.16	**<.001**	.79
d-prime (week 1)					
PBS_1 & $muscimol_{ACx}$	NaN	**.003**	NaN	.01	.90
PBS_2 & $muscimol_{ACx}$	NaN	**<.001**	NaN	**<.001**	.02
PBS_2 & $muscimol_{VCx}$	.57	.12	.11	**<.001**	.04

Table 2.2: ***Single animal muscimol analysis in the first silencing experiment.*** *Listed are p values (Fisher's exact permutation test) for the indicated comparisons and animals. Significant p values are highlighted (bold). Bonferroni corrected $\alpha = 0.0042$ (12 comparisons). PBS_1 referes to the first saline injection in the week, PBS_2 to the second. NaN refers to sessions with too few completed trials to calculate d-prime.* ***Top:*** *Analysis of rejection rates (see methods).* ***Bottom:*** *Same but for discriminability in valid trials (see methods)*

Moreover, the observed effect was specific to the injection site as a silencing of visual cortex using the same craniotomy did not significantly alter trial rejection rates in most animals (Table 2.2). Discriminability, however, was only significantly reduced in one of the animals with sufficient trials performed to calculate this measure. Importantly though, the lack of sufficient trials in two of the animals and the low number of trials available in the remaining ones, does not allow to form a clear statement about a general influence of muscimol silencing on discriminability.
Given this limitation, the silencing procedure was repeated with the same cohort of animals to confirm the effects observed in the first experiment. Interestingly, in the repetition experiment the effect of silencing ACx on the rejection rate was strongly diminished, but still significantly bigger than in the control conditions in most animals (see Table 2.3, Figure 2.4a). Additionally, while two animals show a slight decrease in discriminability, this

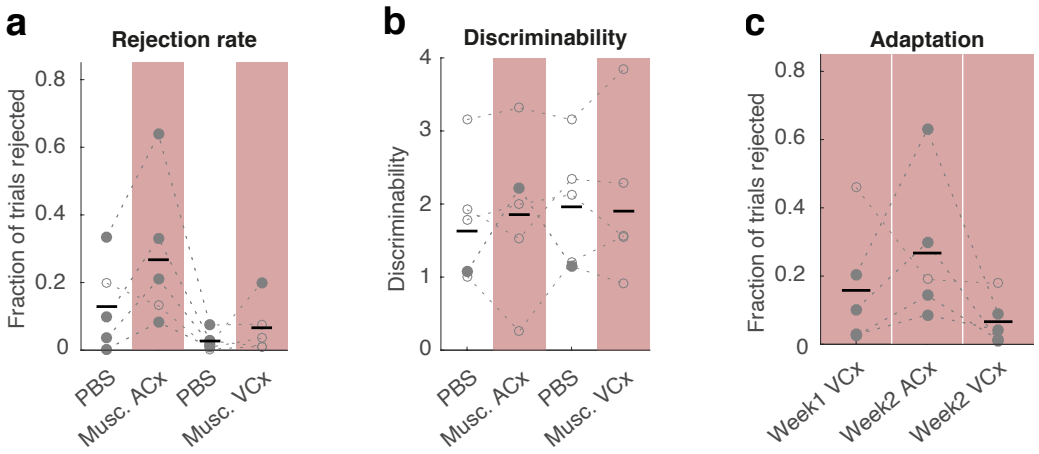

Figure 2.4: ***Repetition of silencing experiments.*** ***a:*** *Trial rejection rate across different manipulations. Pink shades indicate bilateral injection of muscimol in the respective cortical areas, PBS refers to bilateral PBS injections into ACx. Filled dots represent significant muscimol effects compared to PBS injections. Black bars show values obtained in pooled trials per condition.* ***b:*** *Same as a, but showing d-prime in completed trials of each session.* ***c:*** *Format as in a. Shown are effects of the second muscimol injections into ACx and the previous (week 1) and following (week 2) silencing experiments of VCx.*

impairment was not significant compared to both PBS conditions. Indeed, the only animal with a significant change in d-prime increased its discriminability upon silencing in of ACx (Table 2.3). The repetition experiment therefore does not provide evidence that silencing of ACx reduces discriminability in the task.

The differences across the two experiments in the amount of trial rejections suggest that the animals were adapting their behaviour to the procedure. It is possible that the observed trial rejection rate was partially due to the animals' reaction to the procedure. However, as rejections rates following musimol injections into ACx were significantly bigger than both, the following, as well as the preceding day of PBS control injections, a slow adaptation to the procedure can not fully explain the observed effects.

Similarly, rejection rates in both visual cortex silencing sessions are significantly smaller than in the second ACx silencing in most animals and only significantly bigger than expected by chance in the remaining one (Figure

Rejection rate (week 2)					
Animal	1	2	3	4	5
PBS_1 & $muscimol_{ACx}$	**<.001**	**<.001**	**<.001**	**<.001**	.02
PBS_2 & $muscimol_{ACx}$	**<.001**	**<.001**	**<.001**	**<.001**	**<.001**
PBS_2 & $muscimol_{VCx}$	.09	.02	.46	**<.001**	.21
d-prime (week 2)					
PBS_1 & $muscimol_{ACx}$	.01	**<.001**	.24	.52	.72
PBS_2 & $muscimol_{ACx}$	**.001**	**<.001**	.02	.68	.72
PBS_2 & $muscimol_{VCx}$	.33	.39	.84	.05	.13

Table 2.3: ***Single animal muscimol analysis in the second silencing experiment.*** *Format as in Tabble 2.2* ***Top:*** *Analysis of rejection rates (see methods).* ***Bottom:*** *Same but for dscriminability in valid trials.*

2.4c, see Table 2.4). Therefore, the increase in rejection rate is specific to pharmacological silencing of the auditory cortex.

Comparison	Animals				
	1	2	3	4	5
VCx_1 & ACx_2	**<.001**	**.01**	**<.001**	**<.001**	**<.001**
VCx_2 & ACx_2	**<.001**	**.02**	**<.001**	.90	**<.001**

Table 2.4: ***Single animal muscimol adaptation analysis.*** *Listed are p values (Fisher's exact permutation test) for the rejection rate comparisons of the indicated sessions and animals. Significant p values are highlighted (bold). Bonferroni corrected $\alpha = 0.025$ (two comparisons). VCx_1 refers to the first muscimol injection in visual cortex, ACx_2 and VCx_2 to the respective muscimol injections in the second week.*

2.3.3 Laminar single cell selectivity

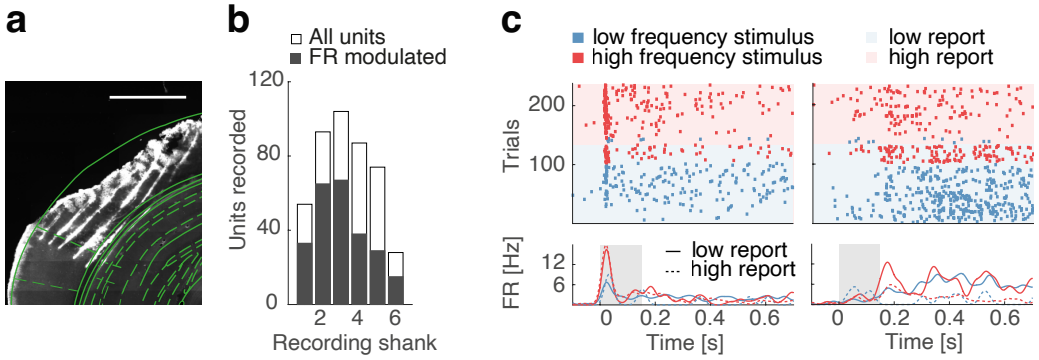

Figure 2.5: ***Recording neural activity in ACx.*** ***a:*** *Histology of acute recording sites. Brain areas are illustrated in green. Probe shanks are inserted mediolaterally to span the cortical layers. Scale bar: 1mm.* ***b:*** *Yield of units recorded in 10 recording sessions across probe shanks for all units (white) and units with significant firing rate changes during the task (dark grey).* ***c Left:*** *Raster plot and PSTH of one example stimulus-tuned cell during one recording session aligned on sound onset (t=0). Spikes are colour coded by the frequency presented in the trial. Background shades indicate the decision reported by the animal. Grey shade in PSTH marks sound presentation.* ***Right:*** *As left, but for one example action-tuned cell.*

Neural activity was recorded from both hemispheres in six animals using a six shank 64 channel silicon probe. Probe shanks were inserted in a mediolateral orientation so that the probe shanks roughly spanned all layers of cortex (Figure 2.5a). Out of the 36 acquired recording sessions 16 sessions were discarded as the mice had either failed to engage in more than 100 valid trials or because less than ten engaged trials were obtained in one of the four combinations of presented stimuli and following responses of the animal (see methods). Moreover, ten recordings were discarded due to unsuccessful targeting of primary auditory cortex, revealed either histologically or by the absence of short latency responses in the multi-unit activity following sound presentation. In the remaining ten recordings, 440 single and multi-units were identified. Of these, 18 multi-units were discarded due to contamination in the refractory period, and another 175 units were excluded from analysis due to a lack of task modulated activity (Table 2.5; see methods for details), resulting in a final population of 247 single and multi-units

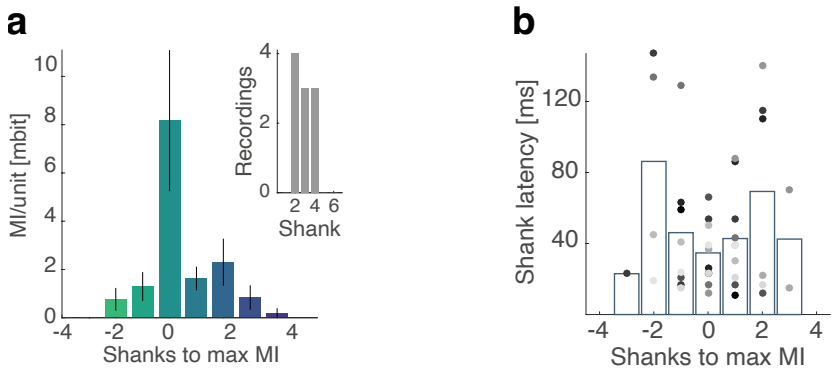

Figure 2.6: ***Alignment procedure.*** ***a:*** *Mean mutual information ± SEM of single unit activity during sound presentation and stimulus identity pooled across recordings. Recordings are aligned on the shank with highest initial sound information. (negative values indicate more superficial, positive numbers deeper shank locations)* ***Inlay:*** *Location of max MI shanks.* ***b:*** *Mean multi-unit peak response latency across aligned recordings. Greyscale of markers denotes single recordings.*

from five animals. Units were preferentially located on the second and third shank from the brain surface, however units from all six recording shanks were included in the analysis (Figure 2.5b). We observed two types of selectivity in the single cell firing rates. Most commonly, units showed tuned, fast latency responses to the presented stimuli. However, in a subset of the recorded units, a preference for the reported decision was observed during the delay period of the trial(Figure 2.5c). We refer to these two types of selective firing as stimulus and action selectivity.
To address the laminar organisation of such single cell activity and selectivity, recordings were aligned on the shanks with highest mean stimulus information per unit in the early sound responses (Figure 2.6a). Interestingly, this alignment showed a a clear peak in Mutual Information (MI) of neural firing rate and the presented stimulus in one of the recordings shanks. This alignment shank, here referred to as max MI shank, was always located in the middle shanks of the electrode and mean sound response latencies in the Multi Unit Activity (MUA) across max MI shanks of all recordings were shorter than latencies of the adjacent shanks (Figure 2.6b). While we did not observe a perfect match of the max MI shank and the fastest latency in the individual recordings, we proceeded on the assumption that the max MI shank is the shank with closest proximity to cortical input layer 4 and

Recording No	All units	Contamination $< .3$	Task responsive	Mid-superficial	Deep units
1	45	45	32	17	15
2	46	44	21	9	12
3	41	40	13	9	4
4	49	39	27	12	15
5	34	33	15	10	5
6	61	61	21	19	2
7	39	39	23	4	19
8	37	37	28	21	7
9	37	35	28	7	21
10	51	49	39	23	16

Table 2.5: ***Number of recorded units across recordings.*** *Number of units identified in each of the ten analysed recording sessions at each step of data processing and recording alignment*

aligned depth across recordings using this reference.
Subsequently, units were grouped into 131 mid-superficial and 116 deep units due to their location relative to the max MI shank (Table 2.5). Mid-superficial units were recorded at either the max MI or at a shank closer to the brain's surface, while deep units were recorded at recording sites medial to the max MI shank.
Activity in mid-superficial units transiently increased in response to both stimuli, but sound responses across units were typically stronger for the low frequency stimulus (Figure 2.7a). After a fast initial sound response, firing rates steadily decreased throughout the late sound presentation and delay period of the task. In contrast, activity in deep units showed both, a fast response to stimulus onset similar to the one observed in mid-superficial units, as well as a slower, less pronounced, increase of activity around the time of sound offset. However, no systematic preference to either of the stimuli was visible across units at any time of the trial, indicating either a lack of specificity in single cell sound responses or diverging stimulus selectivity across individual units. Neither activity in mid-superficial nor deep units showed a systematic firing rate preference associated to the animal's reported choice in the trial epochs prior to the response period.
To assess the magnitude of the selectivity across units at each time point,

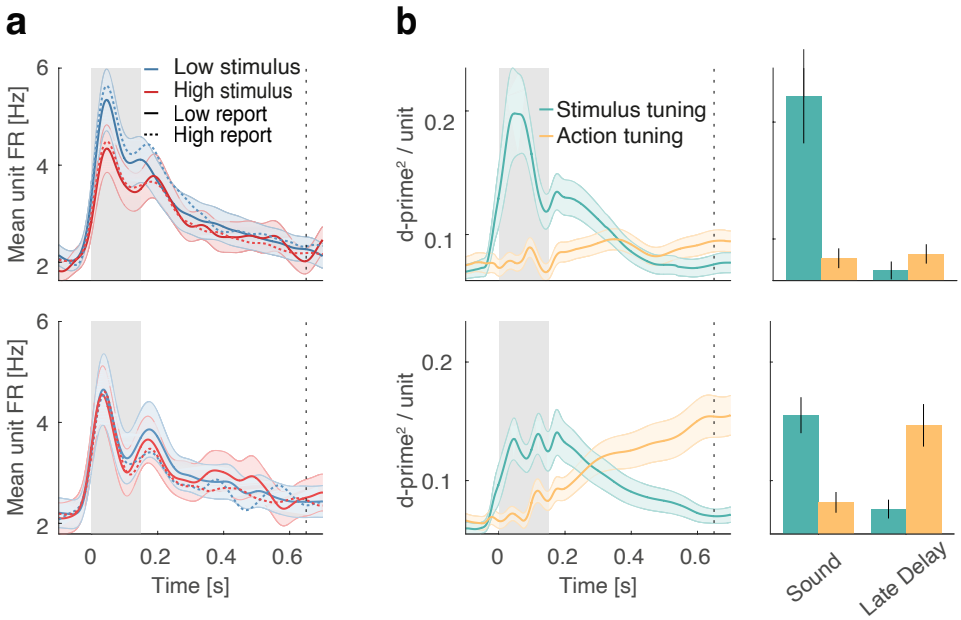

Figure 2.7: ***Laminar activity & selectivity in ACx. a Top:*** *Time course of mean activity ± SEM in mid-superficial units split by presented stimulus and the action performed by the animal. Time of sound presentation (grey shade) and go signal (dotted line) are indicated.* ***Bottom:*** *as top for units recorded in deep shanks.* ***b: Top: Left:*** *Time course of mean unit selectivity ± SEM for presented stimulus and upcoming action in mid-superficial units. Task timing marked as in a.* ***Right:*** *Quantification of average mid-superficial tuning during sound presentation and prior to response period.* ***Bottom:*** *As top for units recorded in deep shanks.*

we calculated the squared discriminability index d-prime across time. This squared measure prevented diverging individual preferences from cancelling out in the population average, thus allowing to correctly quantify the degree of unit selectivity in the population. Because animals perform well in the task (Figure 2.2c), trials of a given stimulus are typically associated to one response. This correlation due to performance of the animal makes it difficult to clearly dissociate stimulus from action-related selectivity as a strong selectivity to either would lead to differences in activity across frequency and action sorted trials. We overcame this issue by calculating stimulus selectivity conditionally on the two response actions and action selectivity conditionally

on the presented frequency. The final selectivity was obtained by averaging across both conditional selectivity measures. Thus, the contribution of stimulus and action selectivity to firing rate changes in a given unit could be unambiguously assigned. Qualitatively following the average firing rates, mean stimulus selectivity in mid-superficial units peaked early after stimulus onset and then rapidly decayed until it reached baseline levels towards the second half of the delay period. In addition, mean action selectivity slightly rose from baseline levels after stimulus offset, but remained low throughout the delay period (Figure 2.7b, top). In contrast, mean stimulus selectivity in deep units increased throughout sound presentation and after sound offset rapidly decreased throughout the delay period of the trials, so that by the end of the delay period stimulus selectivity was close to baseline levels across all layers of ACx. In contrast to mid-superficial units, deep units did exhibit clear action selectivity, forming towards the end of stimulus presentation and continuously rising throughout the delay period. This represents a drastic shift from predominant stimulus selectivity in mid-superficial as well as deep units during sound presentation to a predominant action selectivity in deep units at the end of the delay period with no clear selectivity to either stimulus nor action in mid-superficial units. We investigated the significance of this shift by quantification of the spike counts during these two trial periods (Figure 2.7c). Mean stimulus selectivity signals in both groups were significantly bigger than expected by chance during sound presentation (Mid-superficial: $\overline{d'^2}$=.22; Deep: $\overline{d'^2}$=.16, p <.001 in both, Bonferroni adjusted α = .0063; permutation test, see methods), but not during the late delay, prior to the response period (Mid-superficial: $\overline{d'^2}$=.07, p=.17; Deep: $\overline{d'^2}$=.08, p=.3). Mean action selectivity, on the other hand, was not significantly different from chance during sound presentation in either of the two groups (Mid-superficial: $\overline{d'^2}$=.08,p=.01; Deep: $\overline{d'^2}$=.08, p=.06; Bonferroni adjusted α = .0063). Prior to the response signal however, action selectivity did diverge significantly from chance levels (Mid-superficial: $\overline{d'^2}$=.09,p=.002; Deep: $\overline{d'^2}$=.15, p<.001). These results confirm a qualitative shift in single cell selectivity from exclusive stimulus to exclusive action selectivity. Moreover, even though early sound responses displayed more stimulus tuning in mid-superficial units by construction, mean stimulus selectivity during the full sound presentation did not show a significant laminar difference (difference=.07, p=.28; permutation test, see methods), while action selectivity during the delay period of the trial was significantly bigger in deep than

in mid-superficial units (difference=-.06, p=.002). While significant on the population average, both stimulus as well as response tuning were relatively sparse in the single units. Hence we found that 17% of mid-superficial and 11% of deep units were significantly stimulus selective during sound presentation (22 mid-superficial & 13 deep units, respectively). In the same way, 10% of deep units were significantly action selective prior to the response period, but only 6% of the units recorded at mid-superficial shanks (12 deep & eight mid-superficial units). These differences in selectivity revealed a laminar relation of stimulus information during early sound responses and action selectivity in ACx.

Importantly, alignment on shanks with fastest sound responses instead of highest stimulus MI was not able to reveal the spatial relationship of stimulus and action tuning (Figure 2.8a). Instead, latency aligned selectivity showed ramping action selectivity in both more superficial and deep groups. Moreover, both action selectivity as well as stimulus selectivity during the sound presentation appeared more pronounced in units that are medial to the shank with fastest onset responses.

Therefore, it is possible that selectivity is generally stronger in deep layers of ACx and our alignment on the shank with highest stimulus information concealed this fact. This scenario seems unlikely though, because the location of the max MI shank is relatively reliable across recordings. Indeed, the concentration of late action selectivity in deep units is also visible across unaligned recordings (Figure 2.8b). Therefore, the discrepancy between the latency-aligned tuning and the MI-aligned tuning can either be explained by an unreliable measure of response latency or large deviations in the position of the inserted shanks. Because the shank location was confirmed histologically, it is unlikely that there are drastic differences that might underlie this discrepancy. Moreover, the alignment of stimulus tuning also resulted in an alignment of both, response selectivity as well as the distribution of activity around sound offset across mid-superficial and deep units (Figure 2.7). Therefore it is unlikely that this structure is introduced by variability in electrode placement.

The separation of the recorded units in mid-superficial as well as deep units has therefore revealed a laminar organising principle in ACx. However, it becomes clear from the distribution of stimulus information in figure 2.6a, that the stimulus selectivity during early sound presentation shows considerable heterogeneity. We therefore sought to investigate the heterogeneity of

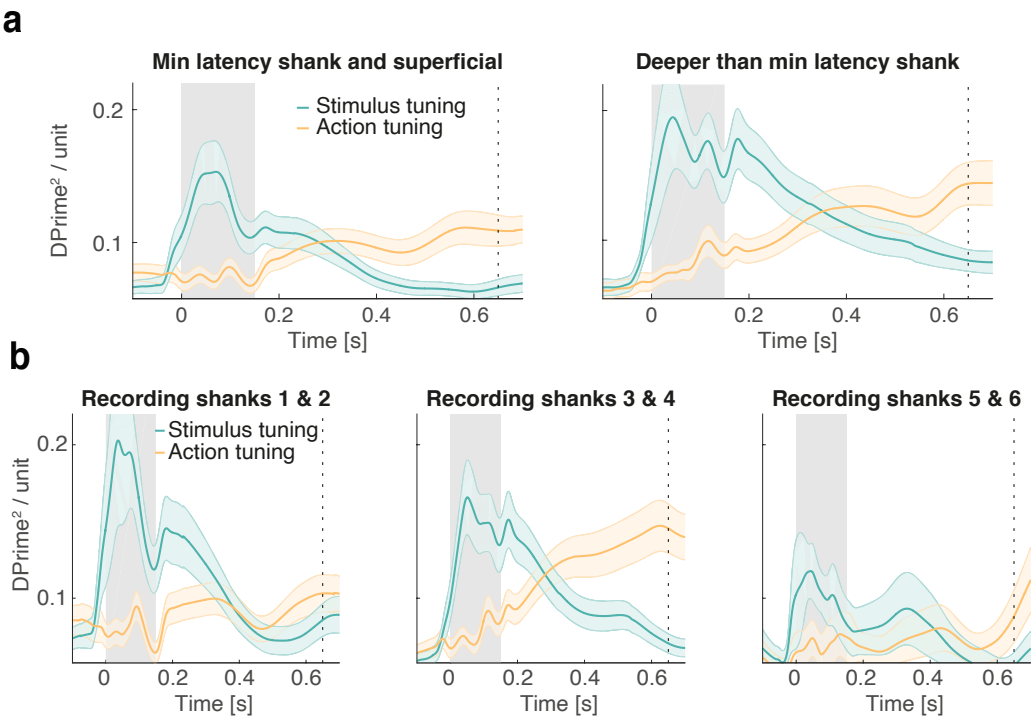

Figure 2.8: ***Alternative alignments.*** ***a:*** *Tuning in latency-aligned recordings.* ***Left:*** *Time course of mean unit selectivity ± SEM for presented stimulus and upcoming action in units recorded at the shank with fastest peak-latency and all more superficial shanks. Time of sound presentation (grey shade) and go signal (dotted line) are indicated.* ***Right:*** *As left but for units recorded in shanks medial to the shank with fastest peak sound response.* ***b:*** *Time course of mean unit selectivity ± SEM for stimulus and upcoming action without alignment. Tuning is shown for pooled units recorded at the two most superficial (left), the two medial (middle) and the two deepest shanks (right). Task timing is denoted as in a.*

stimulus and action selectivity within the two neural populations. To that end, we split mid-superficial units into units recorded at the max MI shank and units recorded more superficially and deep units into units recorded at the shank adjacent to the max MI shank and units recorded at any deeper shank (Figure 2.9).

Analysing heterogeneity within mid-superficial and deep units showed little differences in both action and stimulus tuning across time in deep units. In mid-superficial units, stimulus selectivity during sound presentation was

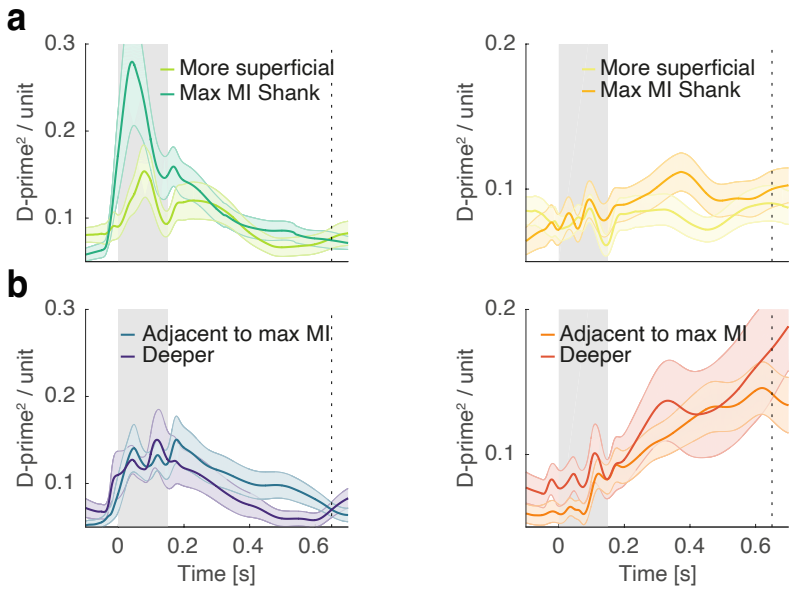

Figure 2.9: ***Heterogeneity in mid-superficial and deep units. a Left:*** *Time course of mean unit selectivity ± SEM for presented stimulus in mid-superficial units, sub-divided by recording location. Time of sound presentation (grey shade) and go signal (dotted line) are indicated.* ***Right:*** *Same but for action selectivity in mid-superficial units.* ***b:*** *Same as a but for sub-divided deep units.*

strongly concentrated in the max MI shank, but no differences in late action selectivity were discovered. Therefore the distinction between mid-superficial and deep units is relatively accurate for action selectivity. While this binary separation cannot capture the heterogeneity in stimulus selectivity in mid-superficial units, these differences are essentially limited to the early sound presentation and therefore reflecting the applied alignment procedure.

Next, we sought to test if the underlying reason for the increase of action tuning during the delay period was a continuous increase of selectivity in the same sparse number of action selective units or if additional action selective units were recruited over time. We therefore calculated the fraction of selective units across time for both stimulus and action in both groups. Importantly, selective units in this analysis were defined as units with p values smaller or equal to 5% without correcting for multiple comparisons. This fraction is qualitatively similar to the mean selectivity time course for

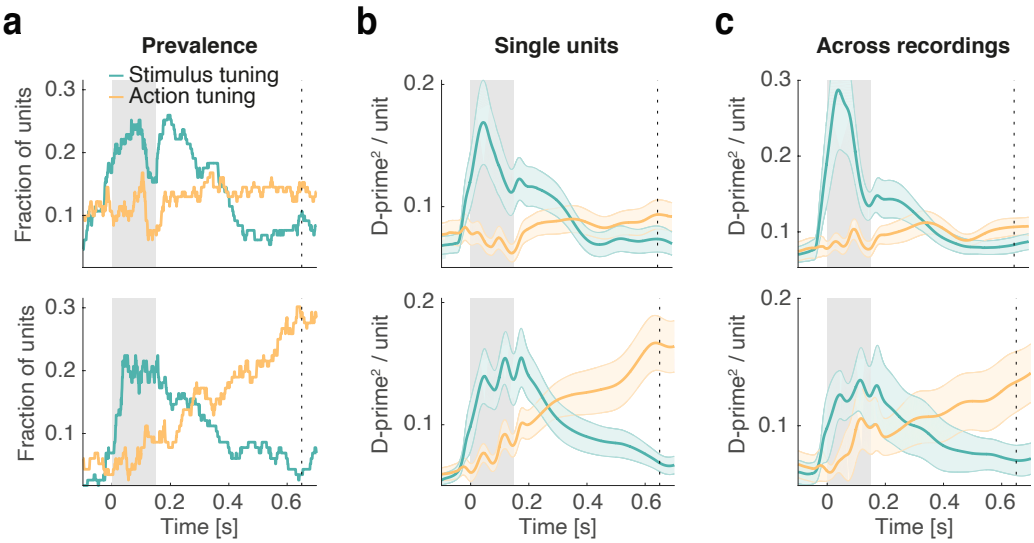

Figure 2.10: ***Laminar selectivity controls. a Top:*** *Fraction of mid-superficial units whose tuning has uncorrected p values* $\leq$ *0.05. Time of sound presentation (grey shade) and go signal (dotted line) are indicated.* ***b: Top:*** *Time course of mean single unit selectivity* $\pm$ *SEM for presented stimulus and upcoming action in mid-superficial units. Task timing marked as in a.* ***c:*** *As b for the average unit-selectivity across recordings.* ***Bottom:*** *As top, but for deep units.*

both stimulus and action selectivity in mid-superficial and deep units (Figure 2.10a). We therefore conclude that the temporal selectivity profiles likely reflect recruitment of larger fractions of units within the population rather than a sole enhancement of selectivity in a constant subset of units.
Moreover, the laminar and temporal separation of action and stimulus selectivity was also apparent when restricting the analysis to single units with less than 10% contamination during the refractory period (Figure 2.10b). Therefore, laminar selectivity differences are unlikely due to distinct levels of contamination shadowing the selectivity of single cells. Additionally, mean unit d-prime^2 across recordings also reliably reproduced the described laminar phenotype. It is therefore unlikely that the observed organisation of action and stimulus selectivity are artifacts of differences in cell number across recordings.

2.3.4 Alternative explanations for action selectivity

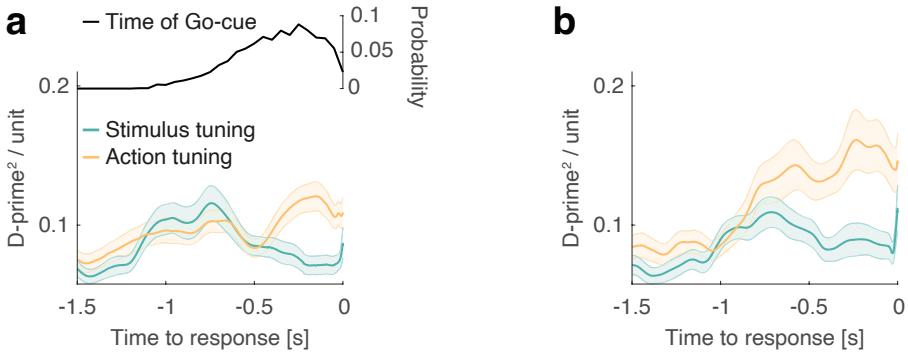

Figure 2.11: ***Response aligned selectivity.*** ***a:*** *Time course of mean unit selectivity ± SEM for presented stimulus and upcoming action in mid-superficial units, aligned on time of the response lick (t=0).* ***Top:*** *Distribution of Go signal.* ***b:*** *As a, but for deep units.*

A possible scenario trivially explaining the observed action selectivity would arise if firing rates in deep units were increasing prior to both response types equally. Systematic differences in response times at the two spouts would then be interpreted as a temporarily ramping action selectivity when aligning neural activity on stimulus onset. To exclude such a misinterpretation, we repeated our analysis by aligning each valid trial on the time of the response lick. Response aligned neural activity in deep units still showed clear action selectivity, therefore excluding the possibility of an unspecific action modulation prior to licking (Figure 2.11). In contrast to stimulus alignment though, aligning neural activity on the time of the response clearly revealed the action selectivity in mid-superficial layers prior to response licks. Notably, while early increases in action selectivity are exclusive to deep layers, a second rise, starting approximately 400ms prior to the response lick, is visible in both mid-superficial and deep units.
Another possible mechanism creating the observed action selectivity might be a broad activation of neurons in the hemisphere opposing the targeted lick spout instead of a diverse action tuning of single neurons. To test this hypothesis we analysed the pooled firing rates and signed action selectivity across layers while grouping the animals lick location relative to the hemisphere of the recording. However, the hence obtained average neural activity

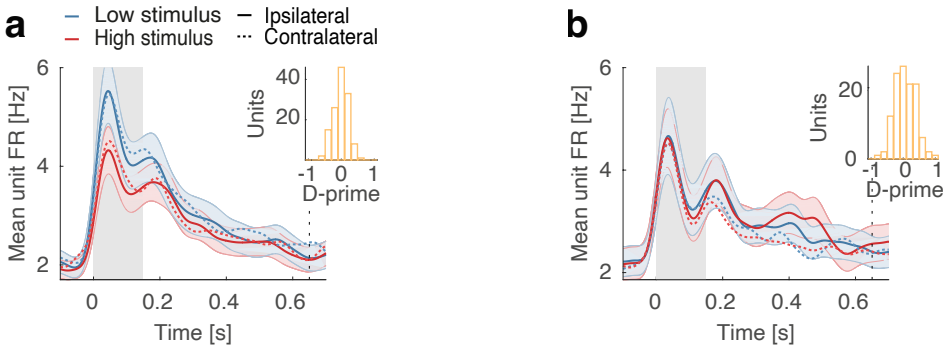

Figure 2.12: ***Action-alignment on recorded hemisphere.*** ***a:*** *Time course of mean activity ± SEM in mid-superficial units split by presented stimulus and the response location relative to the recording site. Time of sound presentation (grey shade) and go signal (dotted line) are indicated.* ***Inset:*** *Distribution of action selectivity prior to the response window. Negative d-primes correspond to a preference of contralateral responses, positive values to ipsilateral ones.* ***b:*** *As a, but for deep units.*

did not reflect the temporal dynamic of action selectivity previously observed in in deep units (Figure 2.7b). Moreover, no common sign in action discriminability could be observed in this analysis (Figure 2.12). It is therefore unlikely that the observed action tuning is due to a broad activation of the hemispheres and more likely that individual action tuned units have specific action selectivity independent of their hemispheric location.

2.3.5 Selectivity to stimulus-action combinations

While neural selectivity is typically attributed to either stimulus or the reported choice, they can also be selective to specific combinations of the presented stimulus and the reported choice [294]. Moreover, because we calculated selectivity conditional on stimulus or action, the resulting selectivity was also always calculated between correct and incorrect trials. Therefore single cell preferences for task outcome or a specific combination of stimulus and action, can be misinterpreted as stimulus or action selectivity.
To distinguish outcome from stimulus or action preferences, signed selectivity measures are needed. Because for a given stimulus, correct outcome is associated with one action, but for the other stimulus with the oppo-

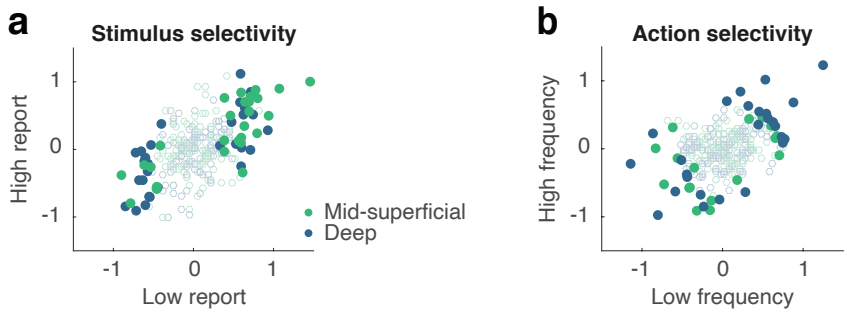

Figure 2.13: ***Reliability of selectivity.*** ***a :*** *Scatterplot of conditional stimulus selectivity during sound presentation in mid-superficial and deep units in low and high report trials. Filled dots depict units with significant overall stimulus tuning.* ***b:*** *As in a but for action tuning prior to response period in low and high frequency trials.*

site action, the d-primes of outcome selective units will change their sign across the two action conditions. Across many such units, the two conditional stimulus d-prime values should consequently be negatively correlated. We therefore calculated the signed conditional d-prime for stimulus selectivity during sound presentation and action selectivity prior to the response window to test if the selectivity was consistent across trial conditions. Stimulus selectivity during the sound presentation (0-150ms) in selective units was consistent across both response-type trials in both layers (Figure 2.13a, correlation$_{mid-superficial}$=.88, p<.001; correlation$_{deep}$=.84, p<.001; Fischer's exact permutation test; correlation across significantly selective units; Bonferroni corrected $\alpha = .0125$.), providing no evidence for an action-bias or outcome selectivity in our stimulus discriminability measure. In contrast, action selectivity prior to the response period (450-700ms) does correlate across trials of both frequencies, too. However some units do show selectivity conditional on one stimulus only and the corrrelation of conditional action measures is only significantly bigger than expected by chance in deep units (Figure 2.13b, correlation$_{mid-superficial}$= 0.57, p=.14; correlation$_{deep}$= 0.74,p=.008;).

2.3.6 Relation of stimulus and action selective neurons

We have so far established two distinct types of task selectivity in ACx with diverging temporal and laminar profiles. It remains unclear though, if and to what extent stimulus and action selective populations are distinct. We

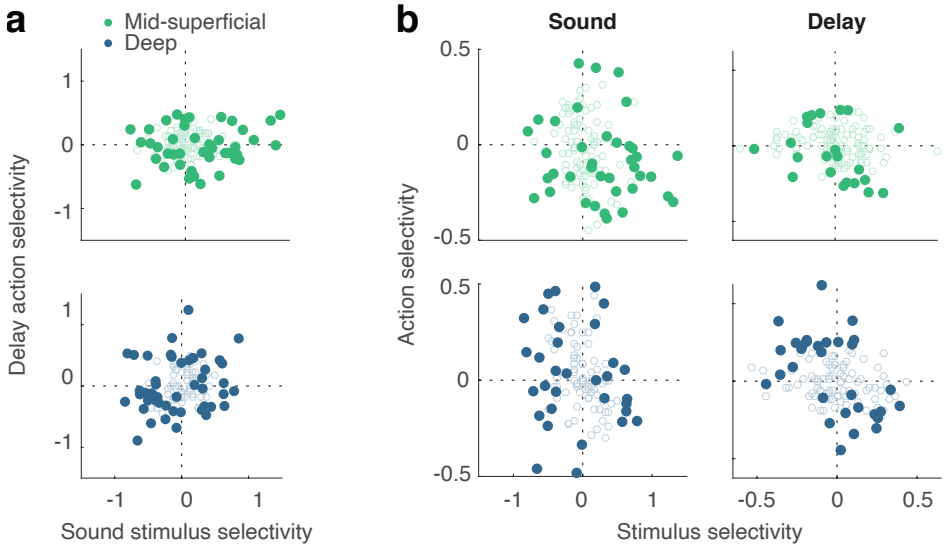

Figure 2.14: ***Relation of stimulus and action selectivity.*** ***a:*** *Scatterplot of signed unit stimulus selectivity during sound presentation and action selectivity prior to the response period for mid-superficial (top) and deep (bottom) units. Filled dots correspond to units with selective tuning (p<=0.05) to at least one modality.* ***b Left:*** *Scatterplot of simultaneous stimulus and action d-prime (during sound presentation for mid-superficial (top) and deep (bottom) units.* ***Right:*** *As left but for selectivity prior to the response period.*

therefore analysed if the sign and magnitude of stimulus selectivity during the sound presentation were correlated with the action selectivity prior to the response period in both mid-superficial and deep populations. While we observed units that displayed both stimulus selectivity during sound presentation and action selectivity prior to the response period, there was no significant correlation between these two signals across mid-superficial or deep units (Figure 2.14a, see Table 2.6 for quantification). Therefore stimulus and action selectivity were conveyed by partially overlapping, but distinct populations of task-selective units.

Depth in ACx	Sound stimulus and delay action	During sound	During delay
Mid-superficial	.07; p=.65	-.29; p=.06	-.21; p=.16
Deep	.21; p=.15	-.05; p=.72	**-.48; p=.001**

Table 2.6: ***Tuning correlations.*** *Quantification of correlations in filled markers of Figure 2.14. Shown are correlation coefficients across units and the p value assessing the probability to observe these correlations by chance (Fischer's exact permutation test). Significant values are highlights (bold). Bonferroni corrected α= .0083 (6 comparisons).*

Even though stimulus and action selectivity occur at distinct time points in the task, it is possible that the action signal in deep units is informed by the stimulus selective sound responses of the population. In this case, the noise in the sound responses of stimulus selective units that either enhances or reduces the specific firing rate induced by stimulus should therefore increase or decrease the chance of a correct decision in the downstream decoding areas [240]. Units preferring one stimulus should therefore have a slight selectivity for the associated response - as higher firing rates for trials of that stimulus should reduce the risk of mistakes, while lower activity will increase the probability of an error. This type of action selectivity during sensory evoked responses with consistent stimulus and action preferences is consistent with the prediction of causal theories of choice probability [240, 89, 47]
We therefore calculated the signed, instantaneous stimulus and action selectivity during both, sound presentation for stimulus selective as well as prior to the response window for action selective units. We discovered a slight correlation of simultaneous stimulus and action selectivity during sound presentation. However, unlike the scenario above, this correlation was negative (Figure 2.14b, see Table 2.6) for quantification). Similarly, action and stimulus selectivity were negatively correlated prior to the response window. Notably, the extent of the negative correlation matched the degree and time of tuning, as mid-superficial units were strongly stimulus selective, while deep units showed stronger action selectivity prior to the response period.
Albeit small, these correlations suggest that sound responses to the preferred stimulus of a stimulus selective unit are slightly bigger in trials where the animal will report the unpreferred stimulus. Consequently, selectivity to task parameters should be slightly higher in incorrect, rather than in

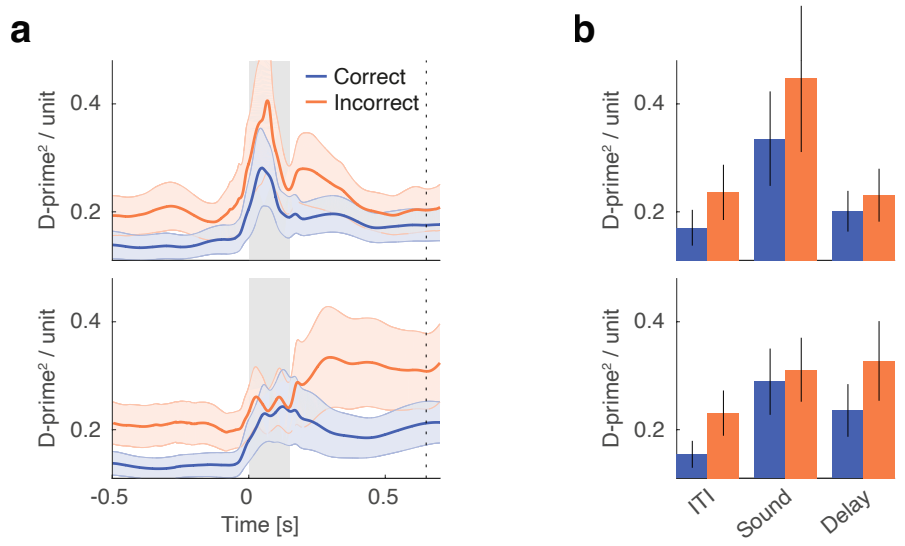

Figure 2.15: ***Outcome dependency. a Top:*** *Time course of mean task selectivity in correct and incorrect trials in mid-superficial units. Thick lines represent distribution means across 1000 iterations of a hierarchical bootstrap, shades denote one standard deviation of the distribution created by the bootstrapping procedure. Time of sound presentation (grey shade) and go signal (dotted line) are indicated.* ***Bottom:*** *Same as top but for units recorded at deep shanks.* ***b Top:*** *Quantification of average mid-superficial tuning during ITI, sound presentation and prior to response period.* ***Bottom:*** *Same as top but for units recorded at deep shanks.*

correct trials, as stimulus and action related firing increases are misaligned. We therefore calculated the selectivity to task conditions in correct and incorrect trials separately. Indeed, task selectivity in incorrect trials iwas constantly higher in incorrect, compared to correct trials both during the sound presentation as well as prior to the response window (Figure 2.15a). Importantly though, the reported differences in selectivity in correct and incorrect trials were very small and not significant at any single time point we investigated (Mid-superficial: p_{ITI}=.22, p_{Sound}=.18, p_{Delay}=.58; Deep: p_{ITI}=.08, p_{Sound}=.76, p_{Delay}=.18; Figure 2.15b). Nevertheless, this trend of stronger task signals in incorrect than correct trials is in line with the observed misaligned stimulus and action selectivity.

2.3.7 Population coding directions

Because we have found indications of outcome dependent differences in task selectivity, we sought to investigate if the population format, rather than the strength of task selectivity is sensitive to the outcome of the trial using the notion of population coding directions (CDs) [60]. CD refers to the linear combination of neural activity best discriminating between two task conditions at a particular time point. To address if stable CDs could be obtained from incorrect and correct trials separately, we calculated CDs on half of the trials obtained in a session and determined their alignment to directions obtained in the remaining trials (see methods). We observed reliable CDs in correct trials in both mid-superficial as well as deep populations during sound presentation as well as prior to the response period (Table 2.7).
In incorrect trials, however, only mid-superficial CDs during sound presentation aligned above chance. Therefore, the lack of stability in the remaining CDs of incorrect trials is unlikely explained solely by the small amount of error trials within a session. It is possible that this discrepancy in alignment of incorrect CDs observed across deep and mid-superficial units during sound presentation is due to the smaller fraction of stimulus selective units in deep populations. Alternatively, the stability of deep stimulus and action coding might also be truly outcome dependent. However, because the measure of CDs did not seem to be stable in incorrect trials, a meaningful comparison of CDs in correct and incorrect trials was not possible.

Depth	Correct trials		Incorrect trials	
in ACx	Sound	Delay	Sound	Delay
Superficial	**.72; p<.001**	**.46; p=.004**	**.45; p=.006**	.08; p=.63
Deep	**.67; p<.001**	**.5; p=.004**	.23; p=.13	.24; p=.25

Table 2.7: ***Reliability of coding directions in correct and incorrect trials.*** *Mean correlations and p values for the indicated populations were obtained in 10000 iterations of a hierarchical bootstrapping procedure. Sound interval: 0:150ms; Delay interval: 450-700ms. Superficial refers to all units recorded in mid-superficial shanks. Significant comparisons are highlighted (bold). Bonferroni corrected α = .0063 (8 comparisons).*

2.3.8 Transformation of coding directions in time

Above, we described a slight correlation in early stimulus and late action signalling of single cells (Figure 2.14a), indicating an overlapping population for stimulus and action representations. To further investigate this similarity of population task signals across time we calculated the correlation of CDs in mid-superficial and deep units across time (Figure 2.16). As this measure is not robust in incorrect trials, this analysis was limited to correct trials. Importantly, this limitation does not allow to distinguish between stimulus and action directions.
In both mid-superficial as well as deep populations we found strong correlations of CDs close in time (Figure 2.16a). This is likely due to overlapping

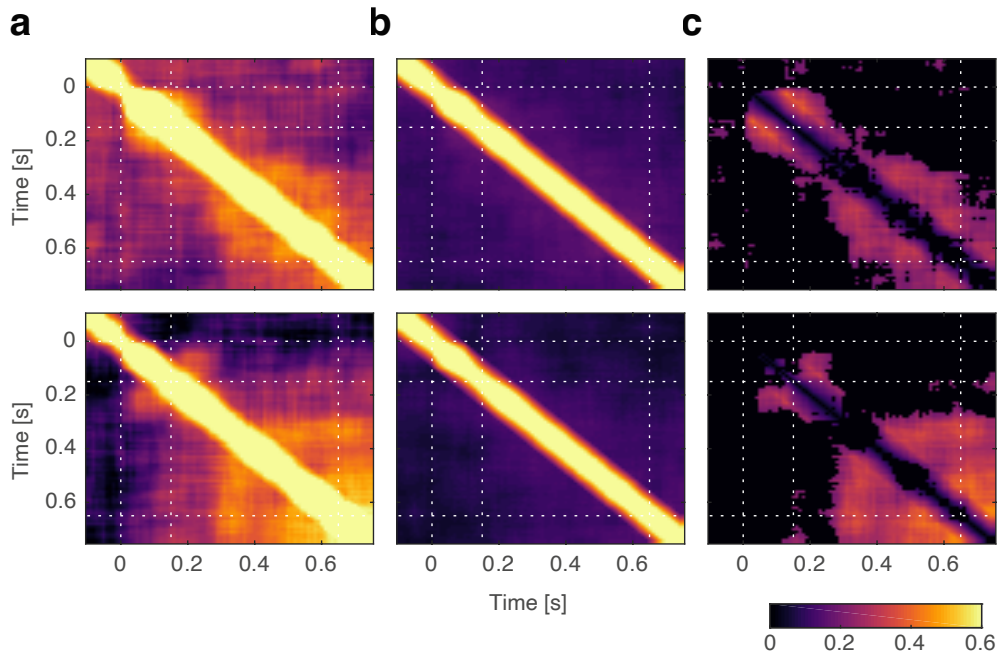

Figure 2.16: ***Stability of coding directions.*** ***a Top:*** *Similarity matrix of coding directions across time in mid-superficial populations. White dotted lines denote sound onset, offset and end of delay period.* ***b:*** *Similarity matrix of random directions in mid-superficial units across time.* ***c:*** *Difference of similarity matrices in a and b at time points with significant alignment of CDs in mid-superficial units (see methods).* ***Bottom:*** *As above but for populations recorded at deep shanks.*

windows of activity and not necessarily indicative of a stable representation of task information. To investigate at what time in the trial task representations are similar more than expected by construction or chance, we computed the correlation expected by chance in both neural populations (Figure 2.16b, see Methods). Due to the overlapping counting windows, CDs close in time were well aligned, while distant time points trypically were almost orthogonal, indicating a low chance of random correlation among CDs. Using these chance distributions, we identified multiple time periods in both mid-superficial as well as deep populations with significantly stronger alignment than expected by chance (Figure 2.16c).

In deep populations, CDs were stably maintained during two distinct time intervals. Thus, both at sound offset as well as during large fractions of the delay period, coding directions remained aligned above chance. Importantly though, these two formats did not correlate with each other stronger than expected by chance, therefore establishing two separate formats of task selectivity in deep populations, likely associated with the stimulus and action selectivity observed in single units. However, because this analysis was limited to correct trials, a direct distinction between the contributions of stimulus and action selectivity in these two formats is not possible.

In contrast, mid-superficial coding directions did not display such a clear distinction between early and late task selectivity. Instead, both during the stimulus as well as the delay period, CDs remained aligned above chance for only approximately 150ms. Importantly, mid-superficial units showed significant task signalling during both sound presentation as well as prior to the response window and CDs at these times in the task have been reliable across sessions halves. Therefore, the short duration of a particular task format is likely not due to noise, but might rather be reflecting a constant rotation of mid-superficial CDs from early stimulus to late action signalling, contrasting the stable format of population discriminability in deep layers.

2.4 Conclusions

We have demonstrated that stimulus and action signalling during a delayed response task have distinct temporal profiles in the rodent ACx. To this end we have successfully implemented a delayed response paradigm for pure-tone frequency discrimination in head fixed mice. Mice performed well in the task with no apparent biases in the responses of completed trials (Figure 2.2c). Interestingly though, animals showed a clear frequency-dependent bias in their premature response rates. This effect was observed across all behavioural setups and did not correspond to a particular location of the response spout. Given that age related hearing loss, especially for high frequencies, is a well know phenomenon in C57BL/6J mice [98], it is possible that low frequencies were more salient and therefore elicited stronger behavioural responses. However, all stimuli were presented well above detection threshold of animals in that age [111, 152]. Moreover, as trial rejection rates were not frequency-dependent (Figure 2.2b) and the ITI was variable, it is unlikely that animals were only acting upon detection of low frequency, rather than a frequency discrimination strategy. Therefore high frequencies might be less salient to the animals, but can still be perceived and elicit reliable behavioural responses.

2.4.1 Involvement of ACx in task performance

Transient silencing of ACx confirmed its involvement in task execution. However, we observed a strong reduction of task engagement rather than a consistent reduction in response accuracy (Figure 2.3). This reduced response behaviour is unlikely reflecting an inability of initiating the appropriate motor commands. While we cannot exclude the possibility that the highly concentrated muscimol solution used for injections diffused far enough to affect thalamic areas, such a scenario would be expected to cause deterioration in discriminability rather than the observed increase in trial rejection [75]. Moreover, all animals were still able and motivated to display licking behaviour, as manually delivered water drops were consumed quickly and reliably. Therefore the impairment does likely not result from an inability to lick in order to receive water.
However, the increased trial rejection rate is consistent with both a temporary loss of sound perception [257] or could reflect a behavioural strategy

in response to impaired sound discrimination or action selection [136, 190]. Because previous studies have shown only mild effects of ACx silencing for frequency discrimination of pure tones [190, 75, 34], the strong behavioural effects observed likely do not reflect reduced discriminability. However, necessity of ACx for discrimination of frequency stimuli with higher complexity [34] and anticipatory behaviour [142] have been reported. Thus the behavioural effects reported here might reflect a cortical involvement due to the fact that mice could only report their choice after a delay period, rather than the discrimination component of the task. While our results were not able to clearly establish the exact nature of its contribution, we have observed clear evidence for the involvement of the ACx in task execution.

2.4.2 Successful laminar recordings

We sought to characterise the task related activity of auditory cortex. A large fraction of the recordings had to be excluded from analysis. This is partially due to very restrictive measures in confirming correct probe location, as all three recordings of one hemisphere were discarded from analysis if the probe placement was incorrect in the histological verification of the last session. Additionally, the recording procedure itself poses a strong disruption of the usual training protocol of behavioural sessions as it includes new waiting times in the setup due to the probe insertion. Therefore additional recordings were excluded because the animals did not engage in enough trials in the recording session. Despite these difficulties, we successfully recorded the activity in the ACx in ten behavioural sessions of five animals, resulting in a total of 422 recorded single and multi-units across recordings. The fact that only about half of these units had firing rates modulated by task parameters is consistent with the reported sparseness of representations of ACx [105], but might also reflect a temporal instability in the units recorded from during the acute recording sessions.

2.4.3 Alignment procedure

We observed stimulus as well as response-type related activity across task responsive units (Figure 2.5c). However, to investigate systematic location differences across recordings an alignment procedure is needed. Traditional studies using linear probes have used Current Source Density (CSD) in the

Local Field Potential (LFP) to determine the location of the granular input layer 4 [222, 296]. However, these methods require a continuous sampling across cortical layers and are not directly applicable in our recordings as we recorded activity at six distinct depths. Moreover, the animals' movements did elicit strong artifacts in the LFP traces, making a clean estimate of CSD unfeasible (data not shown). We therefore sought to identify the shank closest to cortical layer 4 by hypothesising that it should display the highest amount of stimulus information in early sound responses. Reliably estimating information from limited samples is problematic as low amounts of data lead to an overestimation of information. We therefore used an iterative measure of estimating MI that was designed to deal with limited amounts of data and has successfully been used in the rodent ACx [174, 36]. Importantly, while the hence obtained MI might still not unravel the true information content, all simultaneously recorded units suffer from the identical sampling limitation. Therefore MI measures can be compared across probe shanks within the same recording session. If highest stimulus information content in early sound responses is located in input layer 4 as we hypothesised, response latency of neural activity should be shorter at the max MI shank than in neighbouring shanks, as fastest response latencies have been reported in layer 4 and at the intersection of layer 5 and 6 of ACx [222]. Indeed, average response latency was shortest at the max MI shank across recordings. However individual recordings did not show a relationship of max MI shank and the shank with fastest peak-response latency. But while alignment on max MI shanks revealed clear structure in the data, alignment on shanks with fastest response latency failed to do so. The location of the max MI shanks within the six probe shanks did not differ strongly across recordings, indicating a reliable relationship of frequency tuning and depth. The fastest latency shank, however, did not display a clear relationship with depth across our recordings (data not shown). It is therefore likely that our estimate of response latency is unreliable, possibly due to the high variability in neural responses and greatly diverging unit numbers per shank. Thus it is difficult to state the exact relationship of the max MI shank relative to cortical input layer 4. However, alignment on max MI shanks at sound onset across recordings revealed a clear laminar structure in the neural activity and selectivity of the ACx and therefore has shown to mark a relevant position within the cortical layers, consistent with our initial hypothesis.

2.4.4 Activity and selectivity have laminar profiles

Alignment across recordings revealed two main differences in mid-superficial and deep units. While both neural populations demonstrated an initial sound response, only deep units displayed a second, pronounced activation around sound offset (Figure 2.7a). Sound offset responses have been described previously in the ACx [134]. These responses show slightly larger response latencies than onset responses, have a distinct frequency tuning and are most robustly seen in the anterior auditory field [246]. However, closer inspection of the second activation observed in deep units revealed that firing rates already started to increase as early as 50ms prior to sound offset. Thus, this signal does not correspond to offset-triggered responses. Possible explanations of this rise in activity might be a rebound of activity due to decreasing onset-response triggered inhibition [90, 134] or feedback signals selectively targeting deep layers of ACx [92].
Strikingly, the alignment on max MI in early sound responses did not only reveal a relationship to activity around sound offset, but also revealed a laminar structure in single unit selectivity. While stimulus selectivity during the sound presentation did not show significant laminar differences, there was a clear laminar organisation in the selectivity to the action to be performed by the animal. While this signal was not exclusive to deep units, it was significantly stronger than in mid-superficial units (Figure 2.7). This action selectivity could not trivially be explained by diverging response times (Figure 2.11) or broad hemispheric activation (Figure 2.12) and therefore likely represents a true, diverse tuning to the reported decision of the animal. Interestingly, the increase of action selectivity roughly coincided with the reported transient activation of deep units at sound offset. It is therefore possible that these two phenomena are related and the the transient offset activation is inducing the reported choice signaling in deep layers. Moreover, temporal alignment of neural activity on the animal's responses suggested an initial increase in action selectivity in deep units starting as early as 1s prior to the response lick and a later, simultaneous increase in action selectivity in in both populations in the 400ms prior to the response lick (Figure 2.11). This structure could reflect two distinct sources of action-related signals in ACx: Late signals observed in both populations during movement preparation, and earlier signals exclusive to deep units during the delay period of the task. However, a population-level analysis of response aligned action

selectivity in deep units across time will be necessary to further investigate a possible distinction of early and late action signalling in deep populations of the ACx.
Importantly, while action signals have been reported previously in ACx, the delayed response task paradigm used here for the first time demonstrates a clear temporal dissociation of transient stimulus and action-specific signals in ACx [83, 296]. Therefore, task representations in ACx switch from a pure sensory representation to the exclusive representation of action during the delay period. Given that activity in the ACx is sufficient to drive decision behaviour [299, 272], our analysis revealed two possible output signals underlying this biasing effect.

2.4.5 Stimulus and action tuning are misaligned

Action signals observed in neurons of sensory cortical areas have originally been interpreted as evidence for a causal contribution of such neurons to the decision making process, as the decisions reported by the animals correlated with fluctuations in the activity of sensory neurons tuned to the reported stimulus [23, 240]. However, none of the signals described in this chapter support such a notion. Here, action-predictive signals were observed in units distinct from stimulus selective ones (Figure 2.14a). Such differences in choice and stimulus signalling have been reported previously and are interpreted as the result of feedback signalling [298]. Alternatively, distinct representations of stimulus and action-predictive information could be signatures of a local stimulus-choice transformation. The fact that in our data stimulus and action signalling only briefly coincided in ACx challenges this hypothesis and instead supports the interpretation of the observed action selectivity as a feedback-induced phenomenon. A possible source of such feedback projection is supplementary motor area M2, which displays early choice related activity and is involved in action modulation in ACx [230, 224].
As feed forward and feedback-related choice probability likely are observed at different timescales [287], we addressed the possibility of additional classical choice probability signals consistent with a causal contribution. Thus we determined if trial-by trial fluctuations in the sound response of individual neurons were associated with the behavioural choices of the animals (Figure 2.14b). Stimulus representations in both mid-superficial and deep units displayed small, negative choice probability, incompatible with a causal in-

fluence of variations in stimulus response on the reported decision. Such negative choice probability has been previously reported in visual cortices [131] where they are likely caused by feedback projections as they propagate sequentially from higher to lower cortices [81].
Strikingly, we also demonstrated a negative correlation of simultaneous stimulus and action selectivity prior to the response period (Figure 2.14b). This is unlikely due to residual stimulus information as no negative correlation of stimulus selectivity during the sound presentation and late action selectivity has been observed (Figure 2.14a). However, this negative correlation of stimulus and action selectivity implies an interesting misalignment in activity: Firing rates in action selective units prior to the preferred action are higher in incorrect trials. This observation thus suggests the puzzling possibility of increased representations of task information in incorrect compared to correct trials.

2.4.6 Outcome dependency of task signals

We have presented preliminary analysis addressing this possibility and reported a constant, but very small increase in task selectivity in incorrect compared to correct trials (Figure 2.15a). Similar to the initial observation of negative choice probability, these selectivity differences in correct and incorrect trials were not significant (Figure 2.15b). Notably though, we did observe this small outcome-dependent difference in task selectivity not only during the task, but already prior to stimulus presentation. Given that in incorrect trials this task selectivity in deep units was comparable in strength to the selectivity prior to the response period in correct trials, this phenomenon has to be addressed further in future analysis. Indeed, choice probability prior to stimulus presentation has been reported previously [181]. Because animal behaviour in 2AFC tasks is typically modulated by history effects [77, 143, 28], it is possible that such a pre-existing task selectivity reflects these tendencies by selectively coding for the previous action or task outcome. In such a scenario the observed slight outcome-dependent difference in task selectivity could reflect a difference in either strength of or dependency on such history signals or correspond to distinct serial dependencies of task accuracy. To address these scenarios, a reliable measure of population-based selectivity for incorrect trials is needed. However, the measure explored in the analysis presented so far was found to be reliable in

correct but not in incorrect trial conditions (Figure 2.7). It is likely though, that the lack of alignment observed in incorrect trials can be attributed to the low number of incorrect trials available. An analysis approach based on single trial decoding will be employed in future analysis to unequivocally investigate the possibility of outcome dependent signalling in ACx.

2.4.7 Rotation of population coding

Using the measure of a population CD, we successfully demonstrated some of the features described in the single cell analysis on the population level. We hence demonstrated that the direction of population activity best discriminating between high and low frequency trials showed clear laminar differences. In deep units we have described two prolonged, distinct coding formats (Figure 2.16c). A first, short period of stable coding directions was observed around sound offset and a second throughout the second half of the delay period. Given our findings using the single cell analysis, it is likely that these two coding formats are associated with separate stimulus and action representations in deep populations.
Contrasting these temporally distinct coding representations in deep units, mid-superficial populations demonstrated a slow, constant rotation of coding directions throughout the trial. Because mid-superficial units displayed significant stimulus information during sound presentation and weak, but significant action selectivity prior to the response period, this slow rotation might reflect a transformation of stimulus to action representations selectively visible in mid-superficial units. However, this temporally restricted similarity in CDs might also reflect the influence of noise during the beginning of the delay period as it is not clear if population coding directions and the strength of task selectivity are statistically significant throughout the trial.
Because analysis was restricted to correct trials, the analysis presented here did not allow to investigate the existence of population-based action signals during the sound presentation and their relationship to the signals observed prior to the response period. Moreover, as single trial analysis suggested a partial overlap of stimulus and action selective units without providing any evidence for their functional interaction (Figure 2.14), a future population analysis will be used in order to investigate possible interactions of these distinct populations more carefully [236].

Chapter 3

Outcome dependent modulation of task accuracy by cortical state fluctuations

HIGHLIGHTS

- In this chapter, we analyse the contribution of spontaneous baseline fluctuations of neural activity on frequency discrimination accuracy.
- We show that the animals' task accuracy is dependent on the response outcome in the previous trial with higher accuracy in trials following error trials.
- We provide evidence that only in these post-error trials, a clear relationship between neural baseline fluctuations and discrimination accuracy can be established.
- Furthermore, we establish that this response-outcome dependent effect is not due to distinct neural states, but represents a diverging effect of similar neural activity.

3.1 Introduction

In order to identify meaningful features in the stream sensory information and subsequently select appropriate behavioural responses, the dynamics of neural activity have to be in a regime to allow for appropriate processing. In cortex, the degree to which the activity of single neurons fluctuates synchronously has been suggested as an important coordination principle for this issue [15, 252, 279]. The degree of cortical synchrony in spontaneous activity is related to the dilation of the pupil, a known indicator of arousal state and cognitive load [120, 22]. These two phenomena are therefore often jointly referred to as brain state.

As asynchronous cortical activity in rodents has initially been attributed to movement, it is also referred to as the active cortical state in opposition to the inactive state with synchronous activity fluctuations [279]. However, cortical desynchronisation and movement can be dissociated, as certain stereotypical movements can be observed during cortical synchrony [279]. Moreover, cortical desynchronisation has been observed in the absence of movement through arousal in mice and during visual attention in cats [289, 125, 280]. The active cortical state has therefore been suggested to reflect an orientation of cognition to the outside world [278].

Consistent with this idea, the accuracy of the population code during the asynchronous behavioural state can potentially increase, depending of the size and the relation of synchronous fluctuations and stimulus-driven activity [1, 194, 247, 291, 241, 9, 43, 59, 169]. This dependence of the stimulus representation accuracy on the degree of cortical synchronisation has been confirmed in multiple experimental settings and studies [76, 192, 13, 132]. The relevance of these brain state effects for the behavioural performance in a given task, however, is still not fully understood.

Cortical desynchronisation has been suggested to increase discrimination accuracy in monkeys performing in a delayed match to sample task [13]. In rodent studies using detection tasks, on the other hand, a non-monotonic dependency of task accuracy on brain state has been observed, that corresponded to the propensity of the animals to respond in the task [148, 161, 248, 249, 282]. A recent study directly comparing the effects of brain state on discrimination accuracy and task engagement using a 2AFC visual discrimination paradigm suggested that cortical desynchronisation is generally more associated to task engagement, rather than increased behavioural ac-

curacy [113].
Here, we revisited this distinction by analysing neural and behavioural data of head fixed mice performing auditory frequency discrimination in a delayed 2AFC task paradigm. We observed an outcome dependent association of fluctuations in baseline activity and the degree of synchrony with discrimination accuracy, but no correlation of spontaneous neural state fluctuations with the animals' responsiveness in the task.

3.2 Methods

3.2.1 Data inclusion

In this chapter, the data collected as described in chapter 2.2 was analysed. To ensure sufficient trials in each analysed session, only recordings with a minimum of 100 completed trials (= animals responded in the response period) were considered. Moreover, only recordings with a d-prime > 1 were included in the analysis to ensure that the analysed behavioural sessions reflect engaged task responses. Given that spontaneous fluctuations in activity are widespread, non-local phenomena [224, 113], we relaxed the criterion of probe placement applied in the previous chapter. Hence, not only recordings from primary auditory cortex, but also from ventral and dorsal auditory fields were analysed here. Behavioural data of one animal (three sessions) had to be excluded because proper estimation of the pupil size was not possible, as the eye was closed during the majority of the trials. Importantly, exclusion of data obtained from this animal does not affect the reported main results. In total, 20 recording sessions from five animals matched these criteria and all analysis described in this chapter was performed on these data sets.
Trials of all presented frequencies, independently of the difficulty, were included in the analysis. Thus, in 13 of the analysed recordings four different stimuli (Low frequency: 9.9 & 12kHz; High frequency: 16.3 & 20kHz) were presented to the animals. The two difficult stimuli close to the threshold were presented more often (85% of trials, see chapter 2.2). In the remaining seven recordings analysed here, two additional hard stimuli were presented (Low frequency 13kHz; High frequency 15kHz) in 8% of the trials.
Besides neural data and the licking behaviour in the session, additional behavioural measures were considered for analysis. Thus the animals' facial movements were recorded during the behavioural sessions (60 frames per second, camera: ELP) and stored for offline analysis together with synchronisation pulses of stimulus presentation times using a custom Bonsai [147] script and an Arduino Uno board (Arduino). As in the previous chapter, all trails with manual interventions were excluded from analysis. In addition, the last ten trials in each recording session were not considered as session termination was conditional on these trials.

3.2.2 Processing of video data

From the obtained videos, we extracted two global state variables, quantifying the degree of facial movements and the arousal state. For the quantification of facial movements, we computed the average magnitude of Optic Flow (OF) (Lucas-Kanade method [149]) in a Region of Interest (ROI) selected around the face of the animal, consistent with procedures in previous studies [255, 170]. OF values corresponded to the median OF in the analysis window (Figure 3.3c, 2s baseline period prior to sound presentation). For comparisons across sessions, OF measures were z-scored in each recording session separately.
The animal's arousal state was determined by tracking the size of its pupil. For this purpose we used DeepLabCut [156] to detect points around the pupil in each frame of the video. For model training, eight points in 20 frames of each recording session were labelled. To remove frames with poor detection, we considered only frames with an average detection likelihood above 0.8. The pupil size was then given by the major axis of an ellipse fitted with these eight detected points. To increase the robustness of these pupil estimates, the data was smoothed further with a robust local regression using weighted linear least squares and a 1st degree polynomial model (250ms window, rlowess in Matlab). The hence obtained pupil sizes were then normalised within each session by the 2% smallest values, such that pupil size values determined the fraction of size increases relative to the smallest values observed in the sessions. The median pupil size values of each analysis window (2s prior to stimulus presentation, Figure 3.3c) where the computed and used in further analysis.

3.2.3 Quantification of cortical synchrony

We calculated the degree of synchronisation in the recorded neural populations by comparing the standard deviation of their combined activity with the deviation expected in a desynchronised population. In this procedure, the activity of all simultaneously recorded units was combined to calculate the Firing Rate (FR) of the population, defined as the average number of spikes per unit in the analysis window, as well as to form the MUA trace by counting spikes in non-overlapping 20ms windows. Next, we created 100 surrogate activity traces in which the time of each spike was randomly assigned to a recording sample in the 2s time window (Figure 3.1). The 20ms

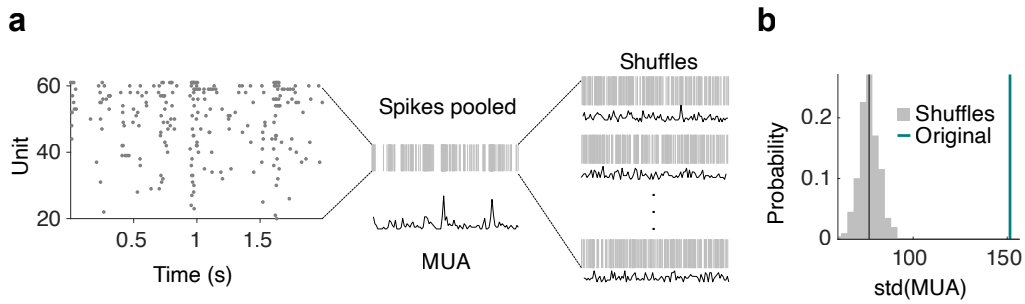

Figure 3.1: ***Schematic of synchrony measurement.*** ***a:*** *Schematic of shuffling procedure.* ***b:*** *Resulting standard deviations in 2s MUA firing in original sample (green) and the distribution across 100 spike time permutations (grey). The final synchrony measure is given by dividing the standard deviation in the original MUA by the mean standard deviation of the shuffle distribution demarcated by the black line.*

binned MUA was calculated for each surrogate and the standard deviation across time determined. The final measure of synchronisation was obtained by:

$$Synch = \frac{\sigma_{MUA}}{\overline{\sigma_{Shuffle}}} \tag{3.1}$$

With σ_{MUA} as the standard deviation of the MUA observed in the real trial and $\overline{\sigma_{Shuffle}}$ being the average standard deviation of the 100 surrogate MUA traces in time.

3.2.4 Whitening of general and neural state predictors

The main goal of this analysis was to determine the effects of spontaneous, trial-by-trial variations of neural state (FR and synchrony), movement (OF) as well as arousal (pupil size) measures on the behaviour of head fixed mice. To separate such spontaneous changes in these variables from session trends and other dependencies, we only used fluctuations in these variables that could not be predicted by past information, referred to as their innovation. To determine the innovation of state predictors, we performed multivariate regression, predicting the expected value of each state variable in a given trial (Figure 3.2). In this process, we considered the values of all four state variables (FR, synchrony, pupil and OF) in the previous ten trials, as well as the outcome of these trials (1 reward; 0 no reward) as model predictors.

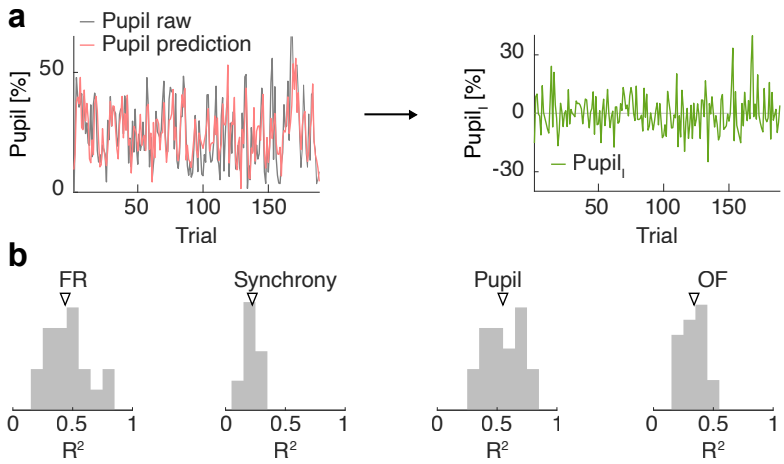

Figure 3.2: ***State predictor whitening.*** ***a:*** *Example of whitening procedure and result. Shown are example traces of actual and predicted trial-by-trial pupil sizes (left) as well as the resulting pupil innovation values (right).* ***b:*** *Distribution of* R^2 *values for multivariate fits of state predictors across recording sessions.*

To account for slow sessions trends we included the current trial number as an additional predictor. The predictor innovations where then defined as the difference of the raw and expected values of each state predictor (Figure 3.2a). The models trained in this process fit the data sufficiently well to strongly limit cross-correlations among the presented state predictor innovations (Figure 3.2b & 3.5a). As a consequence of this procedure, the first ten trials in each session were excluded form analysis. If not mentioned otherwise, all neural and global state predictors in this chapter refer to their respective innovation measures.

3.2.5 Generalised linear mixed modelling

We used generalised linear mixed modelling to analyse behavioural data across recording sessions [72]. Thus models were fit in Matlab (fitglme), using recording session as a random effect. Prior to model fitting, all predictors included were z-scored within a session. Importantly, when splitting trials into different data sets, i.e. trials following correct and trials following incorrect responses, z-scoring was performed independently in each data set. To estimate confidence intervals and corresponding p values, we used boot-

strapped statistics by resampling the data in each recording session (with repetition) so that the number of trials from each recording was preserved in each global surrogate. In each bootstrap iteration, a Generalised Linear Mixed Model (GLMM) was fit for the obtained surrogate data set and the distribution of the resulting fixed effects across 1000 such bootstrap iterations was used to determine if the observed effects were significantly bigger than zero by determining their 95% confidence intervals.
To verify differences in trial accuracy or rejection rate suggested by these models in the data directly, we computed the differences of these measures conditional on the response outcome or neural state predictor values in each recording session and assessed the significance of the obtained distributions using Wilcoxon signed rank test. In models fitting the animals' responses directly, models were fit in Matlab (fitglme), using recording session as a random effect without bootstrapping. The significance of the indicated fixed predictor weights was then calculated using an F-test.

3.2.6 Matching statistics of post-error and post-correct trials

To match the distributions of neural state variables in trials following correct and following incorrect trials, post-correct trials were sub-sampled. Thus in each recording session, for each post-error trial a matching post-correct trial was selected by choosing the trial with the most similar FR and synchrony innovation values (smallest euclidean distance in $\text{Synchrony}_\text{I}$ and FR_I space). Thus similar distributions of FR_I and $\text{synchrony}_\text{I}$ with matching trial numbers were obtained (Figure 3.10b). These distributions were then z-scored and used for GLMM analysis in the above protocol.

3.3 Results

3.3.1 Quantifying baseline activity and synchrony

Neural data recorded from head fixed mice performing in the auditory delayed frequency discrimination task described in the previous chapter was analysed to determine the correlation of spontaneous variations in neural baseline activity and population synchronisation with discrimination accu-

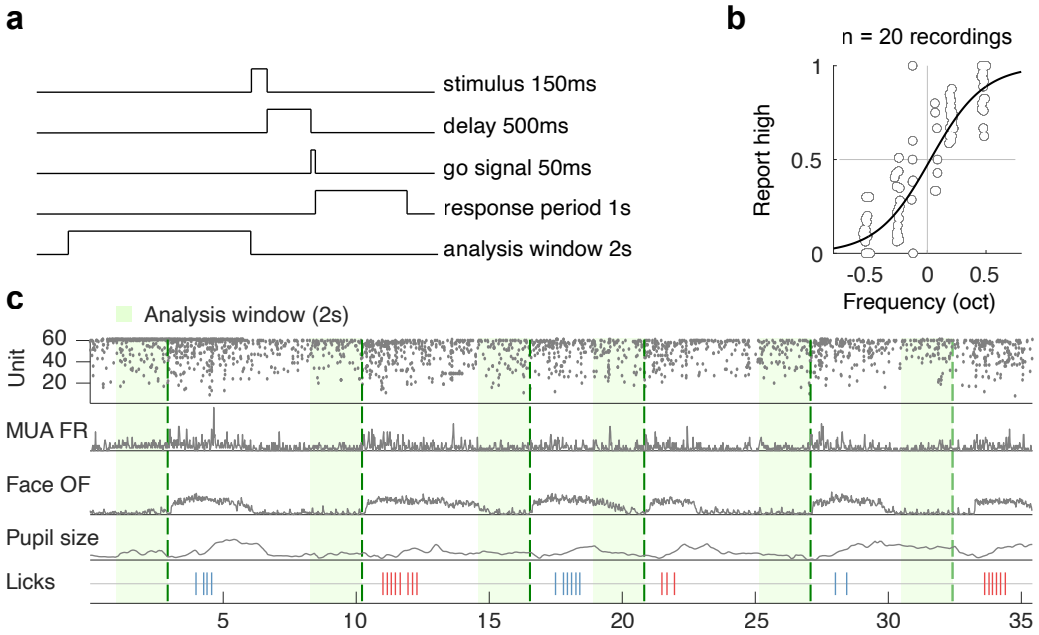

Figure 3.3: ***Task performance and data acquired.*** ***a:*** *Scheme of delayed response task contingency. Each trial, head fixed mice are presented with high or low frequency sounds from two lateral speakers. Animals report 'high' or 'low' by licking at one of two lateral water delivery spouts during the response period.* ***b:*** *Psychometric curves of valid trials across analysed recording sessions. Markers correspond to values in single recordings, black line represents cohort average.* ***c:*** *Example traces of data simultaneously collected during each session. Shown are the spike times of individual units (raster plot, top), their combined activity (MUA FR), the optic flow (OF) induced by facial movements (Face OF), the pupil size and the time and location (red: high report, blue: low report) of licking at the response spouts. Green lines demarcate times of stimulus presentation.*

racy. In the task, mice were presented with pure tones and had to categorise the frequency of the presented stimuli as high or low (category boundary 14kHz, see chapter 2.2). Animals were required to withhold their responses during sound presentation (150ms) and a brief delay period (500ms) until a green LED signalled the onset of the response period. In this task epoch, animals reported their decision by licking at the water delivery spout indicated by the presented sound. Licking at the correct spout triggered a 3μl water reward, incorrect responses prolonged the ITI by a 6s time penalty (Figure 3.3a). Neural activity in the ACx during task behaviour was recorded in six acute recording sessions for each animal (three recordings per hemisphere, see chapter 2.2 for recording and neural selection criteria). To investigate the effect of spontaneous fluctuations in cortical FR and synchrony on discrimination accuracy, we analysed the activity of simultaneously recorded units of recordings with sufficient behavioural engagement (min 100 completed trials, d' >1; see methods for data exclusion criteria). Thus, 20 out

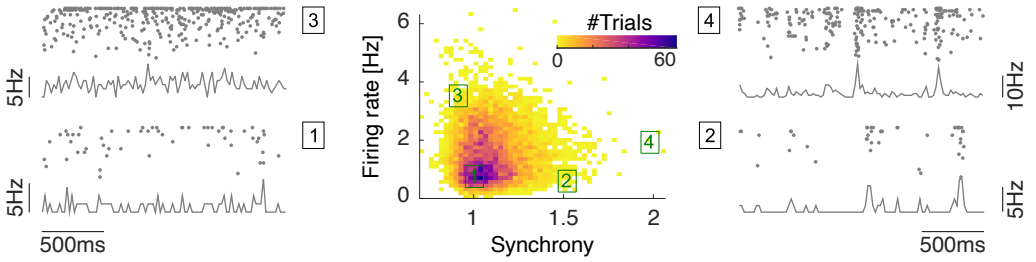

Figure 3.4: ***Distribution of synchrony and FR measures.*** *Heatmap of raw FR and synchrony distributions across all recordings (middle) and the indicated baseline activity examples are shown (left & right). In each example the spike times of individual units (raster plot, top) and the resulting MUA trace (bottom) in the two seconds prior to stimulus presentation are shown.*

of the 36 recording sessions were selected for analysis. Mice showed good behavioural performances in the selected sessions, however across these individual sessions, the response accuracy varied strongly (Figure 3.3b).
To quantify fluctuations in spontaneous neural activity across trials, the baseline activity in the two seconds prior to the sound presentation was characterised by the overall activity level of the population (FR) and the degree of synchrony of that activity (Figure 3.4). This population synchrony was quantified by the standard deviation of the MUA across the 2s analysis window, normalised by the standard deviation expected in a fully asynchronous

population with the same number of spikes (Figure 3.1, see methods for full procedure). As a consequence, this measure of synchrony was independent of the population's activity level. In addition to these neural state measures, we extracted the animal's pupil size as well as the degree of facial movement (given by the average OF across face pixels, see methods) from the recorded video data, two global behavioural variables known to be associated to cortical state fluctuations [224] (Figure 3.3c). Importantly, to reduce auto- and cross-correlations in the neural and global state variables considered here, we only considered their innovation (denoted by the subscript I), defined as the aspect of the signal that could not be predicted from itself and all other state predictors in the past, for further analysis (see methods).
The degree to which these signals could be determined by history varied, with strongest predictability observed in the pupil and weakest in the synchronisation measure ($r^2_{\text{Synchrony}} = 0.22 \pm 0.05$ and $r^2_{\text{Pupil}} = 0.55 \pm 0.13$; median $\pm$ MAD across recordings; Figure 3.2b). Importantly, after this processing

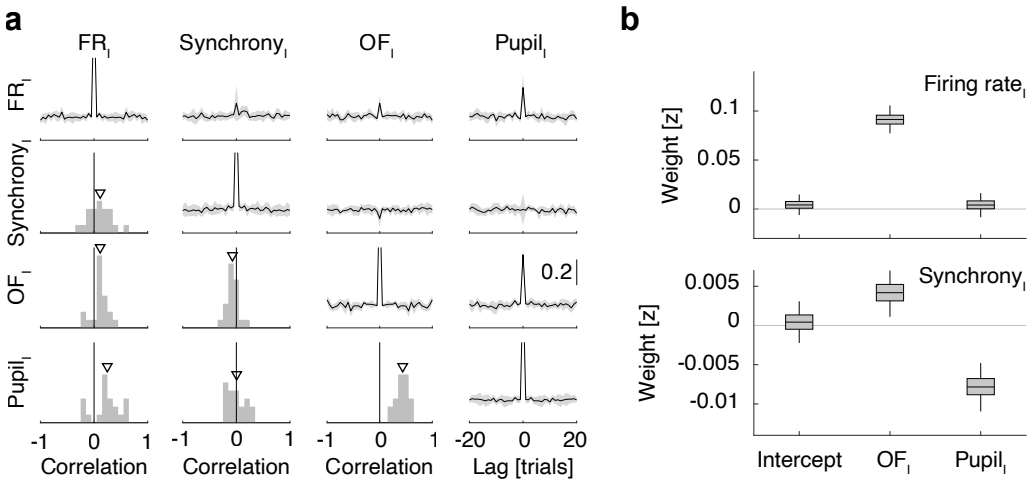

Figure 3.5: ***Cross-correlations of state predictors.*** ***a:*** *Correlation between the four state predictor innovations. Median ± MAD cross-correlations across state predictor innovations (upper triangle) and the correlation of instantaneous values across recordings (lower triangle) are shown. Markers denote medians.* ***b:*** *Distribution of fixed effect weights of the indicated predictors fitting firing rate (top) and synchrony (bottom) innovations. Distribution obtained in 1000 hierarchical bootstrap iterations. Box plot indicates median (mid-line), 50% (box) and 95% confidence intervals (vertical lines).*

step, only 'white' auto- and cross correlations where observed in all state predictors, with only instantaneous correlations between the state predictors remaining (Figure 3.5a).
To determine the degree to which neural baseline fluctuations were determined by the global state measures extracted from the videos, we constructed separate generalised linear mixed models (GLMMs) to fit FR_I and synchrony innovations with the recording session as random effect (see methods). Interestingly, even though FR_I showed positive correlation with both global state predictors, due to their positive correlation with each other, only a positive association of movement with FR_I was observed in our models. $Synchrony_I$, on the other hand was weakly, but significantly associated with both pupil size as well as movement innovations (Figure 3.5b). Our analysis therefore suggests that baseline FR innovations are preferentially associated to movement, while fluctuations in population synchronisation are reflecting the degree of arousal, too.

3.3.2 Effect of firing rate and synchrony on discrimination accuracy

To determine if spontaneous fluctuations in FR and synchrony were correlated with the accuracy in the discrimination task, we constructed a GLMM predicting if the reported decision by the animal was correct, based on the stimulus presented in the trial as well as the four described state related variables (Figure 3.6). In addition, to account for slow changes in task accuracy, the outcome of the previous trial as well as the position of the trial in the session (trial number) were considered as predictors. As expected by the shape of the psychometric curves (Figure 3.3b), the trial accuracy strongly depended on the presented stimulus, reflecting performance differences across the different stimuli (Figure 3.6a). Trial number had a positive effect on accuracy, suggesting a general improvement of discrimination accuracy during the progression of the sessions. All state predictors, on the other hand, had weak predictive power only and were not significantly associated to the discrimination accuracy. Interestingly, the outcome of the previous trial had clear predictive power in this analysis ($p<.001$). As the observed fixed effects were negative, our analysis suggested worse performances in trials following a correct one. Indeed, across recordings accuracy was significantly bigger after error trials ($p=0.025$, signrank test; Figure 3.6b).

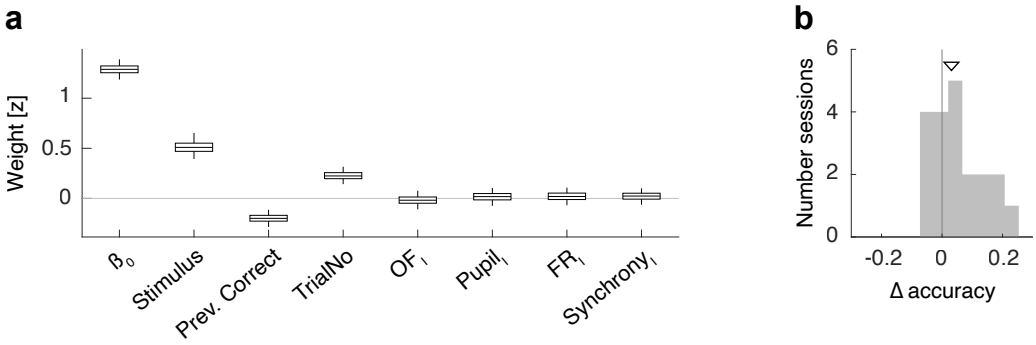

Figure 3.6: ***Effects of state predictors on discrimination accuracy. a:*** *Distribution of fixed effect weights of the indicated predictors. Distribution obtained in 1000 hierarchical bootstrap iterations. Box plot indicates median (midline), 50% (box) and 95% confidence intervals (vertical lines).* ***b:*** *Distribution of accuracy differences in trials following correct and error trials across recordings. Positive values indicate higher accuracy following error trials. Marker denotes median.*

As this analysis revealed significant differences in task accuracy depending on the outcome in the previous trial, we repeated the previous GLMM analysis separately for trials following correct and incorrect responses in order to determine possible differences in the conditional dependencies of task accuracy. Consistent with the previous observations, we discovered increased values for β_0 and the stimulus predictor in trials following incorrect responses, capturing the described differences in task accuracy (Figure 3.7). Remarkably though, in trials following correct responses no other state predictor had a significant effect, while both baseline innovations of neural state variables significantly explained accuracy in trials following errors (p=0.013 and p=0.023 for FR_I and $synchrony_I$ respectively, bootstrap distribution, see methods). Thus, both increased baseline FR_I as well as reduced innovations in synchronisation were associated with higher discrimination accuracy. We therefore refer to these baseline states with high FR_I and low $synchrony_I$ as favourable, while baseline states with low FR innovations and high $synchrony_I$ are referred to as unfavourable in the following. Consistent with previous observations, trial number had a predictive effect on accuracy, indicating improving performances during the session. Fluctuations of pupil size or movement were not associated to the task accuracy irrespective of

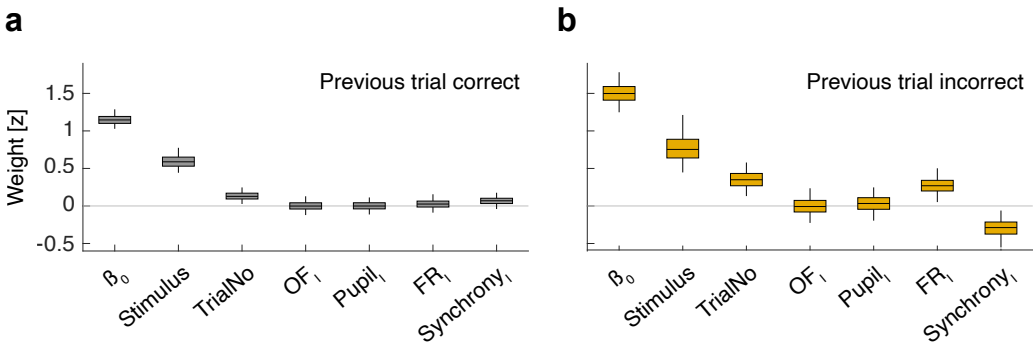

Figure 3.7: ***Conditional effects of state predictors on discrimination accuracy.*** ***a:*** *Distribution of fixed effect weights of the indicated predictors fitting accuracy in trials following correct responses. Distribution obtained in 1000 hierarchical bootstrap iterations. Box plot indicates median (mid-line), 50% (box) and 95% confidence intervals (vertical lines).* ***b:*** *Same, but accuracy fits in trials following errors.*

the outcome history.

To directly determine the accuracy differences associated with neural baseline fluctuations after error trials, the task accuracy as well as psychometric functions in post-error trials were calculated separately for trials with favourable and unfavourable spontaneous baseline activity (Figure 3.8, favourable: FR_I & $synchrony_I$ bigger than recording average, unfavourable: FR_I & $synchrony_I$ smaller than session average). This separation of post-error trials in favourable and unfavourable based on the neural state variables confirmed a significant difference in discrimination accuracy across recording sessions (p=0.03, signrank test) that was reflected by an increased slope (54% increase) in the corresponding psychometric curves (Figure 3.8b). In contrast, separation of trials following correct responses by the same criteria of neural state fluctuations showed no clear differences in the psychometric curves (Figure 3.8a).

Motivated by these findings, we sought to directly investigate the changes in the animals' task responses underlying the observed outcome-dependent changes in task accuracy. We therefore predicted the animals' responses directly in two additional GLMMs trained with trials following correct or error trials, respectively. Analogue to previous models, we considered the presented stimulus, the animals' previous responses as well as session trends

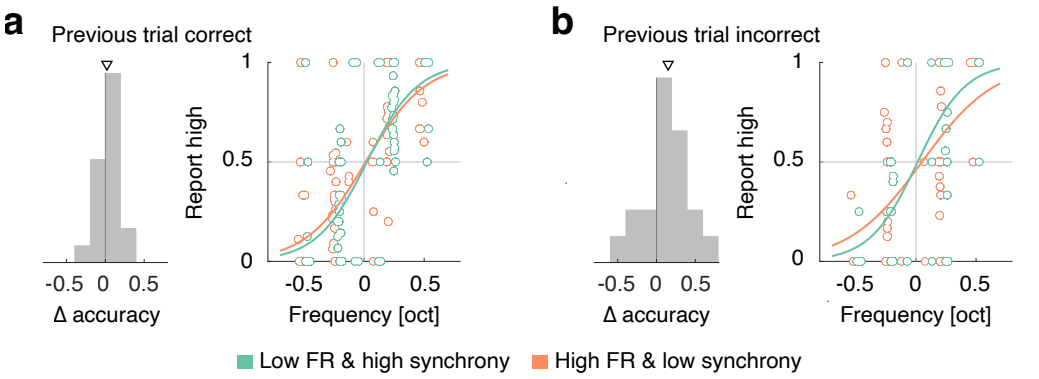

Figure 3.8: ***Conditional psychometric curves. a Left:*** *Distribution of accuracy differences between favourable and unfavourable neural states in trials following correct trials. Marker shows median across recording sessions.* ***Right:*** *Psychometric curves across recordings in trials following correct responses, conditional on the FR_{I} and $synchrony_{\mathrm{I}}$. Only trials with favourable (higher FR_{I} and lower $synchrony_{\mathrm{I}}$ than recording average, lower FR_{I} and higher $synchrony_{\mathrm{I}}$ for unfavourable) and unfavourable neural states were considered in each recording. Markers correspond to values in single recordings.* ***b:*** *Same as in a, but for trials following incorrect responses.*

and neural state innovations as predictors. In addition, we included the interaction of neural state predictors with the presented stimulus and the previous response. The differences in task accuracy associated to neural state fluctuations observed in post-error trials could therefore be captured either by direct effects of neural activity on the animals' responses or by a regulatory effect of neural state predictors on the overall effect of the stimulus or response history.

Consistent with higher accuracy following error trials and an increase in accuracy during the session progression in such trials, we observed slightly higher stimulus weights and a significant interaction term of trial number and the presented stimulus in post-error trials ($p<.017$; Figure 3.9). The effect of favourable neural state fluctuations following error trials was also captured in this analysis. Thus, higher firing rates significantly increased the relative contribution of the stimulus on the animals' responses in this analysis ($p<.004$, Bootstrap). The predictive effect of low synchronisation on accuracy was only weakly reflected ($p=.27$), suggesting that it cannot be fully captured by an increase of the relative stimulus contribution alone.

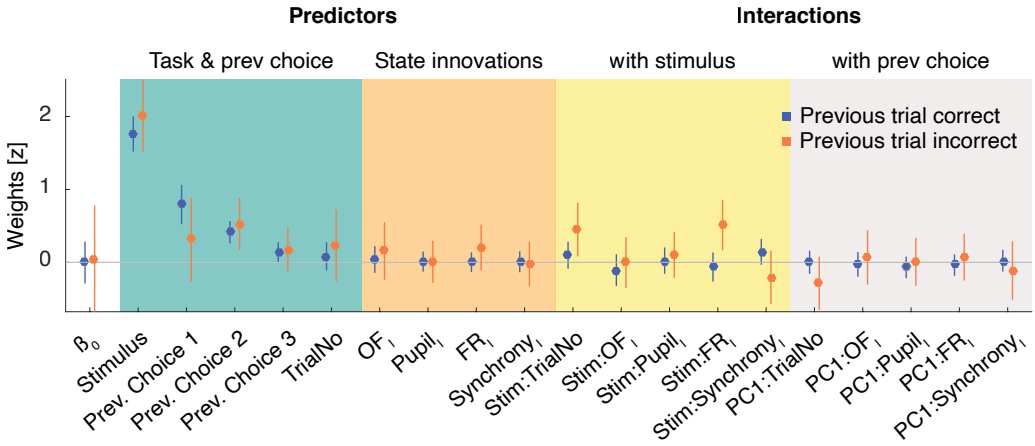

Figure 3.9: ***Conditional dependencies of task responses.*** *Fixed effect weights of the indicated predictors when fitting the animals' responses. Marker colour demarcates the outcome of the previous trial, coloured shades group classes of predictors and ':' indicates an interaction term of two predictors. Vertical lines indicate 95% confidence intervals.*

Consistent with previous observations, neural state predictors had no predictive effect on the animal's behaviour in trials following correct responses. We have demonstrated that discrimination accuracy was only explained by neural state predictors after error trials, but not following correct responses. It is unlikely that this difference is due to outcome dependent modulations of neural activity. While distinct distributions of cortical FR_I and synchronisation innovations following error trials could account for the observed lack of predictive power, the outcome of previous trials was considered in the whitening procedure of all state predictors (see methods). Thus, no systematic differences based on the outcome of the previous trial are expected. We confirmed the lack of systematic differences across post-error and post-correct trials in FR_I and $synchrony_I$ distributions (Figure 3.10a).
To exclude that the small, residual differences present in our data corresponded to the observed out-come dependent differences, the statistics of neural state innovations in both trial groups were matched in each recording using trial sub-sampling (see methods, Figure 3.10b&c). We then constructed two GLMMs predicting the accuracy in the resulting post-error and post-correct data sets with matching distributions in the neural state pre-

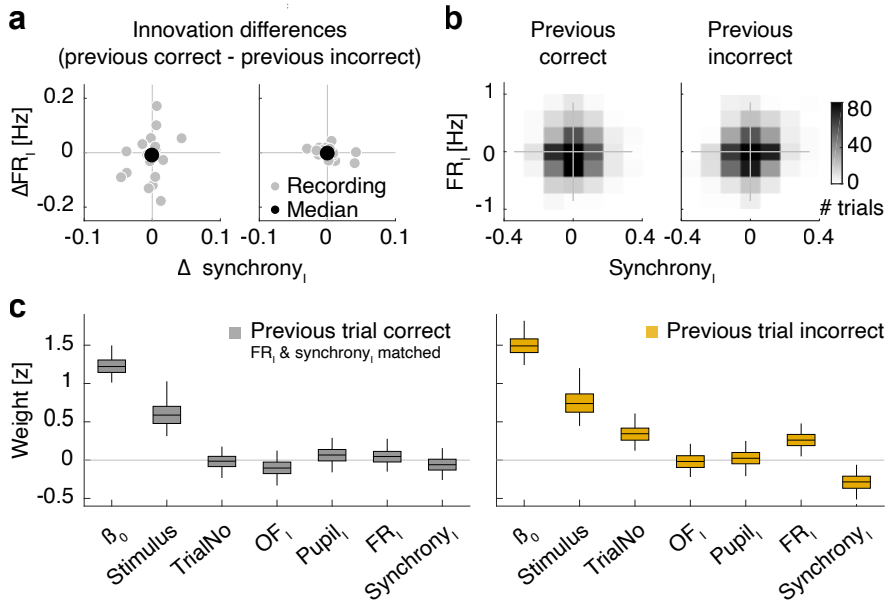

Figure 3.10: ***Response-outcome dependent distributions of neural state variables.*** ***a Left:*** *Scatterplot of differences in FR and synchrony following error trials and correct responses. Positive values indicate higher values in trials following incorrect responses.* ***Right:*** *Same, but after matching distribution statistics by trial sub-sampling (see methods).* ***b:*** *Matched distributions of FR and synchrony in trials following correct (left) and error (right) trials.* ***c:*** *Distribution of fixed effect weights of the indicated predictors in data sets with matched statistics. Distribution obtained in 1000 hierarchical bootstrap iterations fitting task accuracy.*

dictors. As expected, the fixed effects hence obtained remained qualitatively unaltered (Figure 3.10c). The outcome-dependent predictive effects of neural state variables on accuracy were therefore not due to differences in their underlying distributions. Instead, our data established different effects of the same ensemble of neural state innovations depending on outcome of the previous trial.

3.3.3 State innovations and responsivity

Cortical synchronisation and arousal are known to correlate with the responsiveness of animals [162, 113]. Such changes in task responsiveness can

either refer to the propensity of animals to respond in the task at all, and thus reflect a measure of task engagement or, alternatively, also changes in the time mice take to respond. We therefore addressed the association of task and engagement and response time with neural state predictors in our data set.
The degree of task engagement commonly varies across the behavioural session, resulting in periods of disengagement (Figure 3.11a). Because trials were not initiated by the animals in our task paradigm, such periods were reflected by multiple consecutive sound presentations that failed to elicit any licking response (Figure 3.11a). To investigate the relation of fluctuations

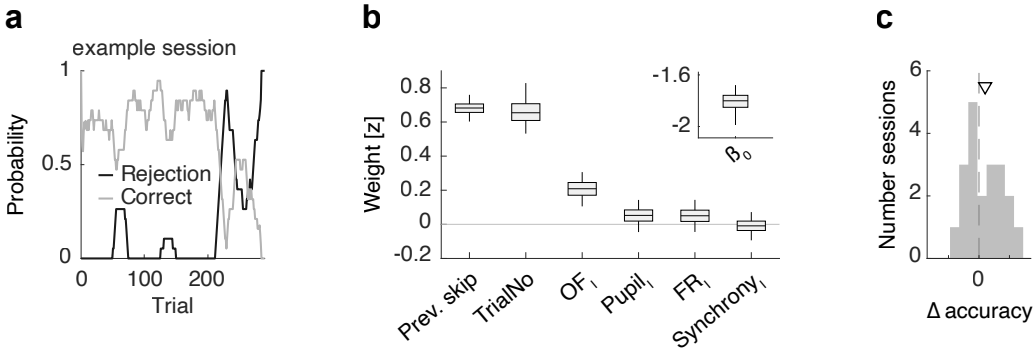

Figure 3.11: ***Effect of state predictors on task engagement.*** ***a:*** *Fraction of rejected trials (skips) and correct responses during an example recording session.* ***b:*** *Distribution of fixed effect weights of the indicated predictors predicting trial rejections. Distribution obtained in 1000 hierarchical bootstrap iterations. Box plot indicates median (mid-line), 50% (box) and 95% confidence intervals (vertical lines).*

of neural state and task engagement in our task paradigm, we constructed GLMMs predicting the animal's propensity to reject the trial. In this analysis, apart from the neural and general state innovations, we considered if the previous trial had been rejected and the trial number to determine the probability of rejecting the current trial. Such rejections were generally scarce in the behavioural sessions, which was reflected by low β_0 weights (Figure 3.11b). Besides from being relatively rare, disengaged trials were predicted strongly by the engagement in the previous trial as well as the trial number. These findings therefore suggested a general loss of task engagement towards the end of the session, where trial rejections were most commonly observed,

as well as a tendency of trial rejections to occur in bouts, as exemplified in figure 3.11a. The increased trial rejection rate towards the session end is partially due to the structure of the behavioural paradigm, as behavioural sessions are terminated due to to persistent lack of engagement (see chapter 2.2). Interestingly, the degree of facial movements (OF_I), but no other state innovation predictor had an additional predictive power ($p_{OF}<.001$, Bootstrap). This association of OF_I with the probability of trial rejection therefore suggested that mice moved more in unengaged trials.
Due to the delay in task structure, response times did not correspond to reaction times in this task paradigm. Nevertheless, we sought to investigate if the timing of these task responses showed a similar correlation with arousal and cortical synchronisation. Response times, defined as the first observed lick after the beginning of sound presentation, varied strongly across trials (Figure 3.12a), but was mostly well within the trials' response period. Interestingly, especially premature responses were associated with lower response accuracy (Figure 3.12a), reminiscent of a speed accuracy trade-off. To determine the relationship of response times in the task with global and neural state innovations, we modelled the animals' response times in a GLMM using recording session as random effect. Among these state innovations,

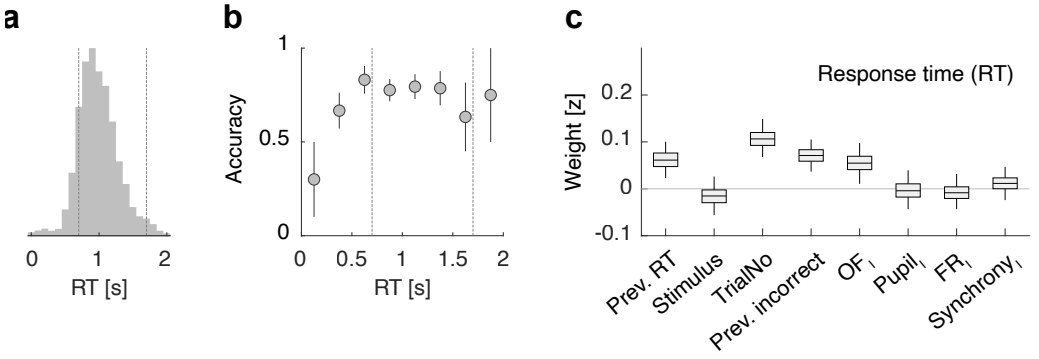

Figure 3.12: ***Effect of state predictors on response time.*** ***a:*** *Distribution of response times (RT) across recordings. Dotted lines demarcate beginning and end of the response period.* ***b:*** *Dependency of task accuracy on response time (Median ± MAD). Trial structure marked as in a.* ***c:*** *Distribution of fixed effect weights of the indicated predictors when fitting response time. Distribution obtained in 1000 hierarchical bootstrap iterations. Box plot indicates median (mid-line), 50% (box) and 95% confidence intervals (vertical lines).*

we considered the response time in the previous trials as well as the trial number as predictors, to account for slow session effects. Moreover, as response times have been shown to depend on the presented evidence [97] and can also be affected by outcome history [49], we included the sensory evidence of the presented stimulus and the outcome of the previous trial for response time predictions. Similar to the observations made in the engagement analysis above, among the four baseline state innovations, only OF_I was significantly associated to the response time in the trial ($p=0.013$, Bootstrap). The strength of the evidence displayed a negative prediction weight, consistent with a speed accuracy trade-off. However, this effect was not significant ($p=0.44$, Bootstrap). Response time was positively associated to errors in the previous trial ($p<.001$, Bootstrap), suggesting an increased response time following error trials. Consistent with slow modulations of reaction time across the session, the trial number as well as the previous response time were predictive of the response timing in the current trial ($p<.001$, Bootstrap).

We therefore conclude that in the context of this task paradigm, our analysis suggested a strong outcome dependent effect of spontaneous neural state fluctuations on task accuracy. The animals' responsiveness in the task, on the other hand, was not associated to neural baseline innovations and only reflected serial dependencies as well as the degree of movement innovations.

3.4 Conclusions

In this chapter we have quantified the effect of fluctuations in the spontaneous baseline firing rate and the degree of cortical synchronisation on accuracy during auditory frequency discrimination. In previous studies, neural synchronisation has typically been quantified using the coefficient of variation [212], the propensity of time periods without cortical firing (silence density) [167] or the power in low frequency bands of population activity [113]. In an effort to quantify the degree of cortical activity and its synchronisation level across multiple acute recordings, we discarded silence density as a measure of cortical synchronisation in our data set, because this measure of spike-free time periods strongly depends on the size of the simultaneously recorded neural population as well as its underlying activity level. Moreover, we refrained from the usage of the coefficient of correlation because in our data this measure correlated with the FR (not shown). Quantification of cortical synchronisation using power in low frequency bands was not possible due to slow, movement related artefacts in the LFP. We therefore introduced a novel estimator for population synchronisation, independent of neural FR, that is based on the observed variability of the MUA in time with respect to the variation expected in a fully desynchronised population with the same FR (Figure 3.1).
While previous studies have shown clear dependencies of spontaneous neural activity on movement and arousal [210, 161, 255, 224], our measures of $\text{synchrony}_\text{I}$ and FR_I revealed a selective correlation of movement innovations with FR_I and an association of $\text{synchrony}_\text{I}$ with movement and arousal innovations (Figure 3.5). This dissociation of FR and synchronisation dependencies is consistent with previous observations in the visual cortex [280]. Trial-by-trial innovations in these neural state measures had little effect on the discrimination accuracy in the task (Figure 3.6), confirming previous observations in head fixed mice [113]. In contrast, task accuracy was predicted by the outcome of the previous trial, indicating a history-dependent component in the animal's behaviour. Influences of task history on behavioural performance are common in 2AFC tasks and typically modulate the subject's tendency to repeat previous choices [28, 77]. Alterations of task behaviour and accuracy following error trials, as observed in this data set, have also been described previously [99, 49].
Importantly, we discovered that these post error changes in behavioural ac-

curacy also increased its association with neural baseline innovations. As expected, the limitation of the predictive effect of neural state fluctuations to post error trials was not due to differences in the distribution of post error and post correct innovations. Instead, our analysis suggested context-dependent differences in the relation of similar ensembles of cortical activity to behavioural accuracy (Figure 3.10). While multiple studies have demonstrated a general dependency of neural stimulus representations and underlying brain state fluctuations [76, 192, 13, 132], our analysis suggested that the behavioural relevance of such changes in representations might be gated by the behavioural context.

Because activity in the ACx is known to modulate the behavioural accuracy in discrimination of pure frequency tones, but is not necessary for performances above chance [299, 4, 190, 34], it is possible that the different effects of spontaneous fluctuations in baseline activity in post-error trials and after correct responses reflect different, context-dependent contributions of the ACx to frequency discrimination. In such a scenario, the impact of cortical silencing would also be expected to display the observed outcome-dependency. However, this hypothesis will have to be tested in future optogenetic silencing experiments.

Importantly, our findings are not in contradiction with previous work, reporting no correlation of cortical state fluctuations with task accuracy [113], as we did not observe significant general effects of brain state fluctuations with accuracy either. Interestingly, in this study by Jacobs et al., weak but significant differences in brain state were reported in auditory tasks with relatively low discrimination accuracy, while these effects were insignificant in visual counterparts of the task with high performance levels. This discrepancy could be explained with a common response-outcome dependent association of brain state with discrimination accuracy. Thus, the fraction of post-error trials, in which neural state predictors are predictive of behavioural accuracy, depends on the overall performance levels, resulting in high fractions of post-error trials in the auditory version of the task, while such trials were mostly absent in the visual counterpart. Different accuracy levels in the task therefore can change the overall presence of brain state effects on discrimination accuracy. However, it is also possible, that the predictive effect of neural state is variable across modalities.

Across modalities, variations in cortical synchronisation are well known to correlate with task performance in rodent Go-NoGo task paradigms as

changes in cortical synchronisation and arousal have been shown to reflect differences in the propensity and speed of task responses [161, 177, 224, 248, 88, 255, 170, 160, 113]. However, in this task, no association of spontaneous fluctuations of neural state predictors and the animals' engagement or response time have been observed (Figure 3.11 & 3.12). Because we only considered the neural signals that could not be accounted for using state predictor history (see methods) and used all obtained state innovations jointly to model the animals' responsiveness, state influences in our analysis were explained by movement fluctuations alone. It is important to state, that the response time analysis performed here is not directly comparable to the previously reported correlations of reaction time and brain state. Even though response times showed some features usually observed in reaction time studies, like post error slowing and a weak speed accuracy trade-off [49, 97, 203, 274] (Figure 3.12), response times in our task paradigms were shaped by the delay structure of the task and therefore do not correspond to reaction times.

Taken together, we have demonstrated a response-outcome dependent association of spontaneous fluctuations in baseline activity in ACx with accuracy in a delayed frequency discrimination task. While a general correlation of such fluctuations with the quality of stimulus representations has been established previously, this is the first demonstration that the corresponding association of spontaneous cortical state fluctuations with discrimination accuracy can be gated by context.

Chapter 4

Sensory and control limitations shape behavioural strategies

HIGHLIGHTS

- In this chapter, we introduce a simple, temporally predictable frequency discrimination task for head fixed mice.
- We show that, independent of the frequency ranges used, animals solve the task by adopting a default-response strategy with anticipatory licking at the lick spout associated with high frequencies.
- We provide theoretical considerations and experimental evidence that this task strategy is rooted in frequency dependent differences in stimulus perception.
- Last, we show that the behavioural strategy adopted by the mice counteracts these sensory asymmetries and is subject to the specific licking control costs of the task paradigm.

4.1 Introduction

A decision is the process that results in a deliberate commitment to a categorical proposition [78]. In sensory-motor decision making, subjects are required to form decisions about certain features of sensory stimuli. Such features can be the direction of cohesively moving dots [178, 153], the frequency of a sound [115] or the location of its source [197]. These decisions then need to be reported by the execution - or omission - of defined actions. These tasks therefore require the subject to infer the state of the outside world given the information provided by their sensory systems [78, 126, 205, 259, 281].
While such tasks have been used in psychophysical studies to determine the perceptual thresholds of the sensory systems to inform decisions [64, 263, 234, 51, 127, 91, 199, 52], behaviour in such tasks is not exclusively representing the degree of sensory evidence available to the subject. Thus, repetitive behaviours, termed choice biases, have been frequently observed in rodent and human performances [28, 5, 99, 143]. The overall magnitude of such choice biases is commonly modulated by the degree of sensory evidence available, but also susceptible to task design and internal factors [265, 143, 266, 37, 182, 277]. Additionally, the cost of cognitive control has been shown to alter task strategies in humans and may therefore cause suboptimal behaviour [103, 19, 18].
While choice bias and repetitive behaviour often lack variability and serve no apparent function in the task [139, 182], recent studies have shown that they can also reflect meaningful task parameters and be updated with response outcome [128, 99]. Choice biases and other task-irrelevant behaviour might therefore offer important insights in the underlying behavioural strategies and potential asymmetries in sensory processing and decision making processes [66, 70, 143]. While sensory decision making has been traditionally studied in primates [30], similar tasks have been developed for mice more recently, thus allowing investigation of the underlying brain function using the rich tools available for genetic alteration and manipulation of brain activity [85, 87, 17, 297, 41, 225].
Among the many experimental settings used to study mouse behaviour, head fixed preparations are increasingly common as they limit additional movement and facilitate the recording of neural activity as well as the arousal state of the animal in addition to movement related data [225, 85, 27, 158, 86, 219]. Two main versions of head fixed preparations have been presented, Go-NoGo

and 2AFC tasks. In Go-NoGo tasks, trials of one category are associated with a response action, typically pressing a lever or licking at a water delivery spout, while these responses have to be omitted in the absence of the respective stimuli. Such tasks are relatively easy to learn, however, their asymmetric response structure can impede the dissociation of dedicated responses and task engagement [30]. These difficulties are minimised in 2AFC tasks. In such paradigms, animals have to select one of two different response actions that are each associated with one stimulus category, allowing for an easier dissociation of response accuracy and task engagement [30]. For frequency discrimination in the auditory domain, both Go-NoGo as well as 2AFC tasks have successfully been implemented [225, 122, 161, 151, 115, 41, 53]. Despite the general interest though, the different factors shaping and limiting task behaviour are poorly understood.

The aim of this work is therefore to investigate the behavioural strategies of head fixed mice during auditory frequency discrimination and identify the underlying performance limiting factors. Despite the symmetric 2AFC task paradigm, we observed clear behavioural asymmetries shared across mice and frequency ranges. We present evidence that this asymmetric behaviour corresponds to an optimal behavioural strategy based on asymmetries in perception and limitations of cognitive control.

4.2 Methods

All proceedings were in accordance with standard operating procedures approved by the Champalimaud foundation's animal welfare body under the project #2018/007 'Principles of Sensory- and Memory-guided Auditory Decision Making: Behavior and Neural Basis'. Surgical procedures and training structure were based on protocols established by Guo et al. [85]. All surgeries used standard antiseptic methods. All experiments were performed using male C57BL/6J mice that were housed on a 12h inverted light/dark cycle.

4.2.1 Head bar surgery

During induction of anaesthesia, animals (6-8 weeks of age, 20-22g body weight) were anesthetized with 2-3% (volume in O_2) isoflurane (Vetflurane, Virbac) and subsequently mounted in a stereotactic apparatus (RWD Life Science) on a heating pad (Beurer). Once animals were stably mounted, isoflurane levels were lowered to 1-1.5% and the eyes were covered with ointment (Bepanthen, Bayer Vital). The head was shaved and the scalp cleaned with betadine. A midline incision was performed to expose lambda and bregma, which were subsequently used to align the skull with the horizontal plane of the stereotactic frame by measuring their position with a thin glass capillary (Drummond Scientific). The skull anterior of bregma was exposed by cutting a small area of skin. The exposed area was cleaned with betadine and slightly roughened by scraping it with a surgical blade (Swann-Morton). This procedure improved the attachment of the glue forming the base of the implanted head bar. Subsequently, the skull was dried with sterile cotton swabs and covered with a thin layer of super glue (UHU). To further increase long-term stability, four 0.9mm stainless steel base screws (Antrin Miniature Specialties) were placed in the skull. The exposed skull and base screws were then covered with dental cement (Tap2000, Kerr). A custom designed head bar (22x4x1mm, aluminium, GravoPlot) was lowered into the dental cement while still viscous until the head bar was in contact with the base screws. Subsequently, an extra drop of dental cement was applied to the centre of the head bar in order to fully engulf its medial part. The remaining skin incision along the midline was then sutured. The animals were injected with buprenorphine (opioid analgesic, 0.05 mg/kg) into the intraperitoneal cavity

and allowed to recover for 3-5 days.

4.2.2 Training procedure

After recovery from head bar implantation the animals were water deprived for 12h prior to the first handling session. In handling sessions mice were accustomed to the experimenter and being placed in an aluminium tube to restrain their movement. In the first days of handling, the tube was placed in the animal's home cage. Once the mouse voluntarily entered the tube, it was presented with water delivered manually from a syringe at the end of the tube. This procedure therefore roughly mimicked the water delivery system in the training apparatus. Mice were allowed to drink a max of 1.5ml of water during each handling session (30min). If animals failed to consume sufficient water they were supplemented to a total of 1ml. The aluminium tube remained in the animal's home cage during the entire week of handling to promote adaptation to it. Animals usually learned to enter the tube and drink in their home cage within three sessions. Subsequently, the tube was presented in the experimenter's hand and, once the animal entered the tube, it was lifted out of the home cage before allowing the mouse to drink. Most animals drank at least 1ml in the restraining tube outside of their home cage within two handling sessions. Once mice were accustomed to receiving water in the aluminium tube and being handled by the experimenter, they were placed in the behavioural setup and head fixed with the two water delivery spouts approximately 1cm in front of their mouth. To adapt them to head fixation, free water was delivered upon licking at either of the water delivery spouts. Lick detection was based on junction potential measures between the aluminium restraining tube and the stainless steel lick spout [94]. After triggering and consuming 15 rewards, training proceeded as summarised in table 4.1.
A brief 10ms green light flash signalled the onset of a trial 200ms before presenting either of two pure frequency sounds (60dB, 10 or 28kHz, duration: 600ms, presentation pseudo random, maximum 3 repetitions per condition), indicating at which of the two water delivery spouts a water reward would be available. Importantly, the mapping of frequency and response spouts was counter balanced in all cohorts trained. Sounds were presented from either of two lateral speakers located at a 2cm distance from each ear. The sound location alternated either in blocks of 50 trials or on a trial-by trial

Stage	Dur	Stimuli [kHz] (Low&High)	Priming	Error	Light [s]
1	.6s	10 & 28	10%	none	.01 at -.2
2	.15s	10 & 28	10%	none	.3 at -.5
3	.15s	10 & 28	none	ITI+6s	.3 at -.5
4	.15s	10,12,14.3 & 20.2,24,28	none	ITI+6s	.3 at -.5

Table 4.1: ***Summary of main training stages.*** *Shown are the final parameters at each stage of the training for sound duration (Dur), high & low frequencies presented, fraction of primed trials with reward delivery prior to response licks, time punishment after error trials and the duration and onset (at) of the light cue.*

basis, depending on the animal. Importantly, sound location was task irrelevant at all times and correct task behaviour required ignoring the location of the stimulus and report if its frequency was high or low instead. The first lick in the response period, which started 150ms after the sound onset and lasted for 2s was considered the animal's response. Responses at the correct spout triggered a 3μl water reward, responses at the incorrect spout did not have any consequence. Following the response period the animals were presented with a new trial after an ITI of 0.5s. To keep the mice engaged in the early phases of training and facilitate the learning of the frequency-to-spout mapping, a free water reward (3μl) was delivered at the onset of the response period in a random 10% subset of the trials. Consumption of these free rewards were recorded as the animals responses and triggered an additional 3μl reward. Importantly, all trials with free water delivery were excluded from later analysis. Animals stayed in this training stage until they responded in more than 90% of unprimed trials (window of 20 trials), independently of their response accuracy. Once animals responded reliably, trial onsets were signalled by a 300ms green light signal, 500ms prior to sound onset. Sound duration was reduced to 150ms and the response period to 1s, followed by a variable ITI of 4-7s. To facilitate their adjustment to the novel timing, incorrect responses were not punished and free reward was delivered in 10% of the trials until the engagement of the animals returned to 90% of 20 consecutive unprimed trials, which typically was achieved within the first 4 days of training.
Subsequently the priming of responses by delivering free water rewards ceased and incorrect responses were punished by increasing the ITI by a

6s penalty. Mice stayed in this training phase until they had learned the basic task contingency and performed stably with a d-prime > 1 across a full session. If at any time during training the animals' responses became heavily biased towards one licking spout, animals were encouraged to respond at the unpreferred spout by manually delivering a free reward at the unpreferred licking spout and temporarily presenting stimuli associated to this spout exclusively until the animals resumed responding. All trials with either free water rewards or sound presentations exclusive to frequencies above or below the threshold were excluded from analysis.
Once animals performed reliably in the basic task paradigm, additional frequencies closer to the threshold were introduced gradually, by adding four additional frequencies (below threshold: 10.5kHz, 10.8kHz; above threshold: 27.6kHz, 26.7kHz) and increasing their difficulty gradually in fives sessions until the final set of frequencies was reached (below threshold: 10kHz, 12kHz, 14.3kHz; above threshold: 20.2kHz, 24kHz, 28kHz).

Training batch	Animals	Low stimuli [kHz]	High stimuli [kHz]
10-28kHz mice	9	10 12 14.3	20.2 24 28
10-20kHz mice	5	10 11.2 12.6	15.9 17.8 20
4 -11kHz mice	10	4 5.1 16.5	7 8.9 11
Early rejection	5	2 2.8 4 5.7	11.3 16 22.6 32

Table 4.2: ***Summary of frequencies used in different training batches.*** *Shown are the final frequencies presented in steady state behaviour. For animals trained to investigate early trial rejection rates, all steady state frequencies were presented from the beginning of training on.*

For animals trained on different frequencies and used for later manipulations of task contingencies, the training progressed in the same way (see Table 4.2 for all low and high stimuli across trained batches). Mice trained to determine the effect of sound frequency on trial rejection rate (n=5, Early rejection cohort) were following the same early progression of training, however, not only the extreme frequencies, but all 8 frequencies (Low frequencies: 2, 2.8, 4, 5.7kHz: High frequencies: 11.3 16 22.6 32kHz) were presented from training stage 1 on.

4.2.3 Analysis of task reponses

For analysis of behavioural data all trials with manual interventions or response priming were excluded. For steady state behaviour, trials from all sessions performed in the final stage of the task were used (minimum 5 sessions). Psychometric curve fits were calculated using the psignifit toolbox [235] for Matlab (MathWorks). Task performance was calculated as the fraction of all trials with correct responses, while accuracy was defined as the fraction of correct responses among all non-rejected trials. If not otherwise mentioned, all summary statistics refer to the population median. Similarly, error bars demarcate the Median Absolute Deviation (MAD), if not otherwise stated.

4.2.4 Signal detection theory predictions

To illustrate how biased decision criteria can represent optimal policies under sensory asymmetries (Figure 4.2), we determined the optimal decision criterion c as the intersection of two Gaussian probability density functions (mean = ±5, -5<c<5) with different widths (standard deviations from .1 to 10, Figure 4.2d).
The optimal decision criterion for multiple frequencies in each category was determined by the intersection of the combined probability density functions of each category (Figure 4.3). Similar to the additional frequencies in the behavioural training paradigm, easy frequency DV distributions remained unaltered (mean=±5, standard deviation$_{Low}$=1, standard deviation$_{High}$ =2) and two additional frequencies per category were introduced, with the mean of the distribution corresponding to stimuli of medium difficulty being placed at the centre between mean$_{Easy}$ and mean$_{Hard}$. For simplicity the standard deviations within one task category did not change with difficulty (narrow distribution: std=1, wide: std=2)
The predicted discrimination accuracy of difficult low and high frequency stimuli was then calculated as the area under the probability density function of difficult stimuli until the decision criterion (Figure 4.3b). The difficulty was given by the distances of the distribution means to the initial easy distributions (displacements 0 to 4 used) and the optimal decision criterion was calculated at each difficulty assuming the presence of easy (difficulty=0), hard (difficulty indicated in the plot) and medium (difficulty=difficulty$_{Hard}$ *0.5) frequencies.

4.2.5 Analysis of anticipatory licking behaviour

Average licking frequency was calculated for each animal by counting licks aligned on sound onset in non-overlapping 20ms bins (Figure 4.7). To quantify pre-stimulus licking (Figure 4.9) the average number of licks at either spout in the 300ms prior to sound presentation was calculated and the difference of pre-stimulus licks at the high and low frequency report spout was formed. To characterise the asymmetry in such pre-stimulus licking across animals, the difference in mean pre-stimulus lick counts at the two spouts was formed and divided by their sum for each animal separately. Therefore, licking asymmetry was not influenced by the general amount of pre-stimulus licking but presented a bounded measure of the asymmetry relative to the overall number of pre-stimulus licks.
To describe licking during early training, the animals' behaviour from the second through the fifth training session was pooled and analysed. Similarly, trial rejection rates in animals exposed to multiple frequencies in early training sessions (Early rejection cohort, Table 4.2) were calculated from the second to the fifth session. Trials were pooled across session for each animal and the relative trial rejection rate for each presented frequency was calculated. The dependency of these relative rejection rates on frequency across the animals was captured by fitting a polynomial of degree 4 in Matlab.

4.2.6 Generalised linear modelling

To dissect the relative contributions of the presented stimuli, anticipatory licking and trial history, the location of response licks of single animals was modelled using a Generalised Linear Model (GLM) approach. Models were implemented using the glmnet toolbox [69] for Matlab. Trials from steady state sessions were pooled for each mouse and the response in each trial was modelled using six binary stimulus predictors, four binary predictors describing anticipatory licking and three choice history predictors. Each of the stimulus predictors was 1 in all trials where a specific stimulus had been presented and 0 in all remaining trials. The predictors describing pre-stimulus licking consisted of 2 pairs of binary predictors indicating the locations of the last and second to last lick prior to the onset of the response window. Thus for a given lick location, the predictor of the respective pair associated to that spout would be 1, the other 0. This structure was chosen in order to allow for asymmetric contributions of licks at the high and the low frequency

report spouts. The first of the three choice history predictors described the response in the previous trial (-1 for low frequency, 1 for high frequency report, 0 if previous trial was rejected), while the remaining two choice history predictors indicated the response in the previous trial depending on the outcome. Thus one predictor indicated the response in the previous trial only if the previous trial was correct, while having the value 0 if the previous trial was rejected or the response was incorrect. Similarly, the last choice predictor had values different from zero only if the response in the previous trial had been incorrect. Logistic regression models were fit predicting the probability of a high frequency report lick using elastic-net parameter α=0.5.

The optimal regularisation parameter λ and the corresponding linear weights β were calculated using cross-validation and choosing the λ with the Mean Squared Error (MSE) one standard deviation away from the smallest MSE. To assess the quality of predictions by models hence obtained, we performed 10 fold nested cross validation. We hence fitted the optimal cross-validated model on 90% of the data and predicted the responses of the animal in the remaining 10%. By repeating this procedure 9 times, probabilities of low or high frequency responses were obtained for the full dataset in each animal. The quality of the predictions was then determined by calculating the Area under the ROC Curve (AUC) in each animal.

To determine the contribution of each predictor, we determined the fraction of the model's variance it captured. In this procedure we determined the best cross validated model for the full dataset of each animal and determined the variance of its responses. We then restricted the model to the predictors of interest and calculated the resulting model responses. The fraction of the full model's variance contained in the variance of these responses was then taken as the contribution of the particular predictor.

To determine the responses of the animals considering only a subset of the predictors, predictions of the models trained on the full data set were used. The probability of high frequency report responses was determined in each trial by calculating the response of the model restricted to the desired predictors. Next, the resulting psychometric curve was calculated with the psignifit toolbox for Matlab as above using the mean probability of high report licks across animals.

4.3 Results

4.3.1 Task and performance

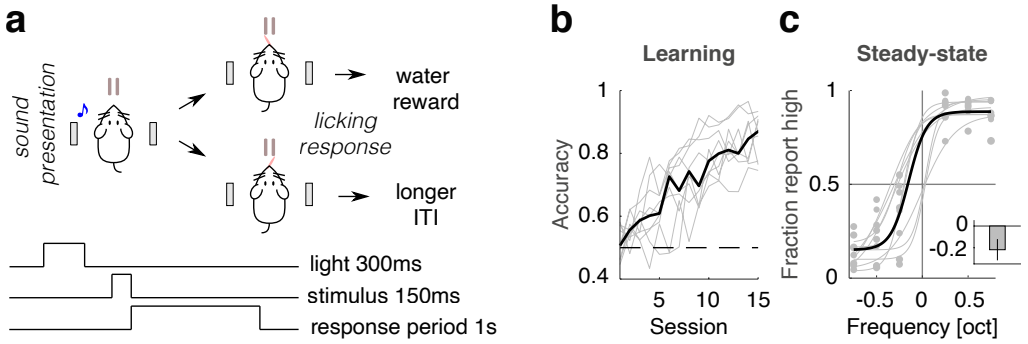

Figure 4.1: ***Task outline and performance. a Top:*** *Scheme of task contingency. Each trial, head fixed mice are presented with high or low frequency sounds from one of two lateral speakers (grey bars). Animals report 'high' or 'low' by licking at one of two lateral water delivery spouts (brown bars).* ***Bottom:*** *Scheme of timing contingencies in a trial.* ***b:*** *Learning of task contingencies. Accuracy of responses in individual mice (grey) and cohort average (black, n=9) in the first sessions of training. Dashed line demarcates chance level.* ***c:*** *Psychometric curves of engaged trials during steady state behaviour. Single animals are shown in grey, black line represents cohort average. Marker size corresponds to the number of trials performed in each condition.* ***Inset:*** *Median threshold of psychometric fits in individual mice ± MAD.*

We trained head fixed mice to discriminate pure frequency tones in a two alternative forced choice (2AFC) paradigm (Figure 4.1a). A 300ms light signal after a random ITI indicated the beginning of a trial. 200ms after light offset, mice were presented with either a high or a low pure frequency sound for 150ms, indicating at which of two water delivery spouts water would be available. Importantly, in this task paradigm, mice were free to lick at the water delivery spouts at any time point prior to the stimulus offset without consequences for the task progression. Instead, we only considered the first lick at a water delivery spout after sound offset to be the dedicated response to the presented stimulus. If this response lick occurred at the spout indicated by the presented stimulus, animals received a 3μl water

reward at that spout. Incorrect responses were punished by a time penalty. Animals learned the task contingencies quickly and accurately licked at the correct lick spout 80% of the trials within two weeks of training (Figure 4.1b). However, while animals reported accurately in easy trials, most well trained animals showed a clear bias towards high frequencies for difficult stimuli, prominently visible in the cohort average (Figure 4.1c).

4.3.2 Optimal strategy under sensory asymmetry

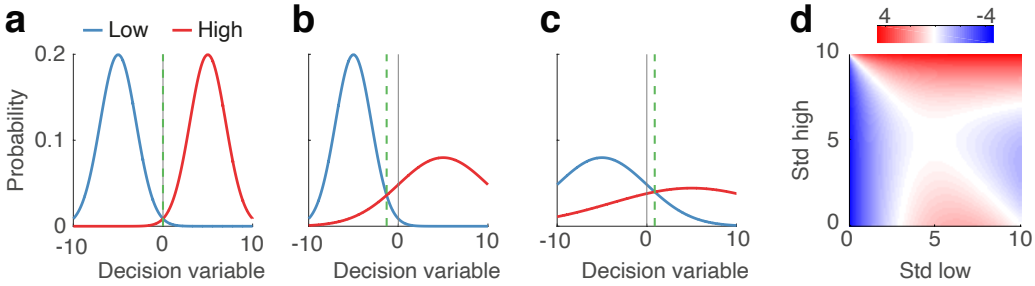

Figure 4.2: ***Dependencies of the decision criterion.*** ***a:*** *Distributions of the decision variable in high and low frequency trials have equal widths. The optimal criterion is demarcated in green (dotted line).* ***b:*** *As a, but for different distribution widths.* ***c:*** *As b, but in a low discriminability scenario.* ***c:*** *Dependency of the ideal criterion on the standard deviation (Std) of DV distributions (distributions means= ±5).*

Under the assumption that our mice performed optimally, we used insights derived from signal detection theory (SDT) to gain intuitions about the factors possibly underlying this generic asymmetry in the task behaviour. In this framework, the observed shift in the psychometric curves should be captured by a non-zero value of the decision criterion c. This decision criterion is given as the value of the decision variable (DV) that is equally likely in the distributions of the two task categories. If these distributions have equal width (Figure 4.2a) and stimuli of the two task categories are presented randomly and with equal probability, the ideal criterion is therefore zero (no evidence for either high or low frequency) and diverging criteria represent a sub-optimal task strategy.
However, non-zero criteria can also reflect optimal behavioural strategies, if the two DV distributions have distinct widths. Interestingly, both shifts

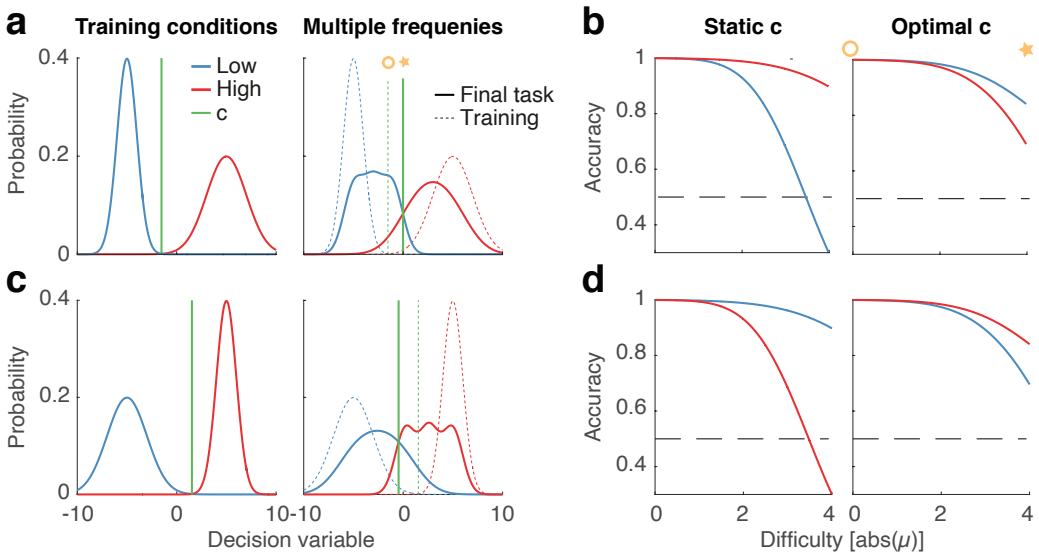

Figure 4.3: ***SDT predictions for multiple frequencies. a Left:*** *Distributions of the DV for easy high and low frequency trials with diverging width (σ_{Low}=1; σ_{High}=2) and the optimal c.* ***Right:*** *Same, but after the introduction multiple frequencies (Means= $\pm 5, \pm 3.5, \pm 2$). Markers demarcate optimal criterion for multiple frequencies per condition (star) or presentation of two easy stimuli only (circle).* ***b:*** *Predicted accuracy in difficult low (blue) and high (red) frequency trials with increasing distance of difficult and easy trial DV distributions (Difficulty). Markers correspond to conditions in a.* ***Left:*** *With static c, optimal for discrimination of the initial two easy frequencies.* ***Right:*** *With optimal c considering multiple frequencies at each difficulty level.* ***c:*** *As a but with wider low frequency DV distributions. σ_{Low}=2; σ_{High}=1) and Means= $\pm 5, \pm 2.6, \pm 0.2$.* ***d:*** *As b, but for distributions in c.*

towards narrower as well as towards the wider DV distribution can represent ideal decision criteria, depending on the underlying discriminability (Figure 4.2b-d). Thus the ideal decision criterion is shifted towards the distribution with the smaller standard deviation in scenarios with relatively high d-primes while this shift inverts towards the wider distribution in low discriminability scenarios (Figure 4.2d).

Importantly though, in these scenarios only the presentation of one frequency per category was considered. While these situations can correspond to the task conditions during early training in which only the two easy stim-

uli are presented, multiple frequencies are presented per task category in the final task paradigm (Figure 4.1c). We therefore investigated the predicted behavioural accuracy arising from an optimal decision criterion adjusted for the presence and difficulty of two additional frequencies per task category (Figure 4.3). Generally, the introduction of additional, medium and hard frequencies was associated with a reduction of the initial bias (Figure 4.3a). In the extreme, with difficult frequencies very close to the threshold separating the two task categories, the sign of the bias was observed to invert (Figure 4.3a, bottom). Whatever the sign of the optimal criterion though, predicted performances reflected the differences in the distribution widths across task categories. Thus task accuracy of frequencies associated to wider DV distributions was affected stronger by increasing difficulty than the corresponding stimuli with narrow distribution width (Figure 4.3b, right). Interestingly, the adjustment of the criterion to difficulty was essential for this robustness as the opposite effect was observed for the predicted accuracy with a static criterion, optimal for the initial training scenario with the two easy frequencies only (Figure 4.3b, left). Thus, due to the biased initial criterion, performances of difficult stimuli with narrow task distribution decrease drastically with increasing task difficulty if the criterion is not adapted to the altered task conditions.
Notably, this scenario of a static criterion strongly resembled the observed task accuracy of our mice (Figure 4.4). Thus, after the introduction of

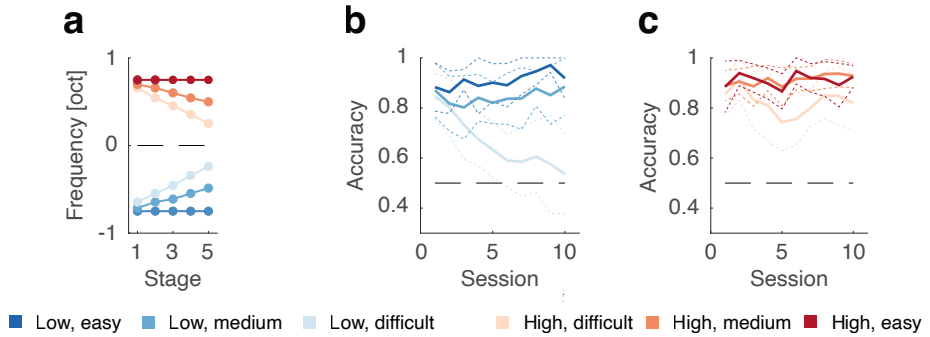

Figure 4.4: ***Discrimination accuracy across difficulty levels.*** ***a:*** *Scheme of increasing difficulty levels during training.* ***b:*** *Accuracy in low frequency trials across mice during sessions with increasing difficulty. Thick lines demarcate cohort median, dotted lines correspond to Median ± MAD.* ***c:*** *As b, but for accuracy in high frequency trials.*

multiple frequencies and while the task difficulty gradually increased across sessions, this increase in difficulty strongly affected the accuracy of low frequency trials only, while no clear effect of increasing difficulty was visible in performance of high frequency trials. Among the previously suggested scenarios, this asymmetry in response accuracy is therefore most compatible with a deficit in the perception of high frequency stimuli, corresponding to a wider distribution of DVs in high frequency trials, in combination with a crystallised decision criterion that is not updated upon the introduction of additional frequencies. While less similar, the higher performances in difficult high frequency trials could however also be explained by a deficit in low frequency perception under an optimal criterion for multiple frequencies presented in each task category.

4.3.3 Frequency-dependent sensory asymmetries

In order to distinguish between these two possible scenarios, we analysed the performance of animals in the early stages of training before multiple frequencies had been introduced. At this stage, both scenarios capable of describing the bias of our animals in difficult low frequency trials predict optimal performance, but assume different sensory asymmetries. As high and low frequencies are presented with equal probability, the optimal criterion for two stimuli is set at the intersection of the two probability density functions corresponding to the distributions of the DV. The width of these distributions therefore determines the distance from this intersection point until the probability has decayed to 0, as slopes will be steeper in the narrower distributions. Importantly though, these differences also correspond to differences in the area under the curve determining the fraction of incorrect decisions (see Figure 4.2b for intuition). Therefore, any difference in discrimination accuracy under the ideal criterion favours the distribution with narrower width.
Interestingly, performances in early training showed clear asymmetries in all animals. Notably though, these differences were mostly due to higher rates of trial rejection, rather than differences in response accuracy (Figure 4.5a). However, both trial rejection rate as well as the smaller differences in task accuracy favoured low frequency trials, consistent with the interpretation of limited high frequency perception and a crystallised decision criterion in later task stages. Because animals have not yet learned the task contin-

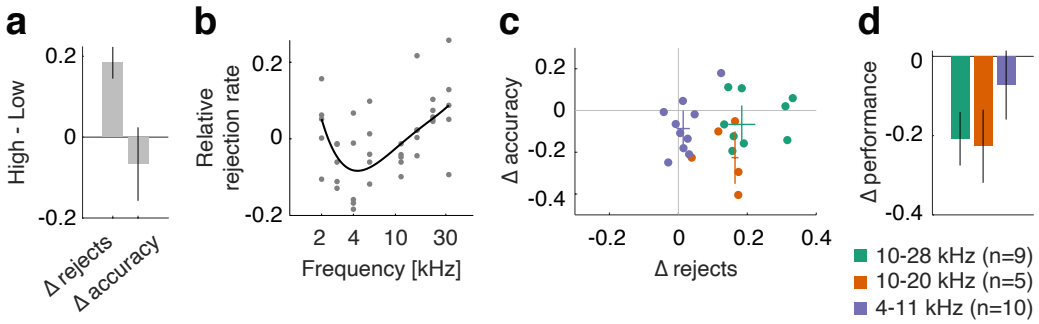

Figure 4.5: ***Asymmetric sound perception.*** ***a:*** *Median difference in trial rejection rate and response accuracy across mice. Errorbars denote MAD.* ***b:*** *Relative rejection rate of naive mice presented with multiple frequencies during the beginning of training (see methods). Markers denote rejection rates in individual animals, black line the cohort fit.* ***c:*** *Early differences (high - low) in trial rejection rate and response accuracy of animals trained with different stimuli. Coloured markers correspond to values of individual animals, lines denote the median ± MAD of each training condition.* ***d:*** *Quantification of performance differences (high - low) of animals presented in c. Bars denote the median, error corresponds to MAD.*

gency at these early stages of the task, the underlying cause of differences in trial rejection rate can not be unambiguously identified from this data. It is possible that the observed difference in trial rejection rates reflect the same sensory limitation responsible for a biased decision criterion - as a limited or more variable perception of high frequency stimuli might also impede learning of the correct stimulus-response mapping. Thus, if high frequency precepts appeared more variable, corresponding to a wider distribution of DV distributions, a mapping of well defined low-frequency stimuli to the appropriate response action can likely be learned faster, while the perceptual variability among high frequency trials could impede the fast learning of the correct task responses.
Alternatively, these diverging trial rejections might indicate a difference in sound detection levels. However, while lowest sound detection thresholds are typically reported at frequencies around 15kHz [152], lowest trial rejection rates were observed for 4kHz stimuli in naive animals presented with multiple stimuli (Figure 4.5b, see methods). Moreover, across multiple frequency pairings, the sign and and degree of differences in trial rejection and accu-

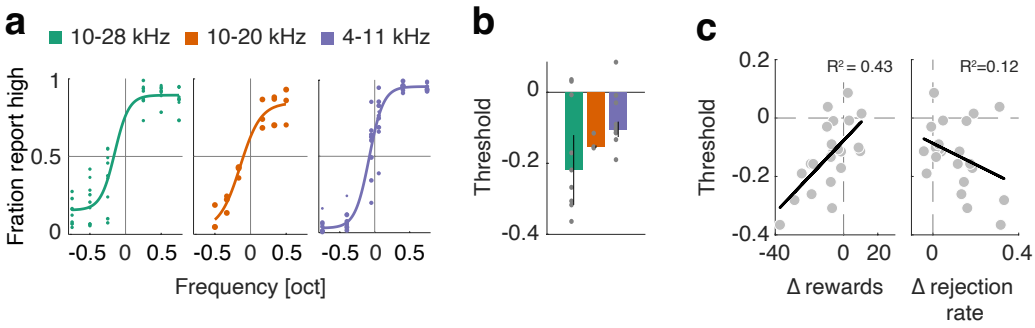

Figure 4.6: ***Early performance differences predict steady state bias.*** ***a:*** *Psychometric curves of animals trained with different frequency sets. Marker sizes correspond to trial numbers, lines show the cohort fit.* ***b:*** *Median ± MAD of threshold of psychometric fits in a. Markers correspond to individual animals.* ***c*** ***Left:*** *Scatter plot of differences in rewards obtained during early training and the biases (thresholds of psychometric fits) during steady state behaviour across all 3 cohorts in a. Markers correspond to individual animals, line shows the linear fit.* ***Right:*** *As left, but for differences in early rejection rate and steady state biases.*

racy across high an low frequency trials matched (Figure 4.5c). We therefore concluded that, due to the similarity of differences in trial accuracy and rejection rates, these behavioural deficits are likely reflecting different effects of the same underlying sensory asymmetry rather than the distinct effects of frequency dependent limitations in sound detection and perception. Notably, as early frequency-dependent differences in task accuracy and trial rejection rate were not limited to our initial training frequencies but were instead observed across all tested frequency pairings, these behavioural differences likely represent general asymmetries in pure frequency perception. Importantly though, cohorts trained to discriminate different frequencies displayed diverging intensities of high frequency performance deficits (Figure 4.5d), indicating different degrees of underlying sensory asymmetries. Because we have proposed initial sensory biases and limitations as the underlying cause of behavioural asymmetries in well trained animals, these diverging sensory asymmetries in early task behaviour should also be reflected in the behaviour of the well trained animals. As stronger sensory asymmetries should correspond to bigger values of the optimal decision criterion in high discriminability scenarios (Figure 4.2d), stronger performance differences in early training should therefore correspond to a bigger shift of

the psychometric curve in the final stage of the task.
Consistent with this prediction, the degree to which performances in low and high frequency trials differed in early training roughly corresponded to the threshold of the psychometric curves in well trained animals (Figure 4.6a&b). To address the relationship of the decision criteria in well trained animals with asymmetries in early training stages more directly, we quantified how well differences in reward and trial rejections rate during early training predicted later biases. Importantly, across all trained cohorts the extend to which animals received different amount of rewards in high and low frequency trials did correspond well to the size of the bias displayed during steady state behaviour (Figure 4.6c, $R^2 = 0.43$). The differences in early rejections rates did correspond roughly to the bias during steady state behaviour across batches as well ($R^2 = 0.12$), indicating a combined relationship of early trial rejections and accuracy differences with steady state biases. Our data therefore suggests that stimulus dependent limitations in naive animals underlie the behavioural asymmetries in well trained animals. Thus the shift of the psychometric curve observed in well trained animals revealed frequency-dependent sensory limitations as well as a limitation in cognitive control preventing the animals from adjusting a previously formed decision rule with the introduction of additional stimuli and difficulty.

4.3.4 Asymmetric task strategy

Given the observed asymmetries in the animals' responses, we wondered if additional asymmetries could be observed in the behavioural strategy of well trained animals. Because licking behaviour prior to the onset of the response period was not relevant for obtaining rewards in the task, we hypothesised that asymmetries in strategy might be reflected in asymmetric anticipatory behaviour. We therefore analysed the licking behaviour prior to the onset of the response period in well trained animals.
Animals did indeed not refrain from licking until the the onset of the response window, but showed an increase in licking frequency briefly after light onset (Figure 4.7a, 10-28kHz cohort). Importantly, while this ramping licking activity occurred at both spouts across animals, the location of this pre-stimulus licking was not arbitrary. Instead, pre-stimulus licking was selective to the spout associated with high frequency sounds in all animals (Figure 4.7b).

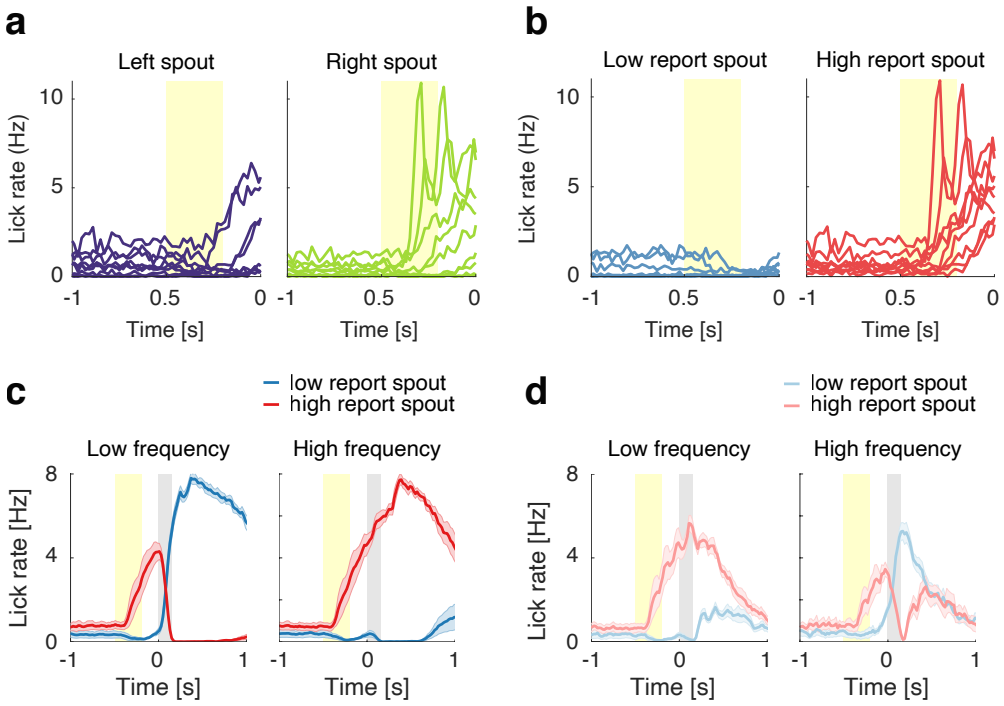

Figure 4.7: ***Pre-stimulus and response licking.*** ***a:*** *Average licking frequency prior to stimulus presentation at the indicated spout locations during steady state behaviour. Individual traces correspond to single animals. Yellow shade denotes the time of light presentation signalling trial start.* ***b:*** *Same as a, but considering low and high frequency report spout.* ***c Left:*** *Time course of licking at the low and high frequency report spout in low frequency trials. Lines denote mean, shades SEM. Grey shade indicates time of sound presentation, yellow shade time of light signaling.* ***Right:*** *Same as left, but for high frequency trials.* ***d:*** *Same as c, but for trials with incorrect responses.*

Importantly though, this pre-stimulus licking did not trivially predict the animals' responses and therefore the observed bias. Instead, anticipatory licking occurred prior to correct low and high frequency trials (Figure 4.7c). Hence animals always started licking at the high frequency report spout and then reported their decision using a stay or switch strategy. Given this preexisting licking at the high frequency spout, it is possible that incorrect responses were associated to this anticipatory licking. However, pre-stimulus licking was similar prior to correct and incorrect trials (Figure 4.7d). Instead,

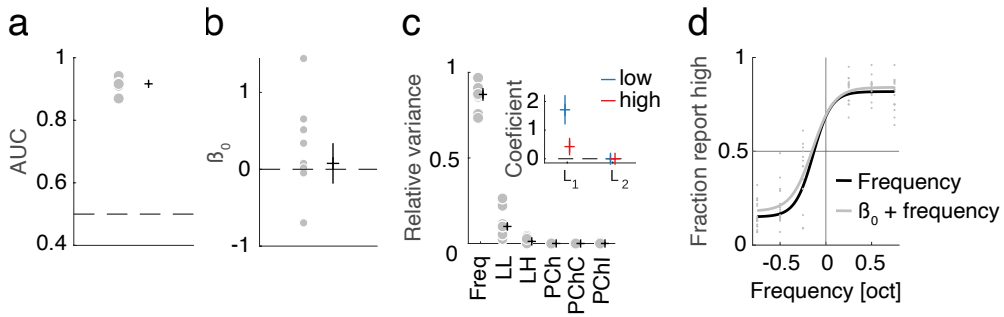

Figure 4.8: ***Generalised linear modelling of licking responses.*** ***a:*** *Model performances. Markers denote cross validated performances of single models, black bars denote median (horizontal) ± MAD (vertical).* ***b:*** β_0 *of models in a.* ***c:*** *Fraction of variance provided by stimulus (Freq), licks at low (LL) and high (LH) frequency report spouts as well as the previous choice (PCh) in correct (PChC) and incorrect (PChI) trials.* ***Inset:*** *Coefficients of low and high spout licks across recordings (median ± MAD).* ***d:*** *Predicted psychometric curves using stimulus coefficients only (black) or in combination with the general bias (grey). Markers denote predicted responses in single mice, curves denote the resulting fits for the cohort averages.*

incorrect 'switching' to the low frequency spout was observed in incorrect high frequency trials while anticipatory licking at the high frequency response spout continued into the response window in incorrect low frequency trials. Importantly though, switches to the low frequency response spout were not completely absent in the latter, but rather appeared to be delayed when compared to correct trials (Figure 4.7d). An alternative explanation of the initially observed shift in the psychometric function might therefore be a failure of the animals to timely alter the licking location.

To investigate further if anticipatory licking was predictive of the observed bias, we modelled the response lick of each mouse in a Generalised Linear Model (GLM), using the presented stimulus, the location of previous licks and the choice history as predictors (see methods). These models very accurately predicted the responses of the mice in trials not used for training the model (Figure 4.8a). As expected by the generally high level of performance in the task (Figure 4.1c), most of the variance of the model was captured by the presented stimulus (Figure 4.8c). The location of prestimulus licking was mildly predictive of the upcoming response, but mostly

through the effect of rare licks at the low frequency response spout (Figure 4.8c). Moreover, β_0 parameters demonstrated, that the observed shift of the psychometric curves was not due to a general bias towards high frequency reports (Figure 4.8b). Instead, we observed clear differences in the weights of low and high frequency stimuli that captured this effect.
Thus, when predicting the responses of the animals based on the frequency components of the models alone, the predicted responses corresponded to a psychometric curve with a similar high frequency bias as the one observed in the behavioural data (Figure 4.8d). Therefore, while pre-stimulus licking did slightly affect the task responses of our mice, it did not explain the general bias, as this effect was captured by the frequency weights of the model, consistent with sensory asymmetries in the task.

4.3.5 Behavioural strategy as compensation of sensory deficits

The observed asymmetric licking behaviour in our animals suggested that they solved the task by using a default, high-frequency-response strategy. Given the previously described deficits in high frequency perception and performance during early training, this behaviour might represent an efficient strategy, compensating for these limitations. As only the perception of a low-frequency stimulus triggers the deviation from a high frequency response, accuracy in the task would only be limited by the degree of low frequency perception in such a scenario.
However, if pre-stimulus licking indeed represents an efficient strategy compensating for differences in stimulus perception, the acquisition of this strategy is expected to simultaneously limit the observed differences in task performance. Additionally, the degree of asymmetry in pre-stimulus licking is also expected to roughly correspond to the strength of the perceptual differences, as this asymmetric strategy might only be efficient in the presence of strong perceptual biases. We therefore compared behaviour of mice in early training sessions with their degree of asymmetric steady-state task behaviour in the final task paradigm.
All animal cohorts trained developed the described asymmetric pre-stimulus licking phenotype (Figure 4.9a). However, consistent with our hypothesis, the speed of acquisition and degree of high-frequency preference in anticipatory licking roughly corresponded to the degree of the observed differences in

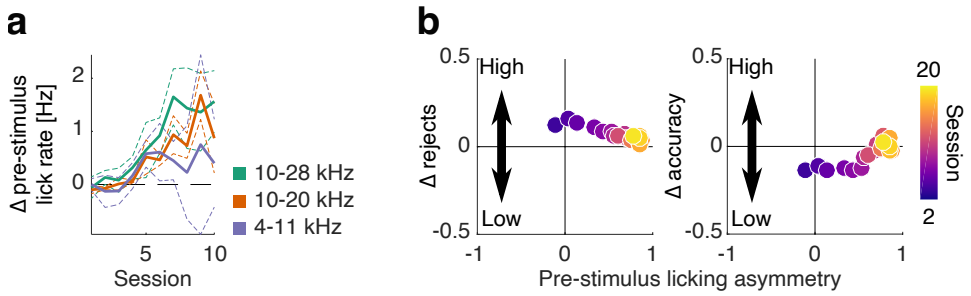

Figure 4.9: ***Default response strategy counteracts sensory bias.*** ***a:*** *Differences in lick rates at high and low frequency spouts in the first sessions of training. Thick lines demarcate cohort medians, thin lines median ± MAD.* ***b Left:*** *Time course of mean licking asymmetry and mean differences in trial rejection in the first 20 sessions of training across all animals with high frequency steady state biases (n=20).* ***Right:*** *Same as a but for licking asymmetry and corresponding accuracy differences.*

early task performance (Figure 4.5d). Thus, strong asymmetries in anticipatory licking were observed in animals trained to discriminate 10 and 20kHz or 10 and 28kHz stimuli, but animals trained with 4 and 11kHz stimuli only showed moderate high-frequency anticipation. Importantly, the acquisition of this licking strategy coincided with the reduction of the observed differences in trial rejections and response accuracy (Figure 4.9b). Anticipatory licking therefore likely develops as part of a behavioural strategy compensating for sensory limitations of high frequency perception by actively exploiting the possibility of task-irrelevant licking prior to the temporally predicable stimulus presentation.

4.3.6 Significance of task structure

To determine the importance of anticipatory licking for task performance and the observed behavioural asymmetries, we exposed well trained animals to two manipulations of the task contingency. First we investigated if animals required anticipatory licking during stimulus presentation in order to maintain their performance. We therefore changed the time of the response window, so that the first lick after sound onset, instead of its offset, was considered the response of the animal. Thus the typical pre-stimulus licking

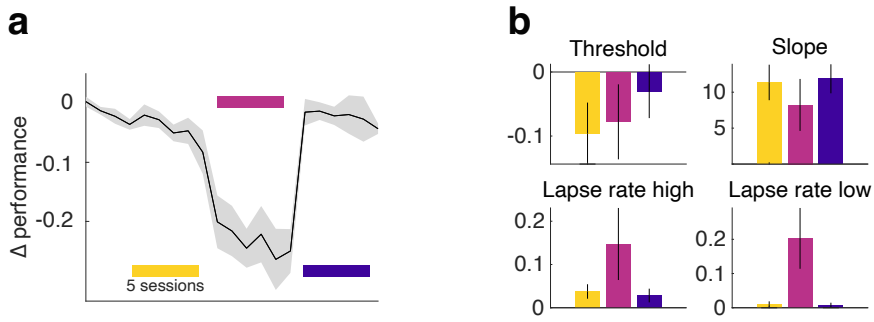

Figure 4.10: ***Manipulations of task contingencies.*** ***a:*** *Performance differences (high - low) of unchanged task contingencies (yellow), immediate response window (magenta) and no-licking contingency (blue). Line shows median across mice (n=9), shades denote MAD.* ***b:*** *Quantification of session performances (sessions = 5) in each task contingency. Bars show median across animals, error bars demarcate MAD.*

would collide with the new response window and thus impede performances. Indeed, animals were strongly affected by this task contingency resulting in performances reduced by 0.2 throughout the full period of this manipulation (Figure 4.10a). Importantly though, this task manipulation did not result in an increased response bias due to unchanged pre-stimulus licking, but rather negatively affected the slope of the psychometric curves as well as the lapse rates of easy low and high frequency stimuli (Figure 4.10b). Thus animals were able to adapt their behavioural strategy in response to the new task requirements, but failed to achieve similar performances.
This reduction in task performance might reflect either an inability of trained animals to appropriately alter their licking behaviour or it could reflect a high cognitive cost of such an alteration. We addressed this distinction with a second manipulation in which the cost of pre-stimulus licking in the task was drastically increased so that the consequences of anticipatory licking should outweigh the internal effort of controlling licks appropriately. To that end, the LED light predicting the stimulus was omitted and stimulus presentation was conditional on a lick-free ITI. Additionally, licking at any time during the ITI triggered an additional ITI until a full interval had been completed without any licking. Interestingly, while the interval between sound presentations grew strongly, the animals performances were not strongly affected by this manipulation (Figure 4.10a). These manipulations of the task

contingency therefore suggest that in addition to sensory limitations, also limitations in licking control shape the observed behavioural strategy.

4.4 Conclusions

We have studied frequency discrimination in a 2AFC task for head fixed mice. Animals were presented with sounds varying in frequency and location and successfully learned to report the if the presented frequency was above or below a threshold while ignoring the sound's location. While animals performed well in the task, they displayed a clear bias towards reporting high frequency sounds (Figure 4.1). Such tendencies to repeat a given response are commonly observed in 2AFC tasks in humans and mice and have been suggested to reflect sensory as well as non-sensory asymmetries [28, 5, 99, 266]. Typically such choice biases arise through influences of previous decisions, which can reflect asymmetries in the sensory evidence as well as the decision making process [99, 70, 143, 275]. However, global choice biases, reflecting a general tendency towards one response, have also been reported [77].
Using GLM analysis we showed that the choice biased observed were explained by asymmetric effects of high and low frequency stimuli on the reported decision (Figure 4.8b&c). Using considerations from SDT we hypothesised a frequency dependent limitation in the sensory perception as the underlying limitation for the observed behavioural asymmetries (Figure 4.2). This explanation required that sensory processes can be reflected in decision criterion variable of signal detection theory and that animals did not update the initial decision criterion upon the introduction of additional, more difficult frequencies.
While the decision criterion c is usually believed to reflect decision making parameters independent of perceptual ones, we have shown that biases in the criterion can also correspond to perceptual limitations and asymmetries (Figure 4.2). Additionally, perceptual and neural coding parameters have recently been shown to affect this measure [290, 117]. Biases in decision criterion therefore do not necessarily have to be indicative of asymmetries in decision making processes, but can reflect perceptual symmetries, too. Our interpretation of the observed bias as the result of deficits in high frequency perception rested on the additional assumption that mice did not update the decision criterion acquired during training with easy stimuli (Figure 4.3). Indeed, mice lose behavioural flexibility with training and age [118] and behavioural strategies established during training are known to limit discrimination capacity [267]. It is therefore possible, that the decision cri-

terion was formed during training with two frequencies only and therefore reflects an asymmetry in low and high frequency perception as well as a limitation of cognitive control preventing its appropriate adjustment.
Notably though, the presented evidence supporting this hypothesis was largely based on data acquired in animals that had not yet fully learned the task paradigm and showed high frequency deficits in task accuracy as well as rejection rates (Figure 4.5). We have raised the possibility that these two differences might reflect the distinct effects of deficits in perception of a detected sound as well as differences in probability of stimulus detection. However, as all stimuli were presented well above the detection threshold of young mice [98, 152], strong failures in stimulus detection are unlikely causing the observed differences in trial rejection rates. Moreover, sound detection thresholds are typically lowest around 15kHz, while trial rejection rates were minimal for 4kHz sounds instead [152] (Figure 4.5b). We therefore concluded that diverging probabilities of sound detection are not responsible for differences in trial rejection rates. Instead, the differences in sensory perception leading to biased responses might also be responsible for the diverging differences in trial rejections causing learning of the appropriate responses to occur at different rates for low and high frequency stimuli. Such a difference in learning speed would be a plausible explanation for the observed development of the default-response strategy revealed by anticipatory licking (Figure 4.7). In temporally predictable task paradigms, such anticipatory behaviours have been described in classical and instrumental conditioning literature [244, 26, 196, 68]. Because the time of the sound presentation is temporally predicted by the light cue, it is not surprising that this anticipatory licking is triggered by the onset of the LED stimulus. However, as this anticipatory licking was strongly associated to the high-frequency report spout, it demonstrated a default response strategy favoring high frequency reports likely corresponding to the differences in sensory perception observed in early training.
Consistent with this hypothesis, we presented evidence that the degree of these sensory differences determined both, the shift of the psychometric function (Figure 4.6) as well as the dependency on a default response strategy to solve the task (Figure 4.9). Similar default strategies and differences in learning speeds have been shown to develop as a consequence of stimulus-specific differences in cortical recruitment [33]. It is therefore possible that the asymmetries observed in our data correspond to similar differences in

cortical activation as low frequency pure tones typically activate larger cortical areas in C57BL/6J mice than frequencies above 10kHz [122, 184, 21]. While the exact perceptual differences underlying the reported behavioural differences in early training remain speculative, we have presented evidence that mice compensated for these asymmetries through the acquisition of a default response strategy exploiting the possibility of task irrelevant anticipatory licking in order to establish a default high frequency response strategy (Figure 4.9). Importantly though, we have demonstrated, that this behavioural strategy can be altered and is likely reflecting the cost of licking control in the precise task paradigm (Figure 4.10).
Taken together, our results therefore have provided evidence that the behavioural strategy of head fixed mice is shaped by sensory and control limitations, as well as the underlying task paradigm. Our work highlights the importance of careful characterisation of behaviour, even in presumably simple task paradigms, as we have argued that symmetric behaviour in our task corresponded to specifics in the task design, rather than symmetry in the underlying perceptual and decision making processes (Figure 4.10b). This distinction suggests that standard approaches of quantifying perception through behaviour, using classical psychometric functions, are limited due to the complex interactions of perception and behaviour. We argue that choice biases and other task-irrelevant behaviour are important measures capable of overcoming these limitations, as they offer valuable insights in the behavioural strategies and their underlying asymmetries as well as limitations in sensory perception and decision making processes.

Chapter 5

Conclusions and closing remarks

HIGHLIGHTS

- In this final chapter we summarise the main findings presented in the previous chapters.
- We discuss possible interpretations in the light of published literature.
- We suggest possible ways to directly address these interpretations by further analysis and additional experimental work.

5.1 Laminar distribution of stimulus and choice-related signals in auditory cortex

In this chapter, the laminar activity of neurons in the ACx of mice performing in a delayed frequency discrimination task was analysed. We have presented a shift from representations of the stimulus towards encoding of the upcoming response action (Figure 2.7). This shift occurred gradually over the duration of the delay period and revealed laminar differences in the task signals present in the ACx. Thus, units across both mid-superficial and deep layers were stimulus informative during its presentation, albeit with slightly different temporal profiles (Figure 2.7 & 2.9). Prior to the animal's

response licks though, task related signals in ACx were exclusively tuned to the action about to be executed and tuning was significantly stronger in the deep layers of cortex.
Given the absence of evidence for a local generation of these action signals (Figure 1.5) and in light of multiple motor related projections to ACx [230, 42], the observed signals likely reflect information about the upcoming action that has been introduced via feedback projections to deep cortical layers. It remains unclear though, if these action-predictive signals in deep layers are relevant for the response execution. Given that primary sensory cortices are sufficient to initiate movement or bias task responses [157, 299], it is possible that these action signals are involved in the initiation of the action. The observed failure to initiate response action following muscimol silencing of ACx (Figure 2.3a), while consistent with this hypothesis, cannot be seen as direct evidence for this interpretation. It can, among others, also be interpreted as resulting from a lack of perceiving the presence of the sound or reflect a coping strategy in trials with limited discriminability. While strong reductions of discriminability are unlikely underlying this effect [75, 190, 34], selective laminar silencing in ACx with temporal specificity using optogenetics will be needed in order to determine if the observed silencing effects can be attributed to the stimulus or action signalling observed. Ideally, targeted manipulations depending on the selectivity of single neurons would be used. Thus the capacity and necessity of the two described neural populations for task performance could be directly addressed with temporal specificity.
A laminar separation of movement and stimulus signals has been previously suggested in rodents [296], however these observations were made in a Go-NoGo task paradigm that does not allow to test the specificity of the observed movement signals. Using a 2AFC frequency discrimination paradigm, we have demonstrated that these signals do not represent generic movement preparation signals commonly observed in cortex [255, 224], but instead are specific to the future response action. Our results therefore represent an important finding, demonstrating the high specificity of movement-related signals in sensory cortex. It remains unclear, however, if this specificity of the observed action signals is limited to response behaviour in the task, or if any upcoming licking behaviour is encoded equally well, irrespective of the behavioural context. Due to a low number of spontaneous licks during the ITI, it was not possible to further explore this distinction in the current

data set. A possible context dependency of such action-related signals will therefore have to be addressed in future experiments.
While the distinct stimulus and action signals in the ACx have been clearly demonstrated, inconsistent observations have been made about the dependency of these neural selectivity on the task outcome. While we demonstrated significant negative correlations of simultaneous action and stimulus d-primes (Figure 2.14b), indicative of increased task information in incorrect trials, no striking outcome-dependent differences in task selectivity were observed (Figure 2.15). The slight differences present in our data set are therefore not indicative of an outcome dependency of task signals in the ACx. However, these small differences could reflect selectivity of a neural sub-population to serial dependencies. We demonstrated that animals performing in the task have a tendency to repeat previous actions (Figure 3.9), introducing a slight correlation of responses in the current and the previous trial. As a repetition of the previous response is expected to be incorrect in 50% of the trials, it is not unreasonable to assume that a correlation of the current with the previous response might be stronger in incorrect than in correct trials. In this scenario, residual activity in the sub-population of the recorded units that is selective to the response actions (Figure 2.7) could account for the observed selectivity differences in correct and incorrect trials. Alternatively, as action signals in sensory cortex can be independent of serial dependencies [150], it is also possible that distinct populations of auditory cortical neurons provide stimulus, action and history information. However, this hypothesis will have to be addressed in future analysis.
Taken together, we have demonstrated the presence of distinct and highly specific stimulus and response signals in the rodent ACx with distinct temporal and laminar features. Our findings therefore represent an important step in mapping the laminar activity of the ACx to its function.

5.2 Outcome dependent modulation of task accuracy by cortical state fluctuations

In this chapter, we have demonstrated response-outcome dependent differences in the frequency discrimination accuracy of head fixed mice and its association to spontaneous fluctuations in baseline activity (Figure 3.7 & 3.8). Animals showed higher performances after error trials than after correct tri-

als. Serial dependencies and behavioural changes upon incorrect responses have been previously observed in rodents [28, 77, 49, 99]. While usually such serial dependencies reflect the the tendency of subjects to repeat previous actions, also differences in perception have been reported [143]. Generalised linear mixed modelling of the animals' responses demonstrated the presence of such history effects in our animals, but suggested that the changes underlying higher performances following error trials were mostly due to changes in the animal's discriminability (Figure 3.9). The increased behavioural accuracy after error trials might therefore reflect an error triggered increase of the animals' attention on the task.

Importantly, we demonstrated that fluctuations in spontaneous neural baseline activity of the ACx only were associated with changes in discrimination accuracy in trials following incorrect responses (Figure 3.7 & 3.8). Thus, following error trials, high firing rates as well as low levels of synchronisation were associated with better accuracy, while no favourable combination of neural activity could be determined in trials following correct responses. As the quality of sensory representations in cortex is know to vary with the cortical state fluctuations, our data thus suggests a possible, context-dependent behavioural relevance of such effects [132, 192, 13, 76]. We have speculated, that this differential effect of brain state changes on behavioural accuracy could be indicative of changes in cortical involvement for task execution. Given that the ACx can influence frequency discrimination behaviour, but is not required for performances above chance level [4, 190, 34], variations of cortical contributions to task performance across the session can not be excluded. We have suggested to address these fluctuations in cortical task contribution by transient, optogenetic silencing of the ACx, as the impact of cortical silencing on the task performance should match the degree of the cortical contribution in the trial. However, because pharmacological silencing of the ACx has been demonstrated to strongly reduce the animals' task engagement (Figure 2.3), this approach might not be suitable.

Alternatively, the hypothesis that variations in the behavioural relevance of cortical state fluctuations might correspond to different degrees of cortical contributions to the task performance could be addressed directly in animals trained to discriminate stimuli with higher complexity. Because the ACx is not essential for frequency-discrimination when presenting pure tones [75, 34, 190], but is required to discriminate more complicated, frequency-modulated stimuli above chance [34], unconditional effects of cortical state

fluctuations would be expected in animals trained to discriminate complex, frequency-modulated stimuli. While this remains a possibility to be addressed in further experiments, it is also worth mentioning that our task paradigm as well as previous studies reporting correlations of fluctuations in cortical synchrony with behavioural accuracy, studied behavioural performance in task paradigms that contained a delay period [13]. While this delay component cannot explain the response-outcome dependency of the effects reported here, it is possible that the working memory load introduced by these task delays increased the otherwise small effects of cortical state fluctuations on behaviour through a broader involvement of cortical areas [39]. Because spontaneous fluctuations in cortical activity are wide-spread phenomena [248, 224], it is possible in this scenario that the behaviourally relevant effects of neural activity fluctuations are not the reported effects on stimulus representations in sensory cortices. Instead, global fluctuations in spontaneous activity of cortices might facilitate task-related functions in higher cortical areas, like the prefrontal or parietal cortex, that are typically associated with working memory tasks [80, 208, 39].
Regardless of the underlying mechanism, we have demonstrated that spontaneous fluctuations in cortical synchronisation and activity prior to stimulus presentation are associated to discrimination accuracy in an outcome-history dependent manner. Our work therefore represents, to our knowledge, the first evidence that such effects of neural activity might be gated by context. This finding might therefore offer important insights in the flexibility of neural processes underlying sensory decision making.

5.3 Sensory and control limitations shape behavioural strategies

In this chapter we have analysed the behavioural strategies of head fixed mice performing frequency discrimination in a simple 2AFC task. We have reported a general bias towards high frequency responses in well trained animals across multiple frequency ranges as well as corresponding anticipatory licking behaviour at the high frequency report spout (Figure 4.1 & 4.9).
Seemingly sub-optimal and repetitive task behaviour is commonly observed in 2AFC task behaviours [28, 70, 143]. However, these behaviours are typically not static, but correspond to the amount of sensory information avail-

able, internal states or parameters of the task [265, 143, 266, 37, 182, 277]. Such behaviour might therefore provide insight in the cognitive processes and limitations underlying the observed behavioural strategy. In humans, conflicts in cognitive processing have been identified as performance limiting factors using the Stroop test [227, 145]. In rodents however, little is known about the factors underlying task-irrelevant behaviour.

In this work, we have presented evidence that the extent of these asymmetric behaviours in well trained mice is predicted by behavioural differences measured during early training (Figure 4.5 & 4.9), suggesting that the observed behavioural asymmetries represented strategies compensating for limitations in sensory perception. The exact nature of these sensory limitations however, remains unclear. We have shown that differences in stimulus detection are unlikely responsible for these differences (Figure 4.5b) and have speculated that frequency-dependent differences in cortical activation might instead shape distinct learning-rates for low and high frequency stimuli, leading to the observed asymmetries. However, this hypothesis will still have to be addressed in future experiments. Because animals can be trained to discriminate activity patters artificially introduced in the sensory cortex [34, 33, 48], similar behavioural asymmetries should form dependent on differences in the sizes of optogenetically activated areas and irrespective of their position within the tonotopic map of the ACx.

While we have demonstrated, that perceptual asymmetries and limitations in flexibly adjusting a learned decision rule might underlie the observed bias in the animals' responses, it remains unclear why animals displayed anticipatory licking. Because the time of stimulus presentation as well as the opening of the response period are temporally well predicted (Figure 4.1), anticipatory licking might correspond to uncertainties in the estimation of the time in the task. In addition to this possibility, manipulations of the task contingency have revealed that these behavioural asymmetries are optional and can be altered or abolished by increasing their cost in the behavioural task, indicating an additional cost in the task-appropriate control of licking behaviour (Figure 4.10).

Our work therefore demonstrates the possibility of determination and qualitative description of cognitive and perceptual limitations in rodent models. Such insight can provide important constraints on the possible neural implementation of task behaviours [135]. However, while these results indicate the presence of multiple limiting factors shaping the behavioural strategy, a for-

mal framework is needed in order to generate testable hypothesis about the quantitative contribution and interaction of these individual factors. Based on the data presented here, such formal models are currently being developed by Juan Castiñeiras and Davide Reato.

5.4 Concluding remarks

Taken together our results highlight the richness of data obtained in mice even in relatively simple, movement restrained behavioural paradigms. Thus, we have identified meaningful structure at all levels of analysis presented here. On the level of task responses, we have shown behavioural asymmetries revealing underlying limitations in perception and cognitive processes. On the level of laminar cortical organisation, we demonstrated temporally and spatially distinct representations of task related signals. Finally, when analysing neural population activity, we revealed a meaningful correlation of it's organisation to the accuracy in the discrimination task.
Our work has demonstrated the necessity of studying decision making processes at these multiple levels of complexity as the observed asymmetries in the displayed task behaviour pose important constraints when modelling its neural implementation [154, 135]. Similarly, the exact tuning properties of single neurons have important consequences for the expected effects of noise correlations on the coding efficiency [169]. The findings we have reported here therefore present an important step towards understanding the complex interactions underlying behaviour.
However, additional research, addressing the remaining and additional questions mentioned above will be needed for a deep understanding of the functional role of activity in the auditory during sensory decision making in mice.

Bibliography

[1] L. F. Abbott and Peter Dayan. The Effect of Correlated Variability on the Accuracy of a Population Code. *Neural Computation*, 11(1):91–101, jan 1999. (Cited on page 66.)

[2] Nixon M Abraham, Hartwig Spors, Alan Carleton, Troy W Margrie, Thomas Kuner, and Andreas T Schaefer. Maintaining accuracy at the expense of speed: stimulus similarity defines odor discrimination time in mice. *Neuron*, 44(5):865–76, dec 2004. (Cited on page 5.)

[3] Hillel Adesnik and Alexander Naka. Cracking the Function of Layers in the Sensory Cortex. *Neuron*, 100(5):1028–1043, 2018. (Cited on pages 11 and 18.)

[4] Mark Aizenberg, Laetitia Mwilambwe-Tshilobo, John J. Briguglio, Ryan G. Natan, and Maria N. Geffen. Bidirectional Regulation of Innate and Learned Behaviors That Rely on Frequency Discrimination by Cortical Inhibitory Neurons. *PLoS Biology*, 13(12):1–32, 2015. (Cited on pages 19, 86, and 120.)

[5] Athena Akrami, Charles D. Kopec, Mathew E. Diamond, and Carlos D. Brody. Posterior parietal cortex represents sensory history and mediates its effects on behaviour. *Nature*, 554(7692):368–372, feb 2018. (Cited on pages 90 and 113.)

[6] Mark L Andermann, Aaron M Kerlin, Demetris K Roumis, Lindsey L Glickfeld, and R Clay Reid. Functional specialization of mouse higher visual cortical areas. *Neuron*, 72(6):1025–39, dec 2011. (Cited on page 5.)

[7] C. Angeloni and M. N. Geffen. Contextual modulation of sound processing in the auditory cortex. *Current Opinion in Neurobiology*, 49:8–15, 2018. (Cited on pages 12 and 19.)

[8] Serin Atiani, Mounya Elhilali, Stephen V. David, Jonathan B. Fritz, and Shihab A. Shamma. Task Difficulty and Performance Induce Diverse Adaptive Patterns in Gain and Shape of Primary Auditory Cortical Receptive Fields. *Neuron*, 61(3):467–480, feb 2009. (Cited on page 13.)

[9] Bruno B. Averbeck, Peter E. Latham, and Alexandre Pouget. Neural correlations, population coding and computation. *Nature Reviews Neuroscience*, 7(5):358–366, may 2006. (Cited on page 66.)

[10] Sophie Bagur, Martin Averseng, Diego Elgueda, Stephen David, Jonathan Fritz, Pingbo Yin, Shihab Shamma, Yves Boubenec, and Srdjan Ostojic. Go/No-Go task engagement enhances population representation of target stimuli in primary auditory cortex. *Nature Communications*, 9(1), 2018. (Cited on page 19.)

[11] Farhan Baluch and Laurent Itti. Mechanisms of top-down attention. *Trends in Neurosciences*, 34(4):210–224, apr 2011. (Cited on page 11.)

[12] Andre M. Bastos, W. Martin Usrey, Rick A. Adams, George R. Mangun, Pascal Fries, and Karl J. Friston. Canonical Microcircuits for Predictive Coding. *Neuron*, 76(4):695–711, nov 2012. (Cited on page 18.)

[13] Charles B. Beaman, Sarah L. Eagleman, and Valentin Dragoi. Sensory coding accuracy and perceptual performance are improved during the desynchronized cortical state. *Nature Communications*, 8(1):1–14, 2017. (Cited on pages 15, 16, 66, 86, 120, and 121.)

[14] A. Berditchevskaia, R. D. Cazé, and S. R. Schultz. Performance in a GO/NOGO perceptual task reflects a balance between impulsive and instrumental components of behaviour. *Scientific Reports*, 6(May):1–15, 2016. (Cited on pages 3, 4, and 5.)

[15] Hans Berger. Über das Elektrenkephalogramm des Menschen. *Archiv für Psychiatrie und Nervenkrankheiten*, 87(1):527–570, dec 1929. (Cited on page 66.)

[16] J. K. Bizley, K. M. M. Walker, B. W. Silverman, A. J. King, and J. W. H. Schnupp. Interdependent Encoding of Pitch, Timbre, and Spatial Location in Auditory Cortex. *Journal of Neuroscience*, 29(7):2064–2075, feb 2009. (Cited on pages 8 and 9.)

[17] J. A. Blake, C. J. Bult, J. A. Kadin, J. E. Richardson, and J. T. Eppig. The Mouse Genome Database (MGD): premier model organism resource for mammalian genomics and genetics. *Nucleic Acids Research*, 39(Database):D842–D848, jan 2011. (Cited on page 90.)

[18] M. M. Botvinick, S. Huffstetler, and J. T. McGuire. Effort discounting in human nucleus accumbens. *Cognitive, Affective, & Behavioral Neuroscience*, 9(1):16–27, mar 2009. (Cited on page 90.)

[19] Matthew M. Botvinick and Jonathan D. Cohen. The computational and neural basis of cognitive control: Charted territory and new frontiers. *Cognitive Science*, 38(6):1249–1285, 2014. (Cited on page 90.)

[20] J. Bourg, N Vasconcelos, and A Renart. Transient competitive amplification during states of cortical activation. In *Cosyne*, 2016. (Cited on page 14.)

[21] Zac Bowen, Daniel E. Winkowski, and Patrick O. Kanold. Functional organization of mouse primary auditory cortex in adult C57BL/6 and F1 (CBAxC57) mice. *Scientific Reports*, 10(1):1–14, 2020. (Cited on page 115.)

[22] Margaret M. Bradley, Laura Miccoli, Miguel A. Escrig, and Peter J. Lang. The pupil as a measure of emotional arousal and autonomic activation. *Psychophysiology*, 45(4):602–607, jul 2008. (Cited on page 66.)

[23] K. H. Britten, W. T. Newsome, M. N. Shadlen, S. Celebrini, and J. A. Movshon. A relationship between behavioral choice and the visual responses of neurons in macaque MT. *Visual Neuroscience*, 13(1):87–100, 1996. (Cited on pages 20 and 62.)

[24] Harriet Brown, Rick A. Adams, Isabel Parees, Mark Edwards, and Karl Friston. Active inference, sensory attenuation and illusions. *Cognitive Processing*, 14(4):411–427, nov 2013. (Cited on page 12.)

[25] M. Christian Brown and Joseph Santos-Sacchi. Audition. In *Fundamental Neuroscience*, pages 553–576. Elsevier, 2013. (Cited on page 7.)

[26] Paul L. Brown and Herbert M. Jenkins. AUTO-SHAPING OF THE PIGEON'S KEY-PECK. *Journal of the Experimental Analysis of Behavior*, 11(1):1–8, jan 1968. (Cited on page 114.)

[27] Christopher P. Burgess, Armin Lak, Nicholas A. Steinmetz, Peter Zatka-Haas, Charu Bai Reddy, Elina A.K. Jacobs, Jennifer F. Linden, Joseph J. Paton, Adam Ranson, Sylvia Schröder, Sofia Soares, Miles J. Wells, Lauren E. Wool, Kenneth D. Harris, and Matteo Carandini. High-Yield Methods for Accurate Two-Alternative Visual Psychophysics in Head-Fixed Mice. *Cell Reports*, 20(10):2513–2524, 2017. (Cited on pages 6 and 90.)

[28] Laura Busse, Asli Ayaz, Neel T Dhruv, Steffen Katzner, Aman B Saleem, Marieke L Schölvinck, Andrew D Zaharia, and Matteo Carandini. The detection of visual contrast in the behaving mouse. *The Journal of neuroscience : the official journal of the Society for Neuroscience*, 31(31):11351–61, aug 2011. (Cited on pages 2, 5, 16, 63, 85, 90, 113, 120, and 121.)

[29] R. A. Butler, I. T. Diamond, and W. D. Neff. ROLE OF AUDITORY CORTEX IN DISCRIMINATION OF CHANGES IN FREQUENCY. *Journal of Neurophysiology*, 20(1):108–120, jan 1957. (Cited on page 19.)

[30] Matteo Carandini and Anne K. Churchland. Probing perceptual decisions in rodents. *Nature Neuroscience*, 16(7):824–831, 2013. (Cited on pages 3, 4, 5, 6, 90, and 91.)

[31] Matteo Carandini and David J. Heeger. Normalization as a canonical neural computation. *Nature Reviews Neuroscience*, 13(1):51–62, jan 2012. (Cited on page 11.)

[32] Ioana Carcea, Michele N Insanally, and Robert C Froemke. Dynamics of auditory cortical activity during behavioural engagement and auditory perception. *Nature Communications*, 8:1–12, 2017. (Cited on pages 18 and 19.)

[33] Sebastian Ceballo, Jacques Bourg, Alexandre Kempf, Zuzanna Piwkowska, Aurélie Daret, Pierre Pinson, Thomas Deneux, Simon Rumpel, and Brice Bathellier. Cortical recruitment determines learning dynamics and strategy. *Nature Communications*, 10(1):1–12, 2019. (Cited on pages 114 and 122.)

[34] Sebastian Ceballo, Zuzanna Piwkowska, Jacques Bourg, Aurélie Daret, and Brice Bathellier. Targeted Cortical Manipulation of Auditory Perception. *Neuron*, 104(6):1168–1179.e5, dec 2019. (Cited on pages 19, 20, 59, 86, 118, 120, and 122.)

[35] S Celebrini and WT Newsome. Neuronal and psychophysical sensitivity to motion signals in extrastriate area MST of the macaque monkey. *The Journal of Neuroscience*, 14(7):4109–4124, jul 1994. (Cited on page 20.)

[36] Gal Chechik, Michael J. Anderson, Omer Bar-Yosef, Eric D. Young, Naftali Tishby, and Israel Nelken. Reduction of Information Redundancy in the Ascending Auditory Pathway. *Neuron*, 51(3):359–368, 2006. (Cited on pages 28, 29, and 60.)

[37] Cathy S. Chen, R. Becket Ebitz, Sylvia R. Bindas, A. David Redish, Benjamin Y. Hayden, and Nicola M. Grissom. Divergent Strategies for Learning in Males and Females. *Current Biology*, pages 1–12, 2020. (Cited on pages 90 and 122.)

[38] Naiyan Chen, Hiroki Sugihara, and Mriganka Sur. An acetylcholine-activated microcircuit drives temporal dynamics of cortical activity. *Nature Neuroscience*, 18(6):892–902, jun 2015. (Cited on page 14.)

[39] Thomas B. Christophel, P. Christiaan Klink, Bernhard Spitzer, Pieter R. Roelfsema, and John-Dylan Haynes. The Distributed Nature of Working Memory. *Trends in Cognitive Sciences*, 21(2):111–124, 2017. (Cited on page 121.)

[40] Andrew M Clark. *Surfing uncertainty: Prediction, action, and the embodied mind*. Oxford University Press, 2016. (Cited on page 18.)

[41] Amanda Clause, Tuan Nguyen, and Karl Kandler. An acoustic startle-based method of assessing frequency discrimination in mice. *Journal of Neuroscience Methods*, 200(1):63–67, aug 2011. (Cited on pages 90 and 91.)

[42] Kameron K Clayton, Ross S Williamson, Kenneth E Hancock, Troy Hackett, and Daniel B Polley. Auditory Corticothalamic Neurons are Recruited by Motor Preparatory Inputs. *bioRxiv*, page 2020.05.28.121459, jan 2020. (Cited on pages 12 and 118.)

[43] Marlene R Cohen and Adam Kohn. Measuring and interpreting neuronal correlations. *Nature Neuroscience*, 14(7):811–819, jul 2011. (Cited on pages 20 and 66.)

[44] Marlene R Cohen and John H R Maunsell. Attention improves performance primarily by reducing interneuronal correlations. *Nature Neuroscience*, 12(12):1594–1600, dec 2009. (Cited on pages 15 and 20.)

[45] Trinity B. Crapse and Michele A. Basso. Insights into decision making using choice probability. *Journal of Neurophysiology*, 114(6):3039–3049, 2015. (Cited on page 20.)

[46] Trinity B. Crapse, Hakwan Lau, and Michele A. Basso. A Role for the Superior Colliculus in Decision Criteria. *Neuron*, 97(1):181–194.e6, jan 2018. (Cited on page 4.)

[47] Bruce G. Cumming and Hendrikje Nienborg. Feedforward and feedback sources of choice probability in neural population responses. *Current Opinion in Neurobiology*, 37:126–132, 2016. (Cited on pages 20 and 53.)

[48] Henry W.P. Dalgleish, Lloyd E. Russell, Adam M. Packer, Arnd Roth, Oliver M. Gauld, Francesca Greenstreet, Emmett J. Thompson, and Michael Häusser. How many neurons are sufficient for perception of cortical activity? *eLife*, 9:1–99, 2020. (Cited on page 122.)

[49] Claudia Danielmeier and Markus Ullsperger. Post-error adjustments. *Frontiers in Psychology*, 2(SEP):1–10, 2011. (Cited on pages 84, 85, 87, and 120.)

[50] Stephen V David, Jonathan B Fritz, and Shihab A Shamma. Task reward structure shapes rapid receptive field plasticity in auditory cortex. *Proceedings of the National Academy of Sciences of the United States of America*, 109(6):2144–2149, 2012. (Cited on pages 18 and 19.)

[51] E de Boer and W A Dreschler. Auditory psychophysics: spectrotemporal representation of signals. *Annual review of psychology*, 38:181–202, 1987. (Cited on pages 2 and 90.)

[52] Beatrice de Gelder, Jari Kätsyri, and Aline W. de Borst. Virtual reality and the new psychophysics. *British Journal of Psychology*, 109(3):421–426, aug 2018. (Cited on pages 2 and 90.)

[53] Livia de Hoz and Israel Nelken. Frequency Tuning in the Behaving Mouse: Different Bandwidths for Discrimination and Generalization. *PLoS ONE*, 9(3):e91676, mar 2014. (Cited on page 91.)

[54] Victor de Lafuente and Ranulfo Romo. Neuronal correlates of subjective sensory experience. *Nature Neuroscience*, 8(12):1698–1703, dec 2005. (Cited on page 20.)

[55] M R DeWeese and M Meister. How to measure the information gained from one symbol. *Network (Bristol, England)*, 10(4):325–40, nov 1999. (Cited on page 3.)

[56] Rodney J. Douglas, Kevan A.C. Martin, and David Whitteridge. A Canonical Microcircuit for Neocortex. *Neural Computation*, 1(4):480–488, dec 1989. (Cited on page 18.)

[57] Joshua D. Downer, Mamiko Niwa, and Mitchell L Sutter. Task engagement selectively modulates neural correlations in primary auditory cortex. *Journal of Neuroscience*, 35(19):7565–7574, 2015. (Cited on pages 15, 19, and 20.)

[58] Joshua D. Downer, Brittany Rapone, Jessica Verhein, Kevin N. O'Connor, and Mitchell L. Sutter. Feature-Selective Attention Adaptively Shifts Noise Correlations in Primary Auditory Cortex. *The Journal of Neuroscience*, 37(21):5378–5392, 2017. (Cited on page 19.)

[59] Alexander S. Ecker, Philipp Berens, Andreas S. Tolias, and Matthias Bethge. The effect of noise correlations in populations of diversely tuned neurons. *Journal of Neuroscience*, 31(40):14272–14283, 2011. (Cited on page 66.)

[60] Michael N. Economo, Sarada Viswanathan, Bosiljka Tasic, Erhan Bas, Johan Winnubst, Vilas Menon, Lucas T. Graybuck, Thuc Nghi Nguyen, Kimberly A. Smith, Zizhen Yao, Lihua Wang, Charles R. Gerfen, Jayaram Chandrashekar, Hongkui

Zeng, Loren L. Looger, and Karel Svoboda. Distinct descending motor cortex pathways and their roles in movement. *Nature*, 563(7729):79–84, 2018. (Cited on pages 31 and 55.)

[61] Steven J. Eliades and Xiaoqin Wang. Neural substrates of vocalization feedback monitoring in primate auditory cortex. *Nature*, 453(7198):1102–1106, jun 2008. (Cited on page 12.)

[62] Steven J. Eliades and Xiaoqin Wang. Contributions of sensory tuning to auditory-vocal interactions in marmoset auditory cortex. *Hearing Research*, 348:98–111, may 2017. (Cited on page 12.)

[63] A. Aldo Faisal, Luc P. J. Selen, and Daniel M. Wolpert. Noise in the nervous system. *Nature Reviews Neuroscience*, 9(4):292–303, apr 2008. (Cited on page 12.)

[64] Gustav Theodor Fechner. *Elemente der Psychophysik*. aug 1860. (Cited on pages 2 and 90.)

[65] D. J. Felleman and D. C. Van Essen. Distributed Hierarchical Processing in the Primate Cerebral Cortex. *Cerebral Cortex*, 1(1):1–47, jan 1991. (Cited on page 18.)

[66] Jason Fischer and David Whitney. Serial dependence in visual perception. *Nature Neuroscience*, 17(5):738–743, may 2014. (Cited on pages 16 and 90.)

[67] Aris Fiser, David Mahringer, Hassana K Oyibo, Anders V Petersen, Marcus Leinweber, and Georg B Keller. Experience-dependent spatial expectations in mouse visual cortex. *Nature Neuroscience*, 19(12):1658–1664, dec 2016. (Cited on page 18.)

[68] David M. Freestone, Mika L.M. Macinnis, and Russell M. Church. Response Rates Are Governed More by Time Cues Than Contingency. *Timing and Time Perception*, 1(1):3–20, 2013. (Cited on page 114.)

[69] Jerome Friedman, Trevor Hastie, and Robert Tibshirani. Regularization Paths for Generalized Linear Models via Coordinate Descent. *Journal of Statistical Software*, 33(1), 2010. (Cited on page 97.)

[70] Matthias Fritsche, Pim Mostert, and Floris P. de Lange. Opposite Effects of Recent History on Perception and Decision. *Current Biology*, 27(4):590–595, 2017. (Cited on pages 16, 90, 113, and 121.)

[71] Jonathan B. Fritz, Mounya Elhilali, and Shihab A. Shamma. Adaptive Changes in Cortical Receptive Fields Induced by Attention to Complex Sounds. *Journal of Neurophysiology*, 98(4):2337–2346, oct 2007. (Cited on page 13.)

[72] Edward E Gbur, WalterW Stroup, Kevon S McCarter, Susan Durham, Linda J Young, Mary Christman, Mark West, and Matthew Kramer. *Analysis of Generalized Linear Mixed Models in the Agricultural and Natural Resources Sciences*. American Society of Agronomy, Crop Science Society of America, and Soil Science Society of America, 2012. (Cited on page 71.)

[73] G A Gescheider, J M Thorpe, J Goodarz, and S J Bolanowski. The effects of skin temperature on the detection and discrimination of tactile stimulation. *Somatosensory & motor research*, 14(3):181–8, 1997. (Cited on page 2.)

[74] George Gescheider. *Psychophysics: The Fundamentals*. 1975. (Cited on page 3.)

[75] Tyler L. Gimenez, Maja Lorenc, and Santiago Jaramillo. Adaptive categorization of sound frequency does not require the auditory cortex in rats. *Journal of Neurophysiology*, 114(2):1137–1145, 2015. (Cited on pages 19, 58, 59, 118, and 120.)

[76] Michael Goard and Yang Dan. Basal forebrain activation enhances cortical coding of natural scenes. *Nature Neuroscience*, 12(11):1444–1449, nov 2009. (Cited on pages 15, 66, 86, and 120.)

[77] Joshua I. Gold and Long Ding. How mechanisms of perceptual decision-making affect the psychometric function. *Progress in Neurobiology*, 103(1):98–114, apr 2013. (Cited on pages 16, 63, 85, 113, and 120.)

[78] Joshua I. Gold and Michael N. Shadlen. The neural basis of decision making. *Annual Review of Neuroscience*, 30:535–574, 2007. (Cited on pages 2, 4, and 90.)

[79] Jay M. Goldberg and William D. Neff. FREQUENCY DISCRIMINATION AFTER BILATERAL ABLATION OF CORTICAL AUDITORY AREAS. *Journal of Neurophysiology*, 24(2):119–128, mar 1961. (Cited on page 19.)

[80] P. S. Goldman-Rakic. Cellular basis of working memory. *Neuron*, 14(3):477–485, 1995. (Cited on page 121.)

[81] Robbe L.T. Goris, Corey M. Ziemba, Gabriel M. Stine, Eero P. Simoncelli, and J. Anthony Movshon. Dissociation of Choice Formation and Choice-Correlated Activity in Macaque Visual Cortex. *The Journal of Neuroscience*, 37(20):5195–5203, 2017. (Cited on pages 20 and 63.)

[82] D.M. Green and J.A. Swets. *Signal Detection Theory and Psycho- physics*. 1966. (Cited on page 3.)

[83] Lan Guo, Jardon T Weems, William I Walker, Anastasia Levichev, and Santiago Jaramillo. Choice-selective neurons in the auditory cortex and in its striatal target encode reward expectation. *Journal of Neuroscience*, 39(19):3687–3697, 2019. (Cited on pages 9, 15, 19, 21, and 62.)

[84] W. Guo, A. R. Chambers, K. N. Darrow, K. E. Hancock, B. G. Shinn-Cunningham, and D. B. Polley. Robustness of Cortical Topography across Fields, Laminae, Anesthetic States, and Neurophysiological Signal Types. *Journal of Neuroscience*, 32(27):9159–9172, jul 2012. (Cited on page 9.)

[85] Zengcai V Guo, S Andrew Hires, Nuo Li, Daniel H O'Connor, Takaki Komiyama, Eran Ophir, Daniel Huber, Claudia Bonardi, Karin Morandell, Diego Gutnisky, Simon Peron, Ning-Long Xu, James Cox, and Karel Svoboda. Procedures for behavioral experiments in head-fixed mice. *PloS one*, 9(2):e88678, jan 2014. (Cited on pages 5, 6, 22, 90, and 92.)

[86] Zengcai V. Guo, Hidehiko K. Inagaki, Kayvon Daie, Shaul Druckmann, Charles R. Gerfen, and Karel Svoboda. Maintenance of persistent activity in a frontal thalamocortical loop. *Nature*, 545(7653):181–186, 2017. (Cited on page 90.)

[87] Channabasavaiah B. Gurumurthy and Kevin C. Kent Lloyd. Generating mouse models for biomedical research: technological advances. *Disease Models & Mechanisms*, 12(1):dmm029462, jan 2019. (Cited on page 90.)

[88] Diego A. Gutnisky, Charles Beaman, Sergio E. Lew, and Valentin Dragoi. Cortical response states for enhanced sensory discrimination. *eLife*, 6:1–23, 2017. (Cited on page 87.)

[89] Ralf M Haefner, Sebastian Gerwinn, Jakob H Macke, and Matthias Bethge. Inferring decoding strategies from choice probabilities in the presence of correlated variability. *Nature Neuroscience*, 16(2):235–242, feb 2013. (Cited on page 53.)

[90] Kenneth E. Hancock and Herbert F. Voigt. Wideband Inhibition of Dorsal Cochlear Nucleus Type IV Units in Cat: A Computational Model. *Annals of Biomedical Engineering*, 27(1):73–87, jan 1999. (Cited on page 61.)

[91] Timothy D Hanks and Christopher Summerfield. Perceptual Decision Making in Rodents, Monkeys, and Humans. *Neuron*, 93(1):15–31, jan 2017. (Cited on pages 2 and 90.)

[92] Kenneth D. Harris and Thomas D. Mrsic-Flogel. Cortical connectivity and sensory coding. *Nature*, 503(7474):51–58, 2013. (Cited on pages xiii, 9, 10, 11, 18, and 61.)

[93] Christopher D Harvey, Philip Coen, and David W Tank. Choice-specific sequences in parietal cortex during a virtual-navigation decision task. *Nature*, 484(7392):62–8, mar 2012. (Cited on page 5.)

[94] Abdallah Hayar, Jeri L. Bryant, John D. Boughter, and Detlef H. Heck. A low-cost solution to measure mouse licking in an electrophysiological setup with a standard analog-to-digital converter. *Journal of neuroscience methods*, 153(2):203–7, jun 2006. (Cited on pages 23 and 93.)

[95] Peter Heil. *The Auditory Cortex*, volume 76. Psychology Press, may 2005. (Cited on page 8.)

[96] Micha Heilbron and Maria Chait. Great Expectations: Is there Evidence for Predictive Coding in Auditory Cortex? *Neuroscience*, 389:54–73, 2018. (Cited on page 18.)

[97] Richard P. Heitz. The speed-accuracy tradeoff: History, physiology, methodology, and behavior. *Frontiers in Neuroscience*, 8(8 JUN):1–19, 2014. (Cited on pages 84 and 87.)

[98] Kenneth R. Henry and Richard A. Chole. Genotypic Differences in Behavioral, Physiological and Anatomical Expressions of Age-Related Hearing Loss in the Laboratory Mouse: Original Papers Travaux originaux. *International Journal of Audiology*, 19(5):369–383, jan 1980. (Cited on pages 58 and 114.)

[99] Ainhoa Hermoso-Mendizabal, Alexandre Hyafil, Pavel E. Rueda-Orozco, Santiago Jaramillo, David Robbe, and Jaime de la Rocha. Response outcomes gate the impact of expectations on perceptual decisions. *Nature Communications*, 11(1):1057, dec 2020. (Cited on pages 85, 90, 113, and 120.)

[100] Adrián Hernández, Verónica Nácher, Rogelio Luna, Antonio Zainos, Luis Lemus, Manuel Alvarez, Yuriria Vázquez, Liliana Camarillo, and Ranulfo Romo. Decoding a Perceptual Decision Process across Cortex. *Neuron*, 66(2):300–314, apr 2010. (Cited on page 20.)

[101] Mark H Histed, Lauren A Carvalho, and John H R Maunsell. Psychophysical measurement of contrast sensitivity in the behaving mouse. *Journal of neurophysiology*, 107(3):758–65, feb 2012. (Cited on page 5.)

[102] Kurt M. Hofstetter and G. Ehret. The auditory cortex of the mouse: Connections of the ultrasonic field. *The Journal of Comparative Neurology*, 323(3):370–386, sep 1992. (Cited on page 9.)

[103] Philip Holmes and Jonathan D. Cohen. Optimality and some of its discontents: Successes and shortcomings of existing models for binary decisions. *Topics in Cognitive Science*, 6(2):258–278, 2014. (Cited on page 90.)

[104] Yuusuke Honma, Hiroaki Tsukano, Masao Horie, Shinsuke Ohshima, Manavu Tohmi, Yamato Kubota, Kuniyuki Takahashi, Ryuichi Hishida, Sugata Takahashi, and Katsuei Shibuki. Auditory Cortical Areas Activated by Slow Frequency-Modulated Sounds in Mice. *PLoS ONE*, 8(7):e68113, jul 2013. (Cited on page 9.)

[105] Tomáš Hromádka and Anthony M. Zador. Representations in auditory cortex. *Current Opinion in Neurobiology*, 19(4):430–433, aug 2009. (Cited on page 59.)

[106] D. H. Hubel and T. N. Wiesel. Receptive fields of single neurones in the cat's striate cortex. *The Journal of Physiology*, 148(3):574–591, oct 1959. (Cited on page 18.)

[107] D. H. Hubel and T. N. Wiesel. Receptive fields, binocular interaction and functional architecture in the cat's visual cortex. *The Journal of Physiology*, 160(1):106–154, jan 1962. (Cited on page 18.)

[108] Daniel Huber, Leopoldo Petreanu, Nima Ghitani, Sachin Ranade, Tomás Hromádka, Zach Mainen, and Karel Svoboda. Sparse optical microstimulation in barrel cortex drives learned behaviour in freely moving mice. *Nature*, 451(7174):61–4, jan 2008. (Cited on page 5.)

[109] T. J. Imig, M. A. Ruggero, L. M. Kitzes, E. Javel, and J. F. Brugge. Organization of auditory cortex in the owl monkey(Aotus trivirgatus). *The Journal of Comparative Neurology*, 171(1):111–128, jan 1977. (Cited on page 8.)

[110] D. R. F. Irvine. *The Auditory Brainstem*. Berlin: Springer-Verlag., 1986. (Cited on page 7.)

[111] James R Ison, Paul D Allen, and William E. O'Neill. Age-Related Hearing Loss in C57BL/6J Mice has both Frequency-Specific and Non-Frequency-Specific Components that Produce a Hyperacusis-Like Exaggeration of the Acoustic Startle Reflex. *Journal of the Association for Research in Otolaryngology*, 8(4):539–550, nov 2007. (Cited on page 58.)

[112] John B. Issa, Benjamin D. Haeffele, Amit Agarwal, Dwight E. Bergles, Eric D. Young, and David T. Yue. Multiscale Optical Ca2+ Imaging of Tonal Organization in Mouse Auditory Cortex. *Neuron*, 83(4):944–959, aug 2014. (Cited on page 9.)

[113] Elina A.K. Jacobs, Nicholas A. Steinmetz, Andrew J. Peters, Matteo Carandini, and Kenneth D. Harris. Cortical State Fluctuations during Sensory Decision Making. *Current Biology*, page 348193, oct 2020. (Cited on pages 6, 15, 16, 67, 68, 81, 85, 86, and 87.)

[114] Santiago Jaramillo and Anthony M Zador. The auditory cortex mediates the perceptual effects of acoustic temporal expectation. *Nature neuroscience*, 14(2):246–51, feb 2011. (Cited on page 5.)

[115] Santiago Jaramillo, Anthony M. Zador, and Santiago Jaramillo. Mice and rats achieve similar levels of performance in an adaptive decision-making task. *Frontiers in Systems Neuroscience*, 8(September):1–11, 2014. (Cited on pages 2, 90, and 91.)

[116] W M Jenkins and R B Masterton. Sound localization: effects of unilateral lesions in central auditory system. *Journal of Neurophysiology*, 47(6):987–1016, jun 1982. (Cited on page 7.)

[117] Miaomiao Jin and Lindsey L. Glickfeld. Contribution of sensory encoding to measured bias. *Journal of Neuroscience*, 39(26):5115–5127, 2019. (Cited on page 113.)

[118] Carolyn Johnson and Linda Wilbrecht. Juvenile mice show greater flexibility in multiple choice reversal learning than adults. *Developmental Cognitive Neuroscience*, 1(4):540–551, 2011. (Cited on page 113.)

[119] Jon H Kaas and Troy A Hackett. Subdivisions of auditory cortex and processing streams in primates. *Proceedings of the National Academy of Sciences*, 97(22):11793–11799, oct 2000. (Cited on pages xiii and 8.)

[120] D. Kahneman and J. Beatty. Pupil Diameter and Load on Memory. *Science*, 154(3756):1583–1585, dec 1966. (Cited on page 66.)

[121] Patrick O. Kanold, Israel Nelken, and Daniel B. Polley. Local versus global scales of organization in auditory cortex. *Trends in Neurosciences*, 37(9):502–510, sep 2014. (Cited on page 8.)

[122] Hiroyuki K. Kato, Shea N. Gillet, and Jeffry S. Isaacson. Flexible Sensory Representations in Auditory Cortex Driven by Behavioral Relevance. *Neuron*, 88(5):1027–1039, 2015. (Cited on pages 91 and 115.)

[123] Tara Keck, Georg B. Keller, R. Irene Jacobsen, Ulf T. Eysel, Tobias Bonhoeffer, and Mark Hübener. Synaptic Scaling and Homeostatic Plasticity in the Mouse Visual Cortex In Vivo. *Neuron*, 80(2):327–334, oct 2013. (Cited on page 18.)

[124] Georg B. Keller and Thomas D. Mrsic-Flogel. Predictive Processing: A Canonical Cortical Computation. *Neuron*, 100(2):424–435, 2018. (Cited on page 18.)

[125] Ian R. Kemp and Birger R. Kaada. The relation of hippocampal theta activity to arousal, attentive behaviour and somato-motor movements in unrestrained cats. *Brain Research*, 95(2-3):323–342, sep 1975. (Cited on pages 15 and 66.)

[126] Daniel Kersten, Pascal Mamassian, and Alan Yuille. Object Perception as Bayesian Inference. *Annual Review of Psychology*, 55(1):271–304, feb 2004. (Cited on pages 2 and 90.)

[127] Vivek Khatri and Raddy Ramos. Rat whisker psychophysics. *The Journal of neuroscience : the official journal of the Society for Neuroscience*, 26(48):12385–6, nov 2006. (Cited on pages 2 and 90.)

[128] Peter R. Killeen, Thomas J. Taylor, and Mario Treviño. Subjects adjust criterion on errors in perceptual decision tasks. *Psychological Review*, 125(1):117–130, jan 2018. (Cited on page 90.)

[129] Juhyun Kim, Chanel J. Matney, Aaron Blankenship, Shaul Hestrin, and Solange P. Brown. Layer 6 corticothalamic neurons activate a cortical output layer, layer 5a. *Journal of Neuroscience*, 34(29):9656–9664, 2014. (Cited on page 11.)

[130] Andrew J. King, Sundeep Teki, and Ben D.B. Willmore. Recent advances in understanding the auditory cortex. *F1000Research*, 7:1555, sep 2018. (Cited on page 12.)

[131] Sue Ann Koay, Stephan Y Thiberge, Carlos D Brody, and David W Tank. Amplitude modulations of sensory responses, and deviations from Weber's Law in pulsatile evidence accumulation. *bioRxiv*, page 2020.06.24.167213, jan 2020. (Cited on page 63.)

[132] Dmitry Kobak, Jose L. Pardo-Vazquez, Mafalda Valente, Christian K. Machens, and Alfonso Renart. State-dependent geometry of population activity in rat auditory cortex. *eLife*, 8:1–27, 2019. (Cited on pages 9, 15, 66, 86, and 120.)

[133] A. Kohn. Stimulus Dependence of Neuronal Correlation in Primary Visual Cortex of the Macaque. *Journal of Neuroscience*, 25(14):3661–3673, apr 2005. (Cited on page 20.)

[134] Conny Kopp-Scheinpflug, James L. Sinclair, and Jennifer F. Linden. When Sound Stops: Offset Responses in the Auditory System. *Trends in Neurosciences*, 41(10):712–728, 2018. (Cited on pages 12 and 61.)

[135] John W Krakauer, Asif A Ghazanfar, Alex Gomez-Marin, Malcolm A Maciver, and David Poeppel. Neuron Perspective Neuroscience Needs Behavior: Correcting a Reductionist Bias. *Neuron*, 93(3):480–490, 2017. (Cited on pages 4, 16, 122, and 123.)

[136] Kishore V Kuchibhotla, Jonathan V Gill, Grace W Lindsay, Eleni S Papadoyannis, Rachel E Field, Tom A Hindmarsh Sten, Kenneth D Miller, and Robert C Froemke. Parallel processing by cortical inhibition enables context-dependent behavior. *Nature Neuroscience*, (October):1–14, 2016. (Cited on pages 18, 19, and 59.)

[137] Kishore V Kuchibhotla, Jonathan V Gill, Grace W Lindsay, Eleni S Papadoyannis, Rachel E Field, Tom A Hindmarsh Sten, Kenneth D Miller, and Robert C Froemke. Parallel processing by cortical inhibition enables context-dependent behavior. *Nature Neuroscience*, 20(1):62–71, jan 2017. (Cited on page 20.)

[138] D.R.J. Laming. *Information Theory of Choice-Reaction Times*. 1968. (Cited on page 3.)

[139] Marieke Langen, Martien J.H. Kas, Wouter G. Staal, Herman van Engeland, and Sarah Durston. The neurobiology of repetitive behavior: Of mice.... *Neuroscience & Biobehavioral Reviews*, 35(3):345–355, jan 2011. (Cited on page 90.)

[140] Seung Hee Lee and Yang Dan. Neuromodulation of Brain States. *Neuron*, 76(1):209–222, 2012. (Cited on page 14.)

[141] H W Leibowitz and L O Harvey. Perception. *Annual Review of Psychology*, 24(1):207–240, jan 1973. (Cited on page 18.)

[142] Jingcheng Li, Xiang Liao, Jianxiong Zhang, Meng Wang, Nian Yang, Jun Zhang, Guanghui Lv, Haohong Li, Jian Lu, Ran Ding, Xingyi Li, Yu Guang, Zhiqi Yang, Han Qin, Wenjun Jin, Kuan Zhang, Chao He, Hongbo Jia, Shaoqun Zeng, Zhian Hu, Israel Nelken, and Xiaowei Chen. Primary Auditory Cortex is Required for Anticipatory Motor Response. *Cerebral Cortex*, 27(6):3254–3271, jun 2017. (Cited on page 59.)

[143] Daniel Linares, David Aguilar-Lleyda, and Joan López-Moliner. Decoupling sensory from decisional choice biases in perceptual decision making. *eLife*, 8:1–16, 2019. (Cited on pages 16, 63, 90, 113, 120, 121, and 122.)

[144] Jennifer F. Linden, Robert C. Liu, Maneesh Sahani, Christoph E. Schreiner, and Michael M. Merzenich. Spectrotemporal Structure of Receptive Fields in Areas AI and AAF of Mouse Auditory Cortex. *Journal of Neurophysiology*, 90(4):2660–2675, oct 2003. (Cited on page 9.)

[145] Ran Littman, Eldad Keha, and Eyal Kalanthroff. Task Conflict and Task Control: A Mini-Review. *Frontiers in Psychology*, 10, jul 2019. (Cited on page 122.)

[146] Sheng Liu, Yong Gu, Gregory C DeAngelis, and Dora E Angelaki. Choice-related activity and correlated noise in subcortical vestibular neurons. *Nature Neuroscience*, 16(1):89–97, jan 2013. (Cited on page 20.)

[147] Gonçalo Lopes, Niccoló Bonacchi, João Frazão, Joana P. Neto, Bassam V. Atallah, Sofia Soares, LuÃs Moreira, Sara Matias, Pavel M. Itskov, PatrÃcia A. Correia, Roberto E. Medina, Lorenza Calcaterra, Elena Dreosti, Joseph J. Paton, and Adam R. Kampff. Bonsai: an event-based framework for processing and controlling data streams. *Frontiers in Neuroinformatics*, 9, apr 2015. (Cited on page 68.)

[148] Matthew Lovett-Barron, Aaron S. Andalman, William E. Allen, Sam Vesuna, Isaac Kauvar, Vanessa M. Burns, and Karl Deisseroth. Ancestral Circuits for the Coordinated Modulation of Brain State. *Cell*, 171(6):1411–1423.e17, 2017. (Cited on page 66.)

[149] Bruce D Lucas and Takeo Kanade. An iterative image registration technique with an application to stereo vision. In *Proceedings of the 7th international joint conference on {Artificial} intelligence - {Volume} 2*. Morgan Kaufmann Publishers Inc., 1981. (Cited on page 69.)

[150] Jan-Matthis Lueckmann, Jakob H Macke, and Hendrikje Nienborg. Can Serial Dependencies in Choices and Neural Activity Explain Choice Probabilities? *The Journal of Neuroscience*, 38(14):3495–3506, 2018. (Cited on page 119.)

[151] Fred Marbach and Anthony Zador. A self-initiated two-alternative forced choice paradigm for head-fixed mice. *bioRxiv*, page 073783, 2016. (Cited on pages 5, 6, and 91.)

[152] Hubert Markl and Günter Ehret. Die Hörschwelle der Maus (Mus musculus). *Zeitschrift für Tierpsychologie*, 33(3-4):274–286, apr 2010. (Cited on pages 58, 104, and 114.)

[153] Tiago Marques, Mathew T. Summers, Gabriela Fioreze, Marina Fridman, Rodrigo F. Dias, Marla B. Feller, and Leopoldo Petreanu. A Role for Mouse Primary Visual Cortex in Motion Perception. *Current Biology*, 28(11):1703–1713.e6, jun 2018. (Cited on pages 5, 6, and 90.)

[154] David Marr. *Vision: A Computational Approach (MIT*. Boston, MA: MIT Press., 1982. (Cited on page 123.)

[155] David Marr. *Vision: A computational investigation into the human representation and processing of visual information*. 2010. (Cited on page 18.)

[156] Alexander Mathis, Pranav Mamidanna, Kevin M. Cury, Taiga Abe, Venkatesh N. Murthy, Mackenzie Weygandt Mathis, and Matthias Bethge. DeepLabCut: markerless pose estimation of user-defined body parts with deep learning. *Nature Neuroscience*, 21(9):1281–1289, sep 2018. (Cited on page 69.)

[157] F. Matyas, V. Sreenivasan, F. Marbach, C. Wacongne, B. Barsy, C. Mateo, R. Aronoff, and C. C. H. Petersen. Motor Control by Sensory Cortex. *Science*, 330(6008):1240–1243, nov 2010. (Cited on pages 11 and 118.)

[158] Johannes M. Mayrhofer, Vida Skreb, Wolfger Von der Behrens, Simon Musall, Bruno Weber, and Florent Haiss. Novel two-alternative forced choice paradigm for bilateral vibrotactile whisker frequency discrimination in head-fixed mice and rats. *Journal of Neurophysiology*, 109(1):273–284, 2013. (Cited on page 90.)

[159] David A McCormick, Matthew J McGinley, and David B Salkoff. Brain state dependent activity in the cortex and thalamus. *Current Opinion in Neurobiology*, 31(1):133–140, apr 2015. (Cited on page 14.)

[160] David A. McCormick, Dennis B. Nestvogel, and Biyu J. He. Neuromodulation of Brain State and Behavior. *Annual Review of Neuroscience*, 43:391–415, 2020. (Cited on pages 12, 13, 14, 15, 16, and 87.)

[161] Matthew J. McGinley, Stephen V. David, and David A. McCormick. Cortical Membrane Potential Signature of Optimal States for Sensory Signal Detection. *Neuron*, 87(1):179–192, 2015. (Cited on pages 14, 15, 16, 66, 85, 87, and 91.)

[162] Matthew J. McGinley, Stephen V. David, and David A. McCormick. Cortical Membrane Potential Signature of Optimal States for Sensory Signal Detection. *Neuron*, 87(1):179–192, 2015. (Cited on page 81.)

[163] Matthew J. McGinley, Martin Vinck, Jacob Reimer, Renata Batista-Brito, Edward Zagha, Cathryn R. Cadwell, Andreas S. Tolias, Jessica A. Cardin, and David A. McCormick. Waking State: Rapid Variations Modulate Neural and Behavioral Responses. *Neuron*, 87(6):1143–1161, 2015. (Cited on pages 13, 14, and 15.)

[164] Michael M. Merzenich and John F. Brugge. Representation of the cochlear partition on the superior temporal plane of the macaque monkey. *Brain Research*, 50(2):275–296, feb 1973. (Cited on page 8.)

[165] Donald R. Meyer and Clinton N. Woolsey. EFFECTS OF LOCALIZED CORTICAL DESTRUCTION ON AUDITORY DISCRIMINATIVE CONDITIONING IN CAT. *Journal of Neurophysiology*, 15(2):149–162, mar 1952. (Cited on page 19.)

[166] Jude F. Mitchell, Kristy A. Sundberg, and John H. Reynolds. Spatial Attention Decorrelates Intrinsic Activity Fluctuations in Macaque Area V4. *Neuron*, 63(6):879–888, sep 2009. (Cited on page 20.)

[167] Gabriela Mochol, Ainhoa Hermoso-Mendizabal, Shuzo Sakata, Kenneth D. Harris, and Jaime de la Rocha. Stochastic transitions into silence cause noise correlations in cortical circuits. *Proceedings of the National Academy of Sciences*, 112(11):3529–3534, mar 2015. (Cited on page 85.)

[168] Anne Morel and Jon H. Kaas. Subdivisions and connections of auditory cortex in owl monkeys. *The Journal of Comparative Neurology*, 318(1):27–63, apr 1992. (Cited on page 8.)

[169] Rubén Moreno-Bote, Jeffrey Beck, Ingmar Kanitscheider, Xaq Pitkow, Peter Latham, and Alexandre Pouget. Information-limiting correlations. *Nature Neuroscience*, 17(10):1410–1417, oct 2014. (Cited on pages 66 and 123.)

[170] Simon Musall, Matthew T. Kaufman, Ashley L. Juavinett, Steven Gluf, and Anne K. Churchland. Single-trial neural dynamics are dominated by richly varied movements. *Nature Neuroscience*, 22(10):1677–1686, oct 2019. (Cited on pages 69 and 87.)

[171] Shiro Nakata, Makoto Takemoto, and Wen-Jie Song. Differential cortical and subcortical projection targets of subfields in the core region of mouse auditory cortex. *Hearing Research*, 386:107876, feb 2020. (Cited on page 9.)

[172] Anirvan Nandy, Jonathan J. Nassi, Monika P. Jadi, and John Reynolds. Optogenetically induced low-frequency correlations impair perception. *eLife*, 8, 2019. (Cited on page 14.)

[173] Michael Neelon. Elastic attention: enhanced, then sharpened response to auditory input as attentional load increases. *Frontiers in Human Neuroscience*, 5, 2011. (Cited on page 13.)

[174] Israel Nelken, Gal Chechik, Thomas D. Mrsic-Flogel, Andrew J. King, and Jan W H Schnupp. Encoding stimulus information by spike numbers and mean response time in primary auditory cortex. *Journal of Computational Neuroscience*, 19(2):199–221, 2005. (Cited on pages 29 and 60.)

[175] Israel Nelken, Alon Fishbach, Liora Las, Nachum Ulanovsky, and Dina Farkas. Primary auditory cortex of cats: feature detection or something else? *Biological Cybernetics*, 89(5):397–406, nov 2003. (Cited on page 9.)

[176] Anders Nelson, David M Schneider, Jun Takatoh, Katsuyasu Sakurai, Fan Wang, and Richard Mooney. A circuit for motor cortical modulation of auditory cortical activity. *The Journal of neuroscience : the official journal of the Society for Neuroscience*, 33(36):14342–53, sep 2013. (Cited on page 12.)

[177] Garrett T. Neske, Dennis Nestvogel, Paul J. Steffan, and David A. McCormick. Distinct waking states for strong evoked responses in primary visual cortex and optimal visual detection performance. *Journal of Neuroscience*, 39(50):1004–10059, 2019. (Cited on page 87.)

[178] William T. Newsome, Kenneth H. Britten, and J. Anthony Movshon. Neuronal correlates of a perceptual decision. *Nature*, 341(6237):52–54, sep 1989. (Cited on pages 2 and 90.)

[179] H. Nienborg. Macaque V2 Neurons, But Not V1 Neurons, Show Choice-Related Activity. *Journal of Neuroscience*, 26(37):9567–9578, sep 2006. (Cited on page 20.)

[180] Hendrikje Nienborg and Bruce G. Cumming. Decision-related activity in sensory neurons reflects more than a neuron's causal effect. *Nature*, 459(7243):89–92, may 2009. (Cited on page 20.)

[181] Mamiko Niwa, Jeffrey S. Johnson, Kevin N. O'Connor, and Mitchell L. Sutter. Differences between primary auditory cortex and auditory belt related to encoding and choice for AM sounds. *Journal of Neuroscience*, 33(19):8378–8395, 2013. (Cited on pages 20 and 63.)

[182] Janja Novak, Jeremy D. Bailoo, Luca Melotti, and Hanno Würbel. Effect of cage-induced stereotypies on measures of affective state and recurrent perseveration in CD-1 and C57BL/6 mice. *PLoS ONE*, 11(5):1–22, 2016. (Cited on pages 90 and 122.)

[183] Monica Noelle O'Connell, Annamaria Barczak, Charles E. Schroeder, and Peter Lakatos. Layer Specific Sharpening of Frequency Tuning by Selective Attention in Primary Auditory Cortex. *The Journal of Neuroscience*, 34(49):16496–16508, dec 2014. (Cited on page 13.)

[184] Shinpei Ohga, Hiroaki Tsukano, Masao Horie, Hiroki Terashima, Nana Nishio, Yamato Kubota, Kuniyuki Takahashi, Ryuichi Hishida, Hirohide Takebayashi, and Katsuei Shibuki. Direct relay pathways from lemniscal auditory thalamus to secondary auditory field in mice. *Cerebral Cortex*, 28(12):4424–4439, 2018. (Cited on page 115.)

[185] F W Ohl, W Wetzel, T Wagner, A Rech, and H Scheich. Bilateral ablation of auditory cortex in Mongolian gerbil affects discrimination of frequency modulated tones but not of pure tones. *Learning & memory (Cold Spring Harbor, N.Y.)*, 6(4):347–62, jan 1999. (Cited on page 19.)

[186] Frank W. Ohl and Henning Scheich. Differential Frequency Conditioning Enhances Spectral Contrast Sensitivity of Units in Auditory Cortex (Field Al) of the Alert Mongolian Gerbil. *European Journal of Neuroscience*, 8(5):1001–1017, may 1996. (Cited on page 13.)

[187] H. Okamoto, H. Stracke, C. H. Wolters, F. Schmael, and C. Pantev. Attention Improves Population-Level Frequency Tuning in Human Auditory Cortex. *Journal of Neuroscience*, 27(39):10383–10390, sep 2007. (Cited on page 13.)

[188] Shawn R. Olsen, Dante S. Bortone, Hillel Adesnik, and Massimo Scanziani. Gain control by layer six in cortical circuits of vision. *Nature*, 483(7387):47–52, mar 2012. (Cited on page 12.)

[189] Michael S. Osmanski and Xiaoqin Wang. Behavioral Dependence of Auditory Cortical Responses. *Brain Topography*, 28(3):365–378, 2015. (Cited on page 12.)

[190] Conor O'sullivan, Aldis P. Weible, and Michael Wehr. Auditory cortex contributes to discrimination of pure tones. *eNeuro*, 6(5):1–14, 2019. (Cited on pages 19, 20, 59, 86, 118, and 120.)

[191] Timothy M. Otchy, Steffen B. E. Wolff, Juliana Y. Rhee, Cengiz Pehlevan, Risa Kawai, Alexandre Kempf, Sharon M. H. Gobes, and Bence P. Ölveczky. Acute off-target effects of neural circuit manipulations. *Nature*, 528(7582):358–363, dec 2015. (Cited on page 19.)

[192] Marius Pachitariu, Dmitry R. Lyamzin, Maneesh Sahani, and Nicholas A. Lesica. State-dependent population coding in primary auditory cortex. *Journal of Neuroscience*, 35(5):2058–2073, 2015. (Cited on pages 15, 66, 86, and 120.)

[193] Marius Pachitariu, Nick Steinmetz, Shabnam Kadir, Matteo Carandini, and Kenneth Harris. Fast and accurate spike sorting of high-channel count probes with KiloSort. *Advances in Neural Information Processing Systems*, (Nips):4455–4463, 2016. (Cited on page 28.)

[194] Stefano Panzeri, Simon R. Schultz, Alessandro Treves, and Edmund T. Rolls. Correlations and the encoding of information in the nervous system. *Proceedings of the Royal Society of London. Series B: Biological Sciences*, 266(1423):1001–1012, may 1999. (Cited on pages 14 and 66.)

[195] Stefano Panzeri and Alessandro Treves. Analytical estimates of limited sampling biases in different information measures. *Network: Computation in Neural Systems*, 7(1):87–107, 1996. (Cited on page 29.)

[196] Efstathios B. Papachristos and C. R. Gallistel. Autoshaped Head Poking in the Mouse: a Quantitative Analysis of the Learning Curve. *Journal of the Experimental Analysis of Behavior*, 85(3):293–308, 2006. (Cited on page 114.)

[197] Jose L. Pardo-Vazquez, Juan R. Castiñeiras-de Saa, Mafalda Valente, Iris Damião, Tiago Costa, M. Inês Vicente, André G. Mendonça, Zachary F. Mainen, and Alfonso Renart. The mechanistic foundation of Weber's law. *Nature Neuroscience*, 22(9):1493–1502, sep 2019. (Cited on pages 2 and 90.)

[198] A J Parker and W T Newsome. Sense and the single neuron: probing the physiology of perception. *Annual review of neuroscience*, 21:227–77, 1998. (Cited on page 4.)

[199] D.H. Passe and J.C. Walker. Odor psychophysics in vertebrates. *Neuroscience & Biobehavioral Reviews*, 9(3):431–467, sep 1985. (Cited on pages 2 and 90.)

[200] Warren W. Pettine, Nicholas A. Steinmetz, and Tirin Moore. Laminar segregation of sensory coding and behavioral readout in macaque V4. *Proceedings of the National Academy of Sciences*, 116(29):14749–14754, jul 2019. (Cited on pages 9, 15, and 19.)

[201] Benjamin A. Porter, Tara R. Rosenthal, Kamalini G. Ranasinghe, and Michael P. Kilgard. Discrimination of brief speech sounds is impaired in rats with auditory cortex lesions. *Behavioural Brain Research*, 219(1):68–74, may 2011. (Cited on page 19.)

[202] James F. A. Poulet and Sylvain Crochet. The Cortical States of Wakefulness. *Frontiers in Systems Neuroscience*, 12, jan 2019. (Cited on page 14.)

[203] Braden A. Purcell and Roozbeh Kiani. Neural Mechanisms of Post-error Adjustments of Decision Policy in Parietal Cortex. *Neuron*, 89(3):658–671, 2016. (Cited on page 87.)

[204] Dale Purves, George J Augustine, David Fitzpatrick, William C Hall, Anthony-Samuel LaMantia, and Leonard E. White. *Neuroscience*. Sinauer Associates, 5th edition, 2012. (Cited on pages 6 and 7.)

[205] Rajesh P.N. Rao. An optimal estimation approach to visual perception and learning. *Vision Research*, 39(11):1963–1989, jun 1999. (Cited on pages 2 and 90.)

[206] David Raposo, John P Sheppard, Paul R Schrater, and Anne K Churchland. Multisensory decision-making in rats and humans. *The Journal of neuroscience : the official journal of the Society for Neuroscience*, 32(11):3726–35, mar 2012. (Cited on page 5.)

[207] Josef P. Rauschecker, Biao Tian, Timothy Pons, and Mortimer Mishkin. Serial and parallel processing in rhesus monkey auditory cortex. *The Journal of Comparative Neurology*, 382(1):89–103, may 1997. (Cited on page 8.)

[208] Justin B. Rawley and Christos Constantinidis. Neural correlates of learning and working memory in the primate posterior parietal cortex. *Neurobiology of Learning and Memory*, 91(2):129–138, feb 2009. (Cited on page 121.)

[209] Gregg H. Recanzone. Perception of auditory signals. *Annals of the New York Academy of Sciences*, 1224(1):96–108, apr 2011. (Cited on page 18.)

[210] Jacob Reimer, Matthew J. McGinley, Yang Liu, Charles Rodenkirch, Qi Wang, David A. McCormick, and Andreas S. Tolias. Pupil fluctuations track rapid changes in adrenergic and cholinergic activity in cortex. *Nature Communications*, 7(May):1–7, 2016. (Cited on pages 14 and 85.)

[211] Anton Reiner. Corticostriatal projection neurons – dichotomous types and dichotomous functions. *Frontiers in Neuroanatomy*, 4, 2010. (Cited on page 11.)

[212] A. Renart, J. de la Rocha, P. Bartho, L. Hollender, N. Parga, A. Reyes, and K. D. Harris. The Asynchronous State in Cortical Circuits. *Science*, 327(5965):587–590, jan 2010. (Cited on pages xiv, 13, 14, and 85.)

[213] Daniel Reznik, Yael Henkin, Noa Schadel, and Roy Mukamel. Lateralized enhancement of auditory cortex activity and increased sensitivity to self-generated sounds. *Nature communications*, 5:4059, jun 2014. (Cited on page 12.)

[214] Daniel Reznik, Ori Ossmy, and Roy Mukamel. Enhanced auditory evoked activity to self-generated sounds is mediated by primary and supplementary motor cortices. *The Journal of neuroscience : the official journal of the Society for Neuroscience*, 35(5):2173–80, feb 2015. (Cited on page 12.)

[215] Ranulfo Romo, Adrián Hernández, Antonio Zainos, Luis Lemus, and Carlos D. Brody. Neuronal correlates of decision-making in secondary somatosensory cortex. *Nature Neuroscience*, 5(11):1217–1225, nov 2002. (Cited on page 20.)

[216] Cedric Roussel, Gethin Hughes, and Florian Waszak. A preactivation account of sensory attenuation. *Neuropsychologia*, 51(5):922–929, apr 2013. (Cited on page 12.)

[217] Douglas A Ruff and Marlene R Cohen. Attention can either increase or decrease spike count correlations in visual cortex. *Nature Neuroscience*, 17(11):1591–1597, nov 2014. (Cited on page 20.)

[218] Brian P Rummell, Jan L Klee, and Torfi Sigurdsson. Attenuation of Responses to Self-Generated Sounds in Auditory Cortical Neurons. *The Journal of neuroscience : the official journal of the Society for Neuroscience*, 36(47):12010–12026, 2016. (Cited on page 12.)

[219] Caroline A. Runyan, Eugenio Piasini, Stefano Panzeri, and Christopher D. Harvey. Distinct timescales of population coding across cortex. *Nature*, 548(7665):92–96, 2017. (Cited on page 90.)

[220] Natalia Rybalko, Daniel Šuta, Fidel Nwabueze-Ogbo, and Josef Syka. Effect of auditory cortex lesions on the discrimination of frequency-modulated tones in rats. *European Journal of Neuroscience*, 23(6):1614–1622, mar 2006. (Cited on page 19.)

[221] S. Sadagopan and X. Wang. Contribution of Inhibition to Stimulus Selectivity in Primary Auditory Cortex of Awake Primates. *Journal of Neuroscience*, 30(21):7314–7325, may 2010. (Cited on page 13.)

[222] Shuzo Sakata and Kenneth D Harris. Laminar Structure of Spontaneous and Sensory-Evoked Population Activity in Auditory Cortex. *Neuron*, 64(3):404–418, 2009. (Cited on pages 10, 12, 18, and 60.)

[223] Aman B Saleem, Aslı Ayaz, Kathryn J Jeffery, Kenneth D Harris, and Matteo Carandini. Integration of visual motion and locomotion in mouse visual cortex. *Nature Neuroscience*, 16(12):1864–1869, dec 2013. (Cited on page 18.)

[224] David B. Salkoff, Edward Zagha, Erin McCarthy, and David A. McCormick. Movement and Performance Explain Widespread Cortical Activity in a Visual Detection Task. *Cerebral Cortex*, 30(1):421–437, 2020. (Cited on pages 12, 15, 62, 68, 75, 85, 87, 118, and 121.)

[225] Joshua I. Sanders and Adam Kepecs. Choice ball: A response interface for two-choice psychometric discrimination in head-fixed mice. *Journal of Neurophysiology*, 108(12):3416–3423, 2012. (Cited on pages 6, 90, and 91.)

[226] Varun Saravanan, Gordon J Berman, and Samuel J Sober. Application of the Hierarchical Bootstrap to Multi-Level Data in Neuroscience. *bioRxiv*, page 819334, jan 2020. (Cited on page 31.)

[227] Federica Scarpina and Sofia Tagini. The Stroop Color and Word Test. *Frontiers in Psychology*, 8, apr 2017. (Cited on page 122.)

[228] D. M. Schneider and R. Mooney. Motor cortex suppresses auditory cortical responses to self-generated sounds. In *Soc. Neurosci. Nov. 11–15, Washington, DC*, 2017. (Cited on page 12.)

[229] David M. Schneider and Richard Mooney. How movement modulates hearing. *Annual Review of Neuroscience*, 41:553–572, 2018. (Cited on pages 12, 13, 18, and 19.)

[230] David M. Schneider, Anders Nelson, and Richard Mooney. A synaptic and circuit basis for corollary discharge in the auditory cortex. *Nature*, 513(7517):189–194, 2014. (Cited on pages 12, 19, 62, and 118.)

[231] David M. Schneider, Janani Sundararajan, and Richard Mooney. A cortical filter that learns to suppress the acoustic consequences of movement. *Nature*, 561(7723):391–395, sep 2018. (Cited on page 12.)

[232] J Schnupp, I Nelken, and A King. *Auditory Neuroscience: Making Sense of Sound*. MIT Press, 2013. (Cited on page 7.)

[233] Jan W. H. Schnupp, Christian Honey, and Ben D. B. Willmore. Neural Correlates of Auditory Object Perception. In *Neural Correlates of Auditory Cognition*, pages 115–149. Springer, 2013. (Cited on page 9.)

[234] Sven Schörnich, Ludwig Wallmeier, Nikodemus Gessele, Andreas Nagy, Michael Schranner, Daniel Kish, and Lutz Wiegrebe. Psychophysics of human echolocation. *Advances in experimental medicine and biology*, 787:311–9, 2013. (Cited on pages 2 and 90.)

[235] Heiko H. Schütt, Stefan Harmeling, Jakob H. Macke, and Felix A. Wichmann. Painfree and accurate Bayesian estimation of psychometric functions for (potentially) overdispersed data. *Vision Research*, 122:105–123, 2016. (Cited on pages 25 and 96.)

[236] João D. Semedo, Amin Zandvakili, Christian K. Machens, Byron M. Yu, and Adam Kohn. Cortical Areas Interact through a Communication Subspace. *Neuron*, 102(1):249–259.e4, 2019. (Cited on page 64.)

[237] Michael N. Shadlen and Roozbeh Kiani. Decision making as a window on cognition. *Neuron*, 80(3):791–806, 2013. (Cited on pages 2 and 12.)

[238] Michael N. Shadlen and William T. Newsome. Noise, neural codes and cortical organization. *Current Opinion in Neurobiology*, 4(4):569–579, aug 1994. (Cited on page 12.)

[239] Michael N. Shadlen and William T. Newsome. The Variable Discharge of Cortical Neurons: Implications for Connectivity, Computation, and Information Coding. *The Journal of Neuroscience*, 18(10):3870–3896, may 1998. (Cited on page 12.)

[240] MN Shadlen, KH Britten, WT Newsome, and JA Movshon. A computational analysis of the relationship between neuronal and behavioral responses to visual motion. *The Journal of Neuroscience*, 16(4):1486–1510, feb 1996. (Cited on pages 20, 53, and 62.)

[241] Maoz Shamir and Haim Sompolinsky. Implications of Neuronal Diversity on Population Coding. *Neural Computation*, 18(8):1951–1986, aug 2006. (Cited on page 66.)

[242] S Murray Sherman. Thalamocortical interactions. *Current Opinion in Neurobiology*, 22(4):575–579, aug 2012. (Cited on pages 7 and 11.)

[243] Stewart Shipp. Structure and function of the cerebral cortex. *Current biology : CB*, 17(12):R443–9, jun 2007. (Cited on pages 10, 11, and 18.)

[244] B. F. Skinner. 'Superstition' in the pigeon. *Journal of Experimental Psychology*, 38(2):168–172, 1948. (Cited on page 114.)

[245] Matthew Smear, Roman Shusterman, Rodney O'Connor, Thomas Bozza, and Dmitry Rinberg. Perception of sniff phase in mouse olfaction. *Nature*, 479(7373):397–400, oct 2011. (Cited on page 5.)

[246] Magdalena Sołyga and Tania Rinaldi Barkat. Distinct processing of tone offset in two primary auditory cortices. *Scientific Reports*, 9(1):1–12, 2019. (Cited on pages 9, 12, and 61.)

[247] Haim Sompolinsky, Hyoungsoo Yoon, Kukjin Kang, and Maoz Shamir. Population coding in neuronal systems with correlated noise. *Physical Review E*, 64(5):051904, oct 2001. (Cited on page 66.)

[248] Anderson Speed, Joseph Del Rosario, Christopher P. Burgess, and Bilal Haider. Cortical State Fluctuations across Layers of V1 during Visual Spatial Perception. *Cell Reports*, 26(11):2868–2874.e3, 2019. (Cited on pages 14, 66, 87, and 121.)

[249] Anderson Speed, Joseph Del Rosario, Navid Mikail, and Bilal Haider. Spatial attention enhances network, cellular and subthreshold responses in mouse visual cortex. *Nature Communications*, 11(1), 2020. (Cited on pages 12, 15, and 66.)

[250] H Stanislaw and N Todorov. Calculation of signal detection theory measures. *Behavior research methods, instruments, & computers : a journal of the Psychonomic Society, Inc*, 31(1):137–49, feb 1999. (Cited on page 3.)

[251] Max-Philipp Stenner, Markus Bauer, Hans-Jochen Heinze, Patrick Haggard, and Raymond J Dolan. Parallel processing streams for motor output and sensory prediction during action preparation. *Journal of neurophysiology*, 113(6):1752–62, mar 2015. (Cited on page 12.)

[252] M. Steriade, P. Gloor, R.R. Llinás, F.H. Lopes da Silva, and M.-M. Mesulam. Basic mechanisms of cerebral rhythmic activities. *Electroencephalography and Clinical Neurophysiology*, 76(6):481–508, dec 1990. (Cited on page 66.)

[253] M Steriade, I Timofeev, and F Grenier. Natural waking and sleep states: a view from inside neocortical neurons. *Journal of neurophysiology*, 85(5):1969–85, may 2001. (Cited on page 14.)

[254] I. Stiebler, R. Neulist, I. Fichtel, and G. Ehret. The auditory cortex of the house mouse: left-right differences, tonotopic organization and quantitative analysis of frequency representation. *Journal of Comparative Physiology A: Sensory, Neural, and Behavioral Physiology*, 181(6):559–571, dec 1997. (Cited on pages 8 and 9.)

[255] Carsen Stringer, Marius Pachitariu, Nicholas Steinmetz, Charu Bai Reddy, Matteo Carandini, and Kenneth D. Harris. Spontaneous behaviors drive multidimensional, brainwide activity. *Science*, 364(6437), 2019. (Cited on pages 69, 85, 87, and 118.)

[256] Nobuo Suga. Sharpening of frequency tuning by inhibition in the central auditory system: tribute to Yasuji Katsuki. *Neuroscience Research*, 21(4):287–299, feb 1995. (Cited on page 13.)

[257] Sanjiv K. Talwar, Pawel G. Musial, and George L. Gerstein. Role of mammalian auditory cortex in the perception of elementary sound properties. *Journal of Neurophysiology*, 85(6):2350–2358, 2001. (Cited on pages 19 and 58.)

[258] Wilson P. Tanner and John A. Swets. A decision-making theory of visual detection. *Psychological Review*, 61(6):401–409, 1954. (Cited on page 3.)

[259] Joshua B. Tenenbaum and Thomas L. Griffiths. Generalization, similarity, and Bayesian inference. *Behavioral and Brain Sciences*, 24(4):629–640, aug 2001. (Cited on pages 2 and 90.)

[260] Thomson. Neocortical layer 6, a review. *Frontiers in Neuroanatomy*, 2010. (Cited on page 11.)

[261] D.J. Tolhurst, J.A. Movshon, and A.F. Dean. The statistical reliability of signals in single neurons in cat and monkey visual cortex. *Vision Research*, 23(8):775–785, jan 1983. (Cited on page 12.)

[262] George J. Tomko and Donald R. Crapper. Neuronal variability: non-stationary responses to identical visual stimuli. *Brain Research*, 79(3):405–418, oct 1974. (Cited on page 12.)

[263] C Trahiotis and D E Robinson. Auditory psychophysics. *Annual review of psychology*, 30:31–61, 1979. (Cited on pages 2 and 90.)

[264] Alessandro Treves and Stefano Panzeri. The Upward Bias in Measures of Information Derived from Limited Data Samples. *Neural Computation*, 7(2):399–407, 1995. (Cited on page 29.)

[265] Mario Treviño. Stimulus similarity determines the prevalence of behavioral laterality in a visual discrimination task for mice. *Scientific Reports*, 4:1–12, 2014. (Cited on pages 90 and 122.)

[266] Mario Treviño, Ricardo Medina-Coss y León, and Belén Haro. Adaptive Choice Biases in Mice and Humans. *Frontiers in Behavioral Neuroscience*, 14(July), 2020. (Cited on pages 90, 113, and 122.)

[267] Mario Treviño, Tatiana Oviedo, Patrick Jendritza, Shi Bin Li, Georg Köhr, and Rodrigo J. De Marco. Controlled variations in stimulus similarity during learning determine visual discrimination capacity in freely moving mice. *Scientific Reports*, 3:1–13, 2013. (Cited on page 113.)

[268] Hiroaki Tsukano, Masao Horie, Takeshi Bo, Arikuni Uchimura, Ryuichi Hishida, Masaharu Kudoh, Kuniyuki Takahashi, Hirohide Takebayashi, and Katsuei Shibuki. Delineation of a frequency-organized region isolated from the mouse primary auditory cortex. *Journal of Neurophysiology*, 113(7):2900–2920, apr 2015. (Cited on pages xiii, 8, and 9.)

[269] Hiroaki Tsukano, Masao Horie, Ryuichi Hishida, Kuniyuki Takahashi, Hirohide Takebayashi, and Katsuei Shibuki. Quantitative map of multiple auditory cortical regions with a stereotaxic fine-scale atlas of the mouse brain. *Scientific Reports*, 6(1):22315, apr 2016. (Cited on page 9.)

[270] Hiroaki Tsukano, Masao Horie, Yuusuke Honma, Shinpei Ohga, Ryuichi Hishida, Hirohide Takebayashi, Sugata Takahashi, and Katsuei Shibuki. Age-related deterioration of cortical responses to slow FM sounds in the auditory belt region of adult C57BL/6 mice. *Neuroscience Letters*, 556:204–209, nov 2013. (Cited on page 9.)

[271] Hiroaki Tsukano, Masao Horie, Shinpei Ohga, Kuniyuki Takahashi, Yamato Kubota, Ryuichi Hishida, Hirohide Takebayashi, and Katsuei Shibuki. Reconsidering Tonotopic Maps in the Auditory Cortex and Lemniscal Auditory Thalamus in Mice. *Frontiers in Neural Circuits*, 11, feb 2017. (Cited on pages 6, 8, and 9.)

[272] Joji Tsunada, Andrew S.K. Liu, Joshua I. Gold, and Yale E. Cohen. Causal contribution of primate auditory cortex to auditory perceptual decision-making. *Nat Neuroscience*, 19(1):1922–2013, 2016. (Cited on pages 19 and 62.)

[273] Naoshige Uchida and Zachary F Mainen. Speed and accuracy of olfactory discrimination in the rat. *Nature neuroscience*, 6(11):1224–9, nov 2003. (Cited on page 5.)

[274] Markus Ullsperger and Claudia Danielmeier. Reducing Speed and Sight: How Adaptive Is Post-Error Slowing? *Neuron*, 89(3):430–432, 2016. (Cited on page 87.)

[275] Anne E. Urai, Jan Willem De Gee, Konstantinos Tsetsos, and Tobias H. Donner. Choice history biases subsequent evidence accumulation. *eLife*, 8:1–34, 2019. (Cited on page 113.)

[276] Michiel van Elk, Bigna Lenggenhager, Lukas Heydrich, and Olaf Blanke. Suppression of the auditory N1-component for heartbeat-related sounds reflects interoceptive predictive coding. *Biological psychology*, 99:172–82, may 2014. (Cited on page 12.)

[277] Peter Van Meer and Jacob Raber. Mouse behavioural analysis in systems biology. *Biochemical Journal*, 389(3):593–610, 2005. (Cited on pages 90 and 122.)

[278] C. H. Vanderwolf. *An odyssey through the brain, behavior and the mind.* Springer Science & Busi- ness Media, 2003. (Cited on page 66.)

[279] C.H. Vanderwolf. Cerebral Activity and Behavior: Control by Central Cholinergic and Serotonergic Systems. In *International Review of Neurobiology*, pages 225–340. Elsevier, 1988. (Cited on pages 15 and 66.)

[280] Martin Vinck, Renata Batista-Brito, Ulf Knoblich, and Jessica A. Cardin. Arousal and Locomotion Make Distinct Contributions to Cortical Activity Patterns and Visual Encoding. *Neuron*, 86(3):740–754, may 2015. (Cited on pages 66 and 85.)

[281] HLF von Helmholtz. *Treatise on Physiological Optics.* New York: Dover, 1925. (Cited on pages 2 and 90.)

[282] Vladyslav V Vyazovskiy, Umberto Olcese, Erin C Hanlon, Yuval Nir, Chiara Cirelli, and Giulio Tononi. Local sleep in awake rats. *Nature*, 472(7344):443–447, apr 2011. (Cited on pages 14 and 66.)

[283] Michael L. Waskom, Gouki Okazawa, and Roozbeh Kiani. Designing and Interpreting Psychophysical Investigations of Cognition. *Neuron*, 104(1):100–112, 2019. (Cited on page 5.)

[284] Carmen Weiss, Arvid Herwig, and Simone Schütz-Bosbach. The self in action effects: selective attenuation of self-generated sounds. *Cognition*, 121(2):207–18, nov 2011. (Cited on page 12.)

[285] Ziv M Williams, John C Elfar, Emad N Eskandar, Louis J Toth, and John A Assad. Parietal activity and the perceived direction of ambiguous apparent motion. *Nature Neuroscience*, 6(6):616–623, jun 2003. (Cited on page 20.)

[286] Ross S. Williamson, Kenneth E. Hancock, Barbara G. Shinn-Cunningham, and Daniel B. Polley. Locomotion and Task Demands Differentially Modulate Thalamic Audiovisual Processing during Active Search. *Current Biology*, 25(14):1885–1891, 2015. (Cited on page 19.)

[287] Klaus Wimmer, Albert Compte, Alex Roxin, Diogo Peixoto, Alfonso Renart, and Jaime De La Rocha. Sensory integration dynamics in a hierarchical network explains choice probabilities in cortical area MT. *Nature Communications*, 6:1–13, 2015. (Cited on pages 20 and 62.)

[288] Ralf D. Wimmer, L. Ian Schmitt, Thomas J. Davidson, Miho Nakajima, Karl Deisseroth, and Michael M. Halassa. Thalamic control of sensory selection in divided attention. *Nature*, 2015. (Cited on page 13.)

[289] Jonathan Winson. Interspecies differences in the occurrence of theta. *Behavioral Biology*, 7(4):479–487, aug 1972. (Cited on page 66.)

[290] Jessica K Witt, J Eric T Taylor, Mila Sugovic, and John T Wixted. Signal Detection Measures Cannot Distinguish Perceptual Biases from Response Biases. *Perception*, 44(3):289–300, mar 2015. (Cited on page 113.)

[291] Si Wu, Hiroyuki Nakahara, and Shun-ichi Amari. Population Coding with Correlation and an Unfaithful Model. *Neural Computation*, 13(4):775–797, apr 2001. (Cited on page 66.)

[292] T. C. Yin and J. C. Chan. Interaural time sensitivity in medial superior olive of cat. *Journal of Neurophysiology*, 64(2):465–488, aug 1990. (Cited on page 7.)

[293] Xiong-jie Yu, J. David Dickman, Gregory C. DeAngelis, and Dora E. Angelaki. Neuronal thresholds and choice-related activity of otolith afferent fibers during heading perception. *Proceedings of the National Academy of Sciences*, 112(20):6467–6472, may 2015. (Cited on page 20.)

[294] Adam Zaidel, Gregory C. DeAngelis, and Dora E. Angelaki. Decoupled choice-driven and stimulus-related activity in parietal neurons may be misrepresented by choice probabilities. *Nature Communications*, 8(1):715, dec 2017. (Cited on page 50.)

[295] Robert J Zatorre. There's more to auditory cortex than meets the ear. *Hearing research*, 229(1-2):24–30, jul 2007. (Cited on page 12.)

[296] Marina M Zempeltzi, Martin Kisse, Michael G.K. Brunk, Claudia Glemser, Sümeyra Aksit, Katrina E. Deane, Shivam Maurya, Lina Schneider, Frank W Ohl, Matthias Deliano, and Max F.K. Happel. Task rule and choice are reflected by layer-specific processing in rodent auditory cortical microcircuits. *Communications Biology*, 3(1):1–21, 2020. (Cited on pages 9, 15, 19, 21, 60, 62, and 118.)

[297] Hongkui Zeng and Linda Madisen. Mouse transgenic approaches in optogenetics. In *Optogenetics: Tools for Controlling and Monitoring Neuronal Activity*, pages 193–213. Elsevier, 2012. (Cited on page 90.)

[298] Yuan Zhao, Jacob L. Yates, Aaron J Levi, Alexander C Huk, and Il Memming Park. Stimulus-choice (mis)alignment in primate area MT. *PLOS Computational Biology*, 16(5):e1007614, may 2020. (Cited on pages 20 and 62.)

[299] Petr Znamenskiy and Anthony M. Zador. Corticostriatal neurones in auditory cortex drive decisions during auditory discrimination. *Nature*, 497(7450):482–485, 2013. (Cited on pages 5, 19, 62, 86, and 118.)

[300] Ehud Zohary, Michael N. Shadlen, and William T. Newsome. Correlated neuronal discharge rate and its implications for psychophysical performance. *Nature*, 370(6485):140–143, jul 1994. (Cited on page 20.)

ITQB-UNL | Av. da República, 2780-157 Oeiras, Portugal
Tel (+351) 214 469 100 | Fax (+351) 214 411 277

www.itqb.unl.pt